

INFORMATION TO USERS

This reproduction was made from a copy of a manuscript sent to us for publication and microfilming. While the most advanced technology has been used to photograph and reproduce this manuscript, the quality of the reproduction is heavily dependent upon the quality of the material submitted. Pages in any manuscript may have indistinct print. In all cases the best available copy has been filmed.

The following explanation of techniques is provided to help clarify notations which may appear on this reproduction.

1. Manuscripts may not always be complete. When it is not possible to obtain missing pages, a note appears to indicate this.
2. When copyrighted materials are removed from the manuscript, a note appears to indicate this.
3. Oversize materials (maps, drawings, and charts) are photographed by sectioning the original, beginning at the upper left hand corner and continuing from left to right in equal sections with small overlaps. Each oversize page is also filmed as one exposure and is available, for an additional charge, as a standard 35mm slide or in black and white paper format.*
4. Most photographs reproduce acceptably on positive microfilm or microfiche but lack clarity on xerographic copies made from the microfilm. For an additional charge, all photographs are available in black and white standard 35mm slide format.*

*For more information about black and white slides or enlarged paper reproductions, please contact the Dissertations Customer Services Department.

U·M·I Dissertation
Information Service

University Microfilms International
A Bell & Howell Information Company
300 N. Zeeb Road, Ann Arbor, Michigan 48106

1328192

Minnis, Steffi Ann

STABLE ISOTOPE PROFILES OF HERMATYPIC CORALS: INDICATORS OF
CHANGING ENVIRONMENTAL CONDITIONS IN UPWELLING AND NON-
UPWELLING REGIONS OF THE EASTERN TROPICAL PACIFIC

Rice University

M.A. 1986

University
Microfilms
International 300 N. Zeeb Road, Ann Arbor, MI 48106

PLEASE NOTE:

In all cases this material has been filmed in the best possible way from the available copy. Problems encountered with this document have been identified here with a check mark ✓.

1. Glossy photographs or pages ✓
2. Colored illustrations, paper or print _____
3. Photographs with dark background ✓
4. Illustrations are poor copy _____
5. Pages with black marks, not original copy _____
6. Print shows through as there is text on both sides of page _____
7. Indistinct, broken or small print on several pages ✓
8. Print exceeds margin requirements _____
9. Tightly bound copy with print lost in spine _____
10. Computer printout pages with indistinct print _____
11. Page(s) _____ lacking when material received, and not available from school or author.
12. Page(s) _____ seem to be missing in numbering only as text follows.
13. Two pages numbered _____. Text follows.
14. Curling and wrinkled pages _____
15. Dissertation contains pages with print at a slant, filmed as received ✓
16. Other _____

University
Microfilms
International

RICE UNIVERSITY

STABLE ISOTOPE PROFILES OF HERMATYPIC CORALS: INDICATORS
OF CHANGING ENVIRONMENTAL CONDITIONS IN UPWELLING AND
NON-UPWELLING REGIONS OF THE EASTERN TROPICAL PACIFIC

by

STEFFI ANN MINNIS

A THESIS SUBMITTED IN PARTIAL FULFILLMENT OF
THE REQUIREMENTS FOR THE DEGREE

MASTER OF ARTS

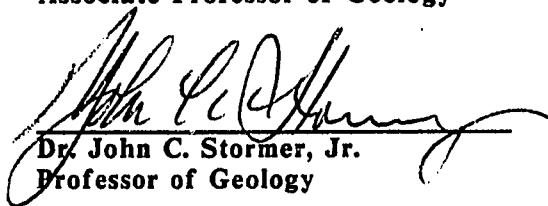
APPROVED, THESIS COMMITTEE:



Dr. Robert B. Dunbar
Associate Professor of Geology
Chairman



Dr. William P. Leeman
Associate Professor of Geology



Dr. John C. Stormer, Jr.
Professor of Geology



Dr. Gerard M. Wellington
Assistant Professor of
Marine Biology
University of Houston,
Galveston

Houston, Texas
May, 1986

To my parents and brother

**STABLE ISOTOPE PROFILES OF HERMATYPIC CORALS:
INDICATORS OF CHANGING ENVIRONMENTAL CONDITIONS IN
UPWELLING AND NON-UPWELLING REGIONS OF THE EASTERN
TROPICAL PACIFIC**

by

Steffi Ann Minnis

ABSTRACT

Subannual and interannual variations in coral skeletal stable isotopes are compared with seasonal water temperature, cloud cover, salinity, and relative skeletal density data from the gulfs of Panama and Chiriqui to establish a cause and effect relationship between skeletal density and variations in certain environmental parameters and to determine how El Niño and upwelling are recorded in coral stable isotope profiles.

Comparison of the magnitude and timing of variations in skeletal stable isotopes of Pavona gigantea and P. clavus with water temperature, salinity, and cloud cover data from the upwelling Gulf of Panama and water temperature and cloud cover data from the non-upwelling Gulf of Chiriqui indicate that $\delta^{18}\text{O}$ and $\delta^{13}\text{C}$ accurately record interannual and subannual variations in these environmental parameters. As a result of seasonal upwelling, the seasonal water temperature variation in the Gulf of Panama is roughly twice that in the Gulf of Chiriqui. In the Gulf of Panama, water temperature variations account for approximately 70% of the observed seasonal variation in skeletal $\delta^{18}\text{O}$, while variations in sea surface salinity account for the remainder. Seasonal variations in skeletal $\delta^{13}\text{C}$ were more pronounced in the Gulf of Chiriqui than in the Gulf of Panama, probably due to an overall greater water clarity in the Gulf of Chiriqui and, therefore, larger seasonal variation in light intensity on the reef.

Although physical oceanographic phenomena associated with El Niño events have been documented in other parts of the eastern tropical Pacific, the

manifestation of El Niño in the stable isotopic records of massive corals from the Gulf of Panama and Gulf of Chiriqui is not obvious. Cessation of normal coral growth and accretion of skeletal material as a result of exposure to prolonged periods of excessively high water temperatures, such as those recorded in the Gulf of Panama during the 1982-1983 El Niño, may have resulted in a hiatus(es) in both the stable isotope and skeletal density band records.

Comparison of skeletal density curves with stable isotope profiles imply the presence of subannual density bands. In samples where large scale skeletal density variations are evident, statistical analyses indicate that skeletal density banding is correlated more significantly with skeletal $\delta^{13}\text{C}$ (sensitive to variations in light intensity and metabolic effects) than $\delta^{18}\text{O}$ (water temperature indicator).

ACKNOWLEDGEMENTS

I would like to thank the following people for their contribution to this thesis:

Dr. Robert B. Dunbar, my advisor and friend, for his patience, wisdom, and inestimable contribution to the conception, execution, and writing of this thesis.

My thesis committee: Dr. John C. Stormer, Dr. William P. Leeman, and especially Dr. G.M. Wellington for his help, guidance, and expertise with understanding coral biology, coral skeletal morphology, and coral reef communities.

The researchers and staff of the Smithsonian Tropical Research Institute, Balboa, Panama for their help in my field work.

My friend, Mark Schurdach, who helped me immensely with the scanning densitometer.

My friends and fellow graduate students at Rice University: Amy, Donna, Howard, Marc, Marian, Jill, Norman, Norio, Rick, and others, who are responsible for my real education.

The Professors, office and technical staff, and all other affiliates to the Department of Geology and Geophysics at Rice University for their contributions.

My very special friends, Lisa and Glen McDowell, whom I love dearly, and on whose emotional and financial support I relied greatly.

And finally, my parents, Burl and Nina Minnis (and my brother, Burl, too, who loaned me money for my income taxes this year). Somehow 'thanks' doesn't seem to be enough because I know that your contribution to my development as a person began a long time before, and will continue long after, my stay at Rice. To you, beloved parents and sibling, this thesis is dedicated.

TABLE OF CONTENTS

Abstract	iii
Acknowledgements	v
List of Figures	vii
List of Tables	viii
Introduction	1
Background	3
Climatic Regime and Coral Reef Development	3
Factors Affecting $\delta^{18}\text{O}$ and $\delta^{13}\text{C}$	11
Coral Growth and Density Banding	22
Anomalous Conditions Associated with El Niño	26
Methods	27
Results and Discussion	29
Gulf of Panama	29
Gulf of Chiriqui	48
Conclusions	66
References	68
Appendix A High and Low Tide Heights: Gulf of Panama	72
Appendix B Stable Isotope Data: Reference and Samples	83
Appendix C Algorithm for Calculating Coral Skeletal Density	111

LIST OF FIGURES

FIGURE 1	Locations of upwelling regions in the eastern tropical Pacific	5
FIGURE 2	Study sites in the Gulf of Panama and Gulf of Chiriqui	7
FIGURE 3	Seasonal variations in certain environmental parameters in the Gulf of Panama and Gulf of Chiriqui	9
FIGURE 4	Generalized depth zonation of <u>Pavona</u> and <u>Pocillopora</u> species in the Gulf of Panama and Gulf of Chiriqui	14
FIGURE 5	Comparison of coral (aragonite) $\delta^{18}\text{O}$ and $\delta^{18}\text{O}$ of inorganic CaCO_3 (calcite) versus water temperature	17
FIGURE 6	Water temperature versus $\delta^{18}\text{O}$ curves of skeletal aragonite for several coral genera	20
FIGURE 7	X-radiograph positive of a massive coral slab	24
FIGURE 8	Skeletal stable isotope and relative density profiles for URABA coral sample	33
FIGURE 9	Skeletal stable isotope and relative density profiles for SOUTH SHORE CONTADORA coral sample	35
FIGURE 10	Skeletal stable isotope profiles and relative skeletal density patterns for CONTADORA 9 coral sample	37
FIGURE 11	Sea surface temperature variations in the Gulf of Panama from January 1982-January 1984	39
FIGURE 12	Sea surface salinity variations in the Gulf of Panama from January 1982-January 1984	41
FIGURE 13	Relationship between skeletal $\delta^{18}\text{O}$ and $\delta^{13}\text{C}$ for the URABA and SOUTH SHORE CONTADORA samples	44
FIGURE 14	Relationship between skeletal $\delta^{18}\text{O}$ and relative skeletal density for the URABA and SOUTH SHORE CONTADORA samples	47

FIGURE 15	Relationship between skeletal $\delta^{13}\text{C}$ and relative skeletal density for the SOUTH SHORE CONTADORA and URABA samples	50
FIGURE 16	Skeletal stable isotope profiles and relative skeletal density patterns for the UVA 56 sample	52
FIGURE 17	Skeletal stable isotope and relative density profiles for the UVA 1 sample	54
FIGURE 18	Skeletal stable isotope and relative density profiles for the SECAS 1 sample	56
FIGURE 19	Relationship between skeletal $\delta^{18}\text{O}$, $\delta^{13}\text{C}$, and relative skeletal density for the UVA 1 sample	59
FIGURE 20	Skeletal stable isotope and relative skeletal density profiles for the AZUERO sample	62
FIGURE 21	Superimposed stable isotope profiles of three massive corals from the Gulf of Panama	65

LIST OF TABLES

TABLE 1	Growth rates of <u>Pocillopora damicornis</u> , <u>Pavona gigantea</u> , and <u>P. clavus</u> in the Gulf of Panama and Gulf of Chiriqui	12
TABLE 2	Sampling date and location, species sampled, and sample names	30

INTRODUCTION

The stable isotopic composition of scleractinian coral skeletons provides useful information about environmental conditions prevalent during coral growth. $^{18}\text{O}/^{16}\text{O}$ ratios record changing water temperatures and salinities (Epstein *et al.*, 1953; Emiliani, 1966; Swart and Coleman, 1980; Epstein and Mayeda, 1953; Craig and Gordon, 1965); $^{13}\text{C}/^{12}\text{C}$ ratios provide information on partitioning among the various carbon sources utilized by the coral (Goreau, 1961; Weil *et al.*, 1981; Land *et al.*, 1975). Variations in growth rate brought on by changes in light intensity, water depth and water temperature are also thought to influence the isotopic composition of the coral skeletal material (Baker and Weber, 1975; Fairbanks and Dodge, 1979; Weber *et al.*, 1975). Comparison of environmental parameters monitored by variations in the stable isotope ratios of carbon and oxygen with density banding provides a new approach for determining the driving mechanism(s) behind seasonal density band formation in massive corals.

Previous studies using corals from the Pacific and Caribbean yield conflicting results regarding which environmental parameters best correlate with density band variations (Highsmith, 1979; Wellington and Glynn, 1983; Goreau, 1977; Weber *et al.*, 1975). Tropical climatic regimes are typically characterized by subannual variations in one or more of the following: light intensity, nutrient supply, water temperature, and salinity. The parameters most often linked to skeletal density variations are light intensity and water temperature (Weber *et al.*, 1975; Buddemeier, 1974; Buddemeier *et al.*, 1974; Buddemeier and Kinzie, 1975; Macintyre and Smith, 1974; Wellington and Glynn, 1983; Highsmith, 1979). The magnitude and timing (eg. leads and

lags) of subannual variations in these parameters with respect to skeletal density band patterns differs between locations thus, making comparison between distant sites difficult. It is, therefore, necessary to compare coral growth and variations in environmental parameters in regions in which skeletal density band patterns develop synchronously, yet provide contrasting subannual variations in water temperature and light intensity.

Massive corals were sampled from the Gulf of Panama, the Gulf of Chiriqui, and the Azuero Peninsula, located within 200km of each other on the Pacific coast of the Republic of Panama. These regions provide the opportunity to study synchronous development of skeletal density banding under conditions of upwelling and non-upwelling. The region off the Azuero Peninsula represents a transition zone between upwelling and non-upwelling conditions. Coral samples were collected in November, 1979 and June, 1983, providing stable isotopic and skeletal density records before and during the 1982-1983 El Niño.

A moderate to strong El Niño event occurs every 2 to 10 years, resulting in increased water temperatures, decreased salinity, increased sea level, and increased depth to the thermocline in the eastern tropical Pacific (Rasmusson and Carpenter, 1982; Philander, 1983). A reduction in coral metabolism, associated with reduced zooplankton concentrations and excessively high water temperatures ($> 28^{\circ}\text{C}$) associated with El Niño, may influence both the $\delta^{18}\text{O}$ and $\delta^{13}\text{C}$ values of coral skeletal material. Recognition of El Niño and upwelling in coral stable isotope profiles may prove useful for studying oceanic circulation in the eastern tropical Pacific through time.

The objectives of this thesis are threefold:

- 1) to determine whether the stable isotopes of carbon and oxygen in the aragonite skeletons of massive coral species in the gulfs of Panama and

Chiriqui accurately record seasonal variations in certain environmental parameters.

2) to determine whether El Niño and upwelling events can be recognized in the skeletal stable isotope profiles of the massive corals, Pavona gigangea and P. clavus.

3) to correlate variations in skeletal stable isotopes and density variations to determine which environmental parameter, water temperature or light intensity, is responsible for density banding in massive corals.

BACKGROUND:

Climatic Regime and Coral Reef Development

The gulfs of Panama and Chiriqui are located on the Pacific coast of the Republic of Panama (Figure 1), representing regions of upwelling and non-upwelling, respectively (Wellington and Glynn, 1983). A strong thermal gradient develops between these two regions off the southeastern tip of the Azuero Peninsula during the tropical dry season (January-April), when water temperatures can drop from approximately 27°C to 18°C (Glynn, 1974; Glynn, 1977; Wellington and Glynn, 1983) (Figure 2).

Seasonal water temperature ranges for the gulfs of Panama and Chiriqui are shown in Figure 3. During the tropical dry season (January-April), the mean water temperature in the Gulf of Panama is 24°C but may fall as low as 15°C for short periods of time during episodes of intense upwelling. Decreased water temperatures associated with upwelling adversely affect coral metabolism, resulting in decreased growth rates for some species. Relief from extreme low water temperatures, however, may come during low tide, when the water over the reef is shallower and insolation causes water temperatures to increase.

Figure 1:

Upwelling regions along the Central American coast are shown by the dot pattern; the stippled pattern represents land; the diagonal lines are elevations greater than 2,000 m (modified from Glynn, et al., 1983).

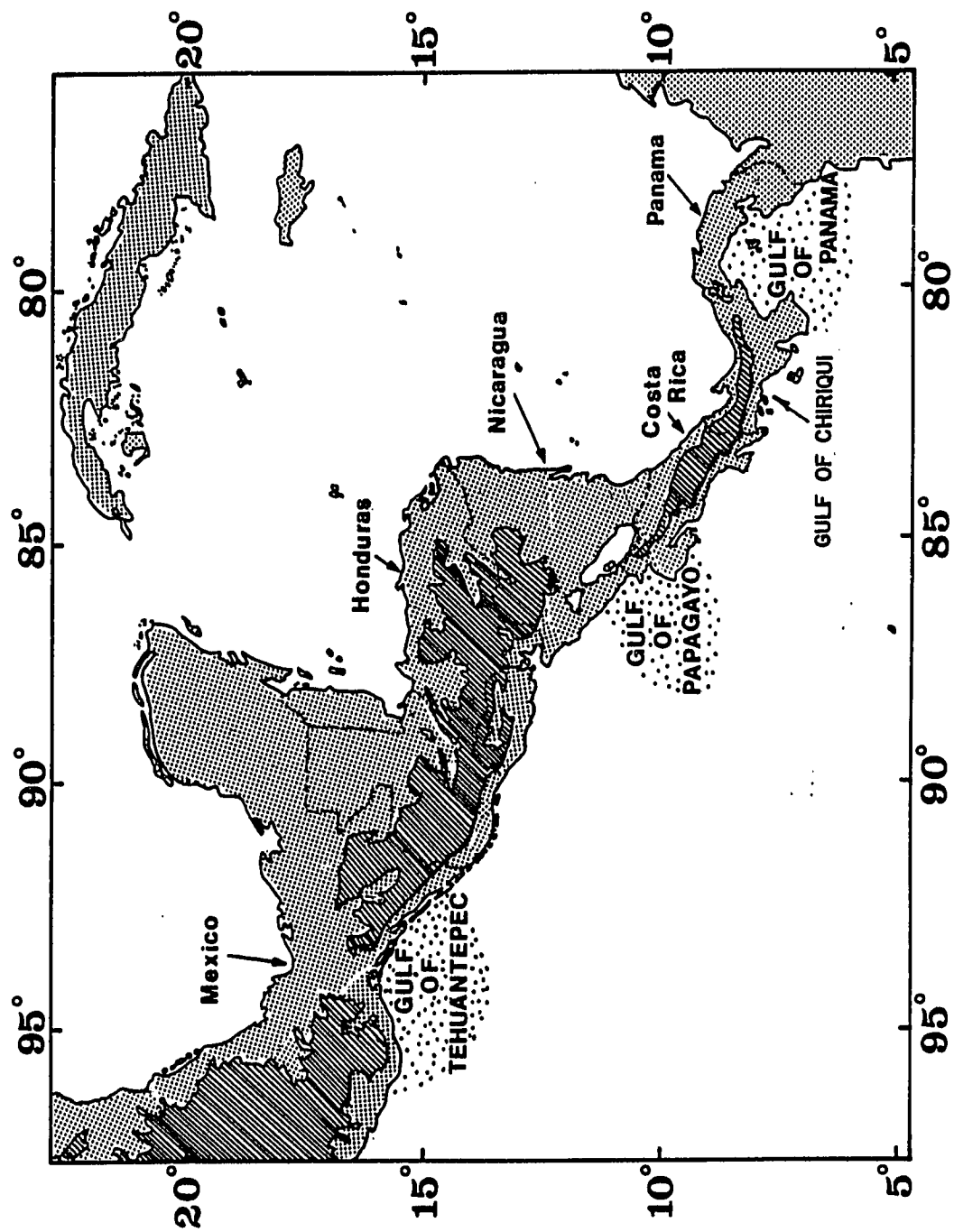


Figure 2:

Study areas from the Gulf of Chiriqui (Uva Island and Secas Islands) and from the Gulf of Panama (Perlas Islands). Sampling locations for this study are shown by the dark triangles. The shaded pattern represents the thermal boundary zone. Dashed contours are 5.4 m isobaths. Modified from Glynn (1977).

SITE LOCATION MAP

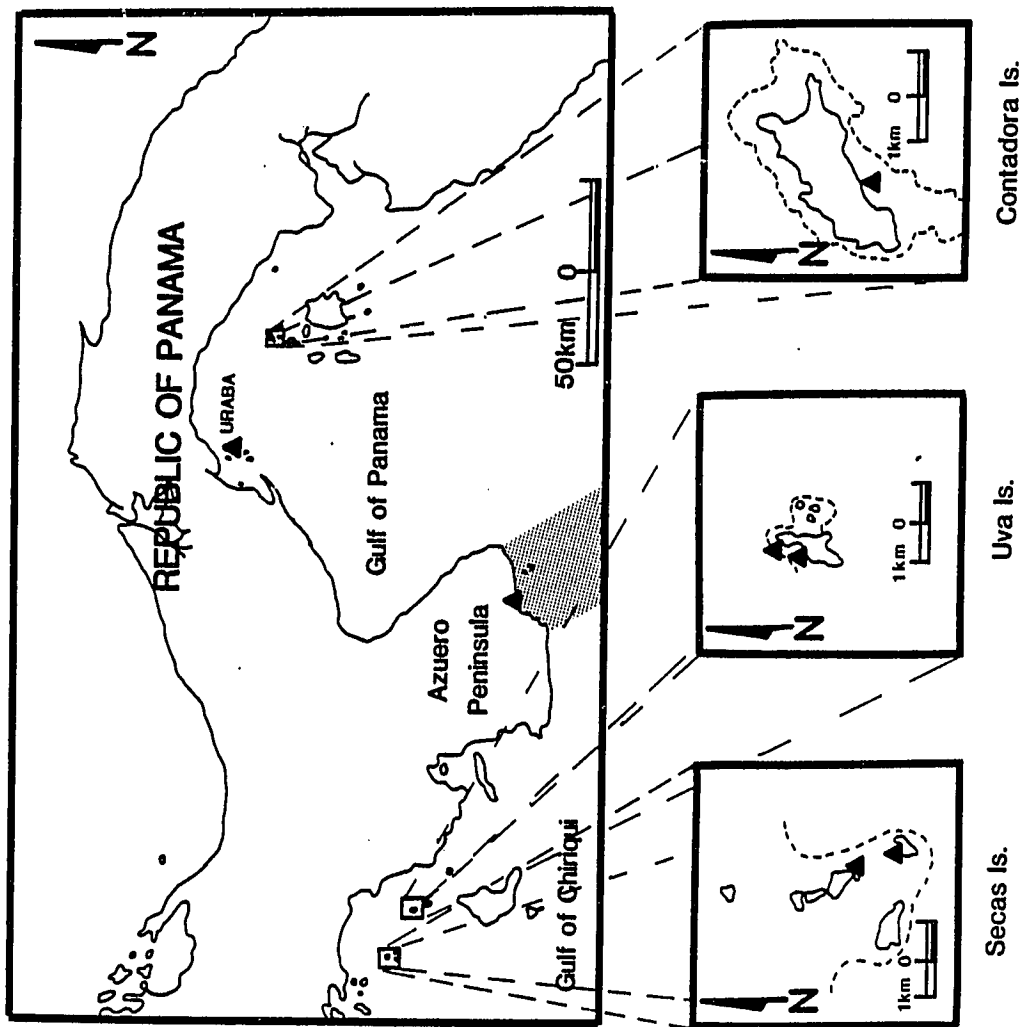
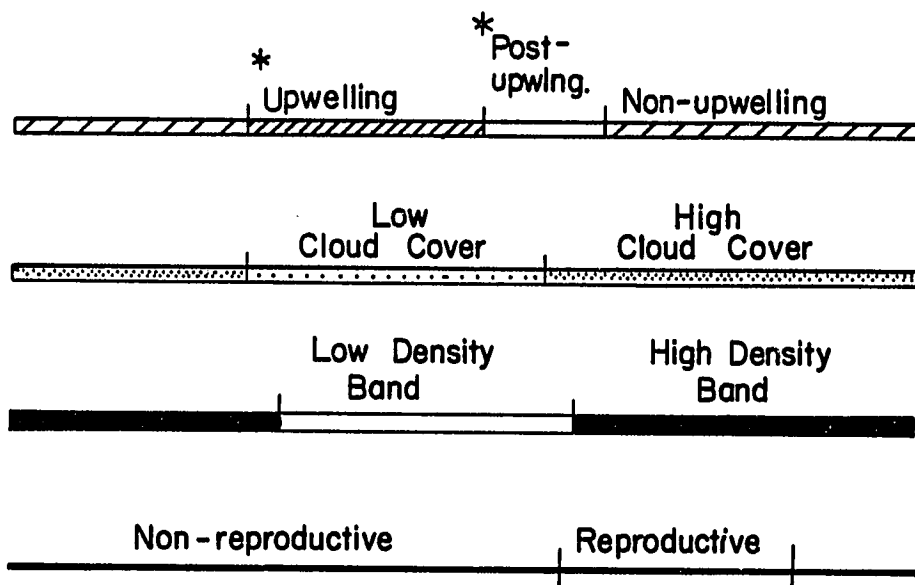
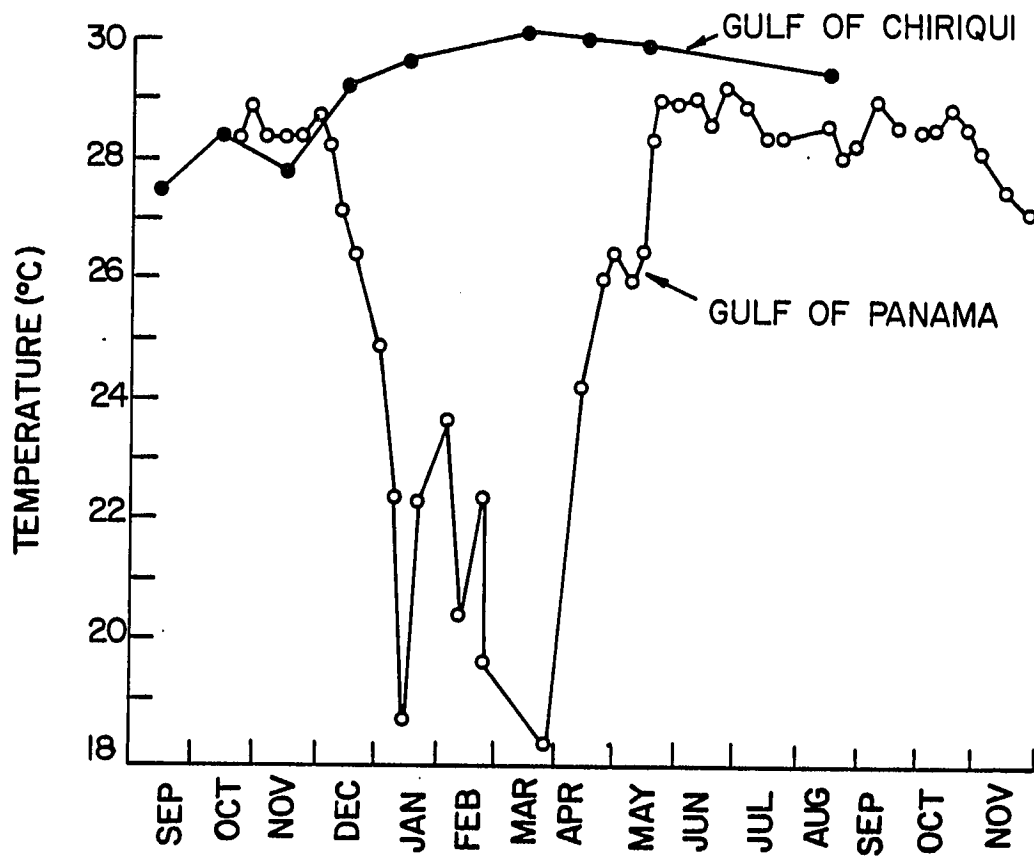


Figure 3:

Seasonal water temperature variations in the gulfs of Panama and Chiriqui (upper part of figure); seasonal variations in upwelling (Gulf of Panama); cloud cover; density band formation; and reproductive status(lower part of figure). Parameters marked with asterisks are those found only in the Gulf of Panama. Gulf of Chiriqui data are monthly averages from 1979-1980; Gulf of Panama data are weekly averages from 1978-1979 (from Wellington and Glynn, 1983).



In the Gulf of Panama, reef structures are more numerous on the lee sides of islands (N and E sides), locations which protect the reefs from direct upwelling and, therefore, provide a more favorable thermal regime (Glynn and Stewart, 1973). Glynn and Stewart (1973) observed that growth rates of the branching coral, Pocillopora damicornis, on the western and southern shores of the Perlas Islands were 65-85% of those on the northern and eastern sides.

Wellington and Glynn (1983) and Glynn and Macintyre (1977) have noted that pocilloporid (branching) and pavonid (massive) species can be found in both gulfs but the reefs in the Gulf of Chiriqui show a greater areal extent and thickness (i.e., vertical build-up) than those in the Gulf of Panama. The decrease in areal extent and thickness of reefs in the Gulf of Panama is presumably due to thermal stress induced by seasonal upwelling (Glynn, 1977). Glynn (1977) observed that the average growth rate of Pocillopora damicornis in the Gulf of Panama decreased from 3.5 to 6.0 mm/month during the period preceding upwelling to less than 1 mm/month during the upwelling season as a result of decreased water temperatures. In the Gulf of Chiriqui, however, water temperatures, water clarity, and light levels remain relatively high (between 27.8 and 30°C, for water temperatures), providing optimum growth conditions for pocilloporid species. Average growth rates for Pocillopora damicornis in the Gulf of Chiriqui range from approximately 2.5 mm/month during the wet season to 3.7 mm/month during the dry season.

Growth rates of Pocillopora damicornis, in the Gulf of Panama decrease during the upwelling season, despite increased concentrations of zooplankton. Growth rates of Pavona gigantea in the Gulf of Panama decrease from 1 mm/month in the upwelling season to 0.5 mm/month in the non-upwelling season. Likewise, average growth rates of Pavona clavus decrease from 2 mm/month during the upwelling season to 0.7 mm/month during the

non-upwelling season (Wellington and Glynn, 1983). Wellington (1982) studied the feeding mode of the branching coral Pocillopora damicornis, and the massive corals, Pavona gigantea and P. clavus in the Gulf of Panama. Coral behavior ranges from phototrophic (deriving their nutrition from translocated by-products of their zooxanthellae) to heterotrophic (deriving their nutrition from zooplankton). He tested whether depth zonation resulted from differential food resource utilization. Pocilloporid and pavonid species were found to be phototrophic but that, although both benefited from nutrient enrichment, pavonid species did so even at reduced light levels. This may explain the higher growth rates of Pavona clavus in the Gulf of Panama despite the lower water temperatures and water clarity (Glynn, 1977; Glynn and Stewart, 1973). When comparing growth rates for similar coral species in the Pacific Ocean, the eastern tropical Pacific corals have some of the highest growth rates. Mean yearly (1972-1974) growth of Pocillopora damicornis on the Saboga reef (Gulf of Panama) was 2.65 cm/yr. and 3.77 cm/yr. on the Secas reef (Gulf of Chiriqui) (Glynn, 1974) (Table 1).

The average tidal range in the Gulf of Panama (2.5m; see Appendix A) is larger than at open ocean sites, for example. This increases the depth range over which warmer, shoal waters and hermatypic coral growth occurs. Branching corals (pocilloporid species) are the chief reef builders in shallow waters (less than 6 m depth) in both the Gulf of Panama and Gulf of Chiriqui. Pavona gigantea and P. clavus are massive corals, generally confined to the lower reef slope and base (7-10m) (Figure 4).

Factors affecting $\delta^{18}\text{O}$ and $\delta^{13}\text{C}$

Oxygen isotopic composition has been used as a paleotemperature indicator in planktonic foraminifera (Emiliani, 1966; Williams, 1976, Malmgren and

TABLE 1

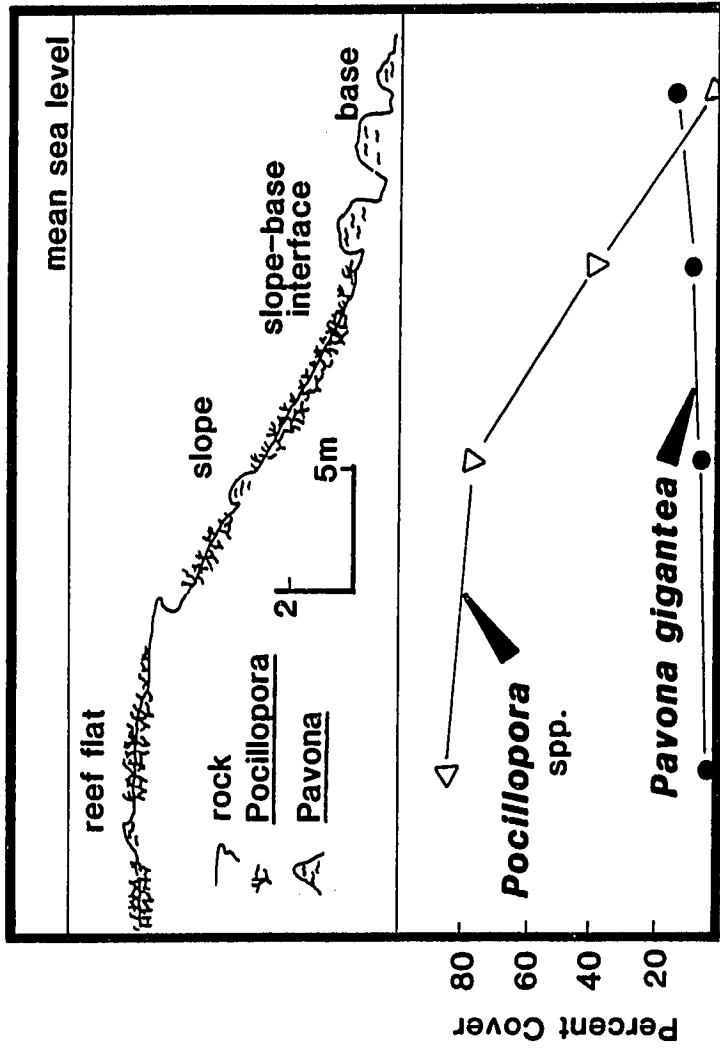
<u>Species/Location</u>	<u>Growth Rate (cm/yr)^{1,2}</u>
<u>Pavona gigantea</u> (Gulf of Panama)	0.85
<u>Pavona clavus</u> (Gulf of Panama)	1.32
<u>Pavona clavus</u> (Gulf of Chiriqui)	0.93
<u>Pocillopora damicornis</u> (Gulf of Panama)	2.65
<u>Pocillopora damicornis</u> (Gulf of Chiriqui)	3.77

(1) Massive coral (pavonid) data from Wellington and Glynn (1983); branching coral (Pocillopora damicornis) data from Glynn (1977).

(2) Average growth rates of Pocillopora damicornis from 3.2 to 3.3 meters depth during period of January through April, 1974; growth rates of Pavona are annual (1978-1979) and are taken from corals between 5 and 7 meters depth.

Figure 4:

Depth zonation of Pavona and Pocillopora species. Pocillopora species are shown to be more abundant in the shallow reef slope and flat; Pavona species, on the reef base (from Wellington, 1982).



Kennett, 1978; and many others), benthic calcareous algae (Wefer and Berger, 1980), and mollusk shells (Killingly and Berger, 1979). $\delta^{18}\text{O}$ of coral skeletal aragonite is dependent on water temperature (Epstein *et al.*, 1953), $\delta^{18}\text{O}$ of the water (Swart and Coleman, 1980), and a "vital" effect (Weber and Woodhead, 1972).

Salinity changes also influence the $^{18}\text{O}/^{16}\text{O}$ ratio of the water and, subsequently, the coral skeleton (Swart and Coleman, 1980). Increased salinity is generally accompanied by greater $^{18}\text{O}/^{16}\text{O}$ ratios of a water mass due to evaporation of the lighter isotope. For open ocean regions, this effect was originally quantified by Epstein and Mayeda (1953) and later modified by Craig and Gordon (1965) and can be expressed:

$$\delta^{18}\text{O}(\text{‰}) = -21.2 + 0.61 \{ \text{salinity}(\text{‰}) \} \quad (1)$$

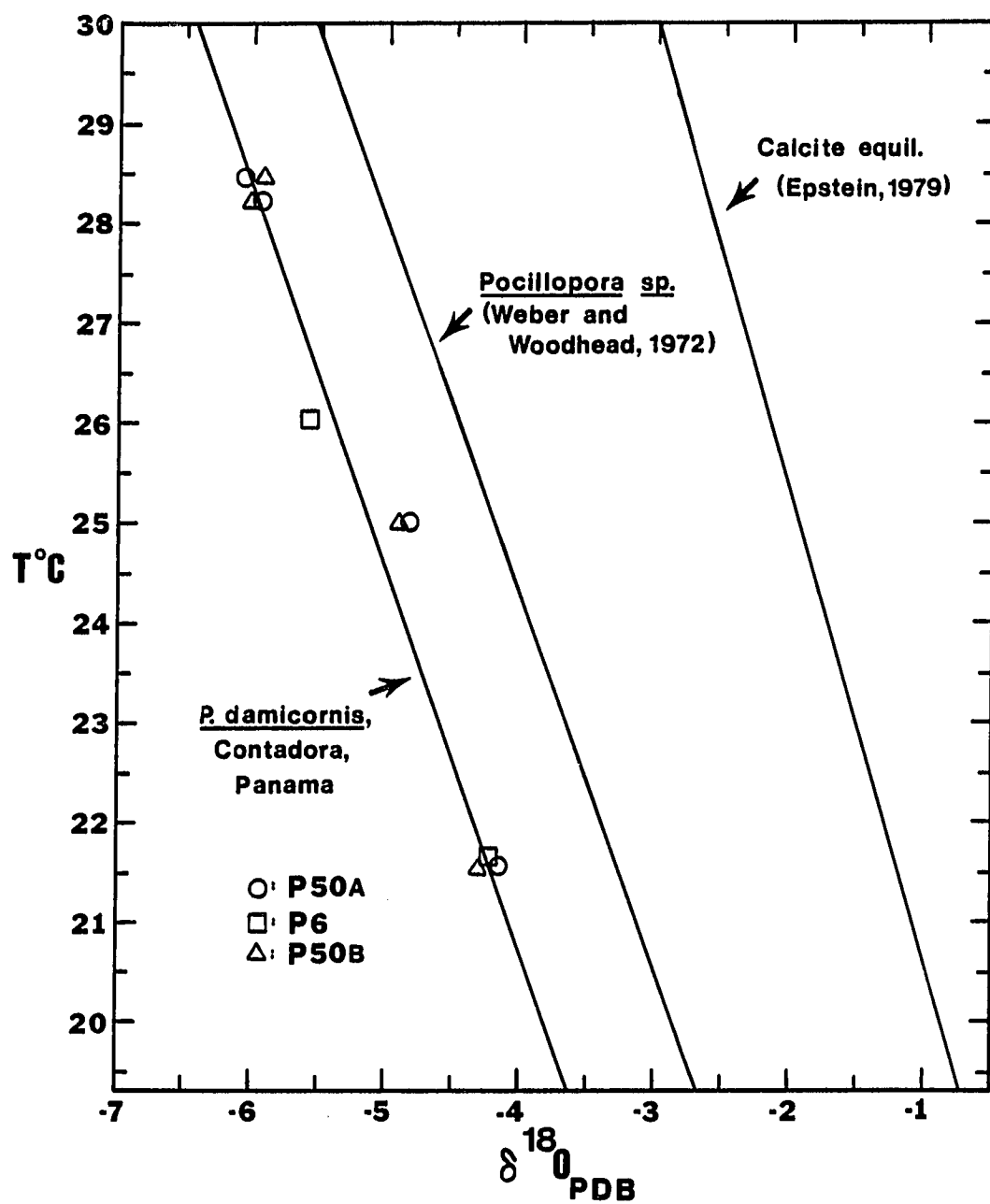
Equation (1) was derived from mean ocean salinities and seawater $\delta^{18}\text{O}$ values. Based on salinity and seawater $\delta^{18}\text{O}$ measurements in the Gulf of Panama, Dunbar and Wellington (1981) determined that 70% of the $\delta^{18}\text{O}$ variation in corals from the Gulf of Panama is caused by seasonal temperature changes while the remainder is due to changes in salinity. They expressed this relationship using the following equation:

$$d\delta^{18}\text{O}/dS(\text{‰}) = 0.12 \quad (2)$$

The $\delta^{18}\text{O}$ versus temperature curves for 44 different coral genera roughly parallel the paleotemperature curve established by Epstein *et al.* (1953) (Figure 5). Coral skeletal $^{18}\text{O}/^{16}\text{O}$ ratios are typically 2-5‰ lower than $^{18}\text{O}/^{16}\text{O}$ ratios of CaCO_3 (calcite) precipitated in isotopic equilibrium with average

Figure 5:

Water temperature versus $\delta^{18}\text{O}$ curves of Pocillopora species compared to $\delta^{18}\text{O}$ versus water temperature curve for inorganic CaCO_3 precipitated from seawater at a given temperature (from Dunbar, 1981).

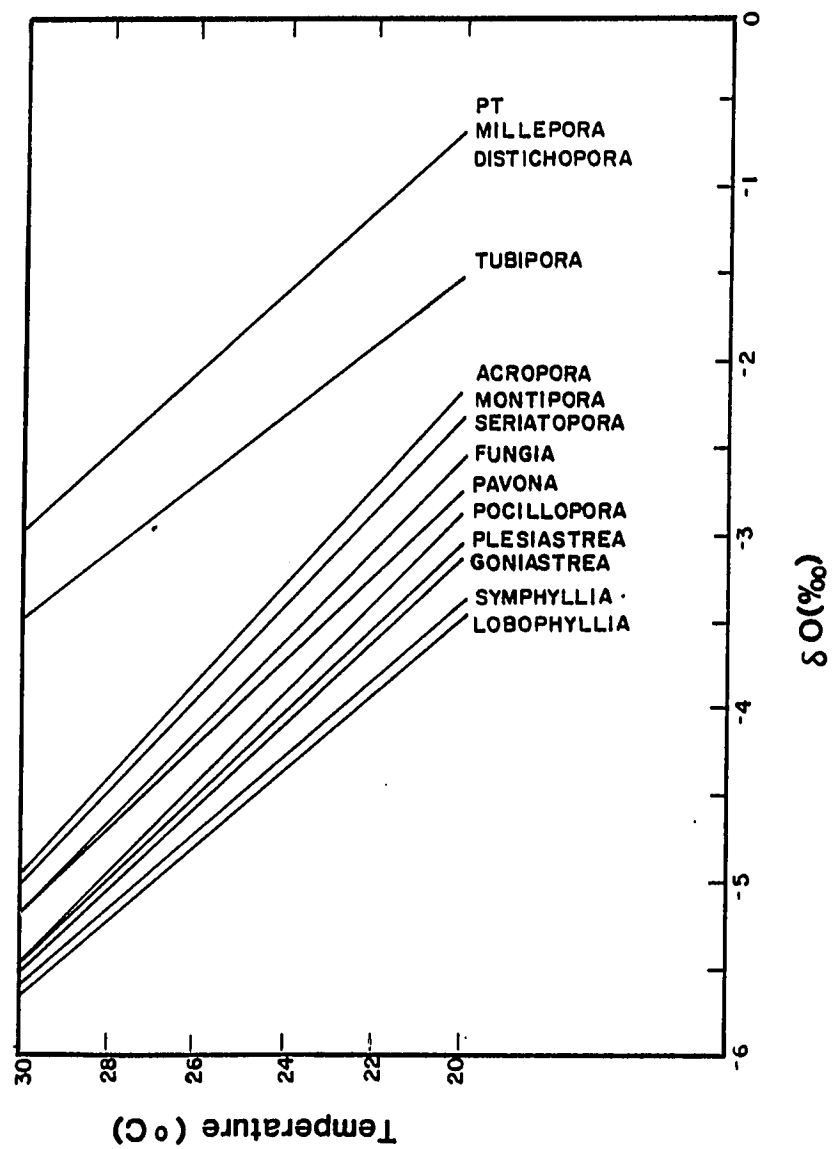


seawater at the same water temperature (Weber and Woodhead, 1972) (Figure 6). This effect was also noted by Weber and Woodhead (1972) who suggested dual sources of carbon and oxygen are utilized during skeletogenesis: seawater bicarbonate and metabolic CO_2 . Metabolic CO_2 is depleted relative to seawater bicarbonate by about 13-17‰ for ^{13}C and 10‰ for ^{18}O (Emiliani *et al.*, 1978). The proportions of the two sources utilized remains roughly constant for a given genus but varies between genera, suggesting a ranking according to their ability to excrete metabolic CO_2 by diffusion or uptake by symbiotic zooxanthellae (Weber and Woodhead, 1972). High polyp density or reduced light intensity would inhibit elimination of metabolic CO_2 , increasing the opportunity for isotopic exchange between metabolic CO_2 and seawater bicarbonate, and, therefore, lowering the $^{18}\text{O}/^{16}\text{O}$ and $^{13}\text{C}/^{12}\text{C}$ ratios of the coral skeleton (Weber and Woodhead, 1972). Goreau (1977) has established that for Montastrea annularis from Jamaica, approximately 60% of the carbon utilized in skeletogenesis is derived from metabolic CO_2 and 40% from seawater bicarbonate. This proportion is not constant, however. With increasing photosynthetic activity, the discrimination against the heavier seawater bicarbonate ion decreases, causing an enrichment of the heavier isotopes in the coral skeleton.

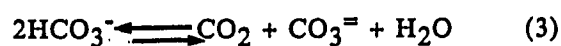
Erez (1978) studied corals and benthic foraminifera from the Gulf of Eilat, Israel and concluded that with increasing photosynthetic activity, the metabolism of the coral was enhanced, causing an increase in the metabolic CO_2 produced and, therefore, incorporated during skeletogenesis. Goreau (1977), however, believes that the accumulation of CO_2 during a period of increased photosynthetic activity, would be used in photosynthesis rather than skeletogenesis, as Erez (1978) suggests. Skeletal $^{13}\text{C}/^{12}\text{C}$ ratios would, therefore, increase during periods of enhanced photosynthetic activity.

Figure 6:

Water temperature versus $\delta^{18}\text{O}$ curves for several coral genera. Note the increasing slope with decreasing $\delta^{18}\text{O}$ values (from Weber and Woodhead, 1972).



Goreau (1977) summarized the partitioning of the internal carbon pool with the following formula:



Therefore, with increasing photosynthetic activity, the internal CO_2 supply is depleted, causing an increased carbon demand by the zooxanthellae. Uptake by the zooxanthellae of metabolic CO_2 produced by the coral during respiration, results in a relative increase in the $\text{CO}_3^{=}$ ion concentration, which is eventually used by the coral in skeletogenesis.

Variations in growth rate brought on by changes in water temperature, light intensity, and water depth affect the $\delta^{13}\text{C}$ of coral skeletal material. Weber et al. (1976), however, believe that growth rate per se does not have a significant effect on skeletal $\delta^{13}\text{C}$, but that the proportion of seawater bicarbonate and metabolic CO_2 utilized, relative to the zooxanthellae's ability to remove the metabolic CO_2 influences the $\delta^{13}\text{C}$ of the coral skeletal material. Skeletal $\delta^{13}\text{C}$ values decrease with decreasing light intensity (Fairbanks and Dodge, 1979) and increasing water depth (Baker and Weber, 1975). Decreasing light intensity and increasing water depth reduce photosynthetic activity, reducing the zooxanthellae's ability to remove the metabolic CO_2 produced by the coral, and ultimately decreasing the overall $\delta^{13}\text{C}$ value of the coral skeleton.

In summary, $\delta^{18}\text{O}$ is dependent on water temperature, $\delta^{18}\text{O}$ of seawater, and a "vital" effect. Many authors believe that the slope of the $\delta^{18}\text{O}$ versus temperature curve for corals is primarily dependent on water temperature and seawater $\delta^{18}\text{O}$ and the intercept (and offset from equilibrium) is dependent on "vital" effects (e.g. Weber and Woodhead, 1972). The offset from the Epstein et al. (1953) calcite- H_2O equilibrium curve is due to isotopic partitioning among

the sources of carbon and oxygen for skeletogenesis. The predominance of one source over the other changes with changing growth rate and taxa. Both $\delta^{18}\text{O}$ and $\delta^{13}\text{C}$ "vital" effects change with changing proportions of metabolic CO_2 and seawater bicarbonate. An empirical measurement is required to quantify the "vital" effect on the $\delta^{18}\text{O}$ signal.

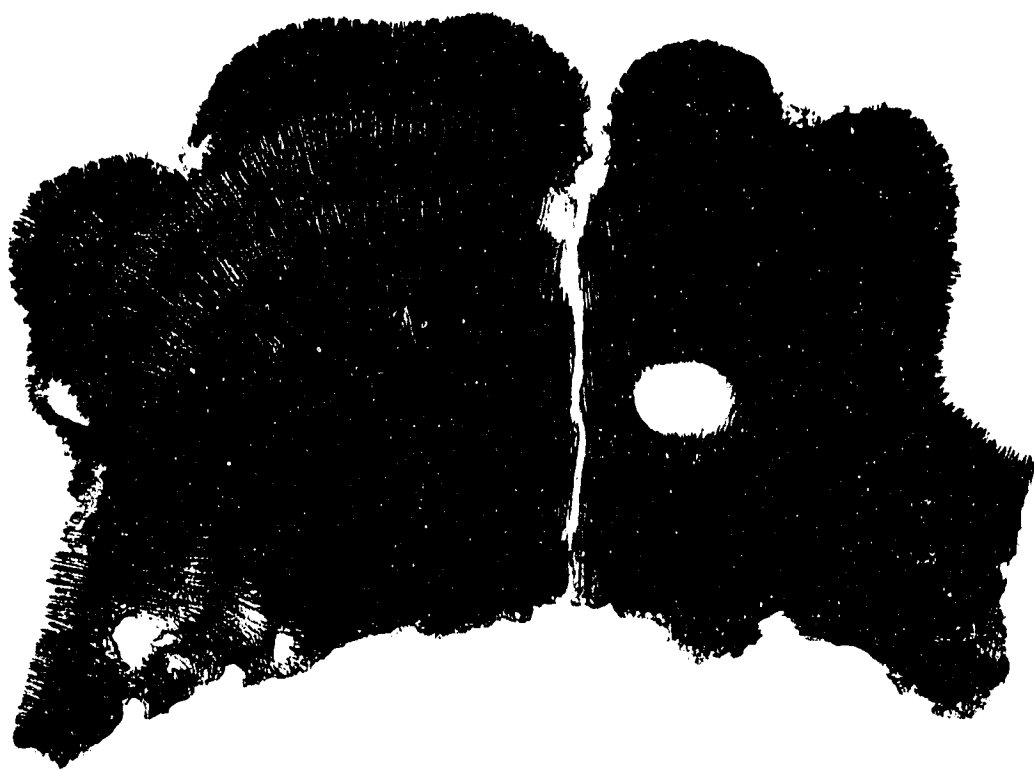
Factors affecting $\delta^{13}\text{C}$ are changes in water depth, water temperature, and light intensity. Variations in these parameters cause changes in coral growth rate which result in changes in the ability of the zooxanthellae to remove isotopically light metabolic CO_2 . Large diurnal variations in $\delta^{13}\text{C}$ of surface seawater ΣCO_2 occur on coral reefs (e.g. from a 0.59‰ variation at Saipan to a 1.46 ‰ variation at Heron Island; Weber and Woodhead, 1971). The temperature dependence of the carbon isotope for fractionation between CaCO_3 and HCO_3^- is small, with a 10°C change in water temperature corresponding to a 0.35‰ variation in the $\delta^{13}\text{C}$ of CaCO_3 , if the $^{13}\text{C}/^{12}\text{C}$ ratio of HCO_3^- is constant (Emrich *et al.*, 1970).

Coral Growth and Density Banding

Density banding is a growth phenomenon exhibited by all massive coral species, including *Pavona clavus* and *P. gigantea*. Figure 7 is a positive print of an X-radiograph of a specimen of *Pavona gigantea* from the Gulf of Panama. The alternate light and dark bands are the low density and high density bands, respectively. Radioisotopic studies on coral aragonite show the low density-high density band pairs are annual (Knutson *et al.*, 1972; Macintyre and Smith, 1974; Moore and Krishnaswami, 1974; Dodge *et al.*, 1974).

Coral growth is a two stage process involving both linear extension and calcification (Wellington and Glynn, 1983). Linear extension involves secretion of an aragonite matrix framework, which is later infilled during calcification .

Figure 7: X-radiograph positive of Pavona gigantea, collected from Contadora Island, Gulf of Panama, June, 1983.



The relative rates at which these two steps occur determines whether a low or high density band is formed. When linear extension is greater than calcification rates, a low density band forms. Conversely, when linear extension is reduced such that calcification rates are proportionately higher, a high density band forms. Two models have been proposed relating variation in certain environmental parameters to observed skeletal density band patterns. Wellington (1982) and Wellington and Glynn (1983) are proponents of one model which suggests that linear extension and tissue growth are positively related and are primarily influenced by changes in light intensity, nutrient supply, and reproductive status. Calcification rates are controlled by changes in algal photosynthetic rates which occur in response to changes in light intensity (Fairbanks and Dodge, 1979; Goreau, 1959). Highsmith (1979) proposes another model which suggests water temperature as well as light intensity are important in controlling skeletal band formation. Highsmith maintains that linear extension is related to zooxanthellar activity and that this activity decreases outside an optimum water temperature range (23.7 - 28.5°C). While the reduction of zooxanthellar activity decreases both linear extension and calcification rates, linear extension is more severely curtailed, resulting in the formation of a high density band.

Comparison of the timing of skeletal density band formation with the timing and magnitude of seasonal variations in water temperature and light intensity in the gulfs of Panama and Chiriqui support the Wellington and Glynn (1983) model. Wellington and Glynn (1983) observed that low density band formation occurs in both the Gulf of Panama and the Gulf of Chiriqui during the dry season (January-April). In the Gulf of Panama, the dry season corresponds to a time when water temperatures and cloud cover are low and nutrient supplies are high. High density bands are formed during the tropical

wet season (May-December) when water temperatures and cloud cover are comparably high in both the Gulf of Panama and the Gulf of Chiriqui but when nutrient supplies are low (Figure 3). In the Gulf of Panama, for 10 time series samples collected from January through November, 1979, nearly 60% of the low density bands formed when water temperatures were below 23.7°C (Wellington and Glynn, 1983). High density bands are formed in both the Gulf of Panama and Gulf of Chiriqui when water temperatures are within the optimum range quoted by Highsmith (1979); i.e., conditions for the formation of low density bands. The synchronous development of density band patterns in regions in which the magnitude of seasonal water temperature variations are so different and formation of low density bands during upwelling of cold ($< 21^{\circ}\text{C}$) water are observations not predicted by Highsmith's (1979) model. Seasonal variations in cloud cover show a closer correlation with density band formation than temperature, per se in areas such as the Pacific coast of Panama (Wellington and Glynn, 1983); Hawaii (Buddemeier and Kinzie, 1974); Christmas and Fanning Islands (Buddemeier, 1974); and Eniwetok (Buddemeier *et al.*, 1974). In Panama, during the dry season (January-April), reduced cloud cover results in increased photosynthetic activity and increased linear extension which produces low density bands. When cloud cover increases, photosynthetic activity and linear extension decrease, resulting in the formation of a high density band. To test this model, coral stable isotope profiles are compared to skeletal density variations to determine whether $\delta^{18}\text{O}$ (a water temperature indicator) or $\delta^{13}\text{C}$ (sensitive to light intensity and metabolic effects) correlate better with coral density band formation.

Anomalous Conditions Associated with El Niño

Upwelling in the Gulf of Panama was modified by an El Niño event

beginning in late 1982 (Firing *et al.*, 1983; Halpern *et al.*, 1983; Philander, 1983). Warm, low salinity water propagated from the western Pacific following cessation of prolonged, strong southeast tradewinds. As a result, sea level increased and the normally shallow thermocline was depressed by as much as 50m in the eastern tropical Pacific (Halpern *et al.*, 1983; Philander, 1983; Firing *et al.*, 1983).

Coincident with the 1982-1983 El Nino was the mortality of 75 to 90% of the living coral cover in this region (Lasker *et al.*, 1984). The first signs of perturbation of the coral community, a "whitening" of the coral tissue, began to appear in the Gulf of Chiriqui in April 1983 and eventually spread to the Gulf of Panama in May or June of 1983. "Whitening" of coral tissue is associated with expulsion of the algal symbionts (zooxanthellae) and often precedes the death of the coral host. Encrusting algae rapidly overgrow dead coral skeletons. Thermal stress associated with the 1982-1983 El Niño appear to be the best explanation for reef mortality in the eastern tropical Pacific (Glynn, 1983).

METHODS

Carbon and Oxygen Isotopes

Coral samples were prepared for isotopic analyses using a technique similar to that used by Dunbar and Wellington (1981). Corals were air-dried for 24-48 hours. Massive corals were slabbed with a Hilquist rock saw. Approximately 2 mg of powder was extracted with a 0.5 mm Dremel Drill tool at regular intervals (eg. 1-3 mm) along vertical growth axes. Coral powder was roasted for approximately 1 to 2 hours at 250°C under a vacuum to drive off volatile organics.

Stable isotope determinations were performed by reaction of powdered, roasted CaCO_3 (aragonite) with 100% H_3PO_4 at 50°C . The CO_2 gas evolved was then analyzed in a V.G. Micromass 602 mass spectrometer. Values are reported in standard delta notation:

$$^{18}\text{O}(\text{‰}) = \{ (^{18}\text{O}/^{16}\text{O}_{\text{sx}} - ^{18}\text{O}/^{16}\text{O}_{\text{std}}) / (^{18}\text{O}/^{16}\text{O}_{\text{std}}) \} \times 1000 \quad (4)$$

where $^{18}\text{O}/^{16}\text{O}_{\text{sx}}$ is the oxygen isotopic ratio of the sample; $^{18}\text{O}/^{16}\text{O}_{\text{std}}$ is the known oxygen isotopic ratio of a reference material (PDB). A similar formula is used to calculate $\delta^{13}\text{C}$. Reproducibility of isotope values is based on replicate analyses of an internal laboratory standard, RICE-1, with averages and standard deviations of -1.06 ± 0.15 for $\delta^{18}\text{O}_{\text{PDB}}$ and -0.78 ± 0.11 for $\delta^{13}\text{C}_{\text{PDB}}$. Average standard deviations for coral isotope replicate analyses are 0.13 for $\delta^{18}\text{O}_{\text{PDB}}$ and 0.13 for $\delta^{13}\text{C}_{\text{PDB}}$. Coral stable isotope and RICE-1 values are reported in Appendix B.

Density Measurements

Massive coral slabs and an Al stepwedge were X-rayed with Kodak X-OMAT TL X-ray film using a Radifluor 360 medical X-ray unit. The X-ray tube had a potential of 90kV and 3 mamps. Coral slab and Al stepwedge thicknesses were measured to the nearest 0.02 mm with a Vernier caliper. The Al stepwedge is used as a standard of known density for calibration of the densitometer. One 5-step Al stepwedge was used, increasing in thickness 0.120 cm per step. The densitometer used was a Transidyne 2955 RFT Scanning Densitometer. The massive coral slabs X-rayed were slightly thicker than one polyp diameter, reflecting density variations among different skeletal elements of a single polyp, rather than large scale density variations. The thicknesses of

the coral slabs should, therefore, be at least 2 to 3 times that of the average polyp diameter (Houck, 1978). Although skeletal density values obtained using a computer program developed by Houck (1978) after a method developed by Buddemeier (1974) are actual skeletal densities, they are reported as "relative" skeletal densities, which are unitless. A brief explanation of the theory, the computer program, and sample data is given in Appendix C.

Correlation coefficients and probabilities for skeletal $\delta^{18}\text{O}$, $\delta^{13}\text{C}$, and relative skeletal density data were calculated using the Pearson Product-Moment Correlation. R is the correlation coefficient and P is the probability that |R| is zero based on the Null Hypothesis. Correlations are defined as significant if $P < 0.05$ and not significant if $P > 0.05$ (Sokal and Rohlf, 1969).

RESULTS AND DISCUSSION

Coral stable isotope profiles are compared to temperature, salinity, and cloud cover data from the Gulf of Panama and Gulf of Chiriqui to determine whether seasonal variations in $\delta^{18}\text{O}$ and $\delta^{13}\text{C}$ accurately monitor variations in these environmental parameters. Stable isotope profiles are also compared to known El Niño occurrences to establish how El Niño is recorded in the carbonate skeletons of eastern tropical Pacific reef corals. Stable isotope and skeletal density data for the Gulf of Panama and Gulf of Chiriqui coral samples are presented in Figures 8 through 10, 16 through 18, and Figure 20. Coral sample locations, species, and sampling dates are shown in Table 2.

Gulf of Panama

Interpretation of $\delta^{18}\text{O}$

The magnitude of skeletal $\delta^{18}\text{O}$ variations correspond closely with the

TABLE 2

<u>Sample</u>	<u>Location</u>	<u>Species</u>	<u>Sampling date</u>
SOUTH SHORE CONTADORA	Gulf of Panama	<i>Pavona gigantea</i>	June 1983
URABA	Gulf of Panama	<i>Pavona gigantea</i>	June 1983
CONTADORA 9	Gulf of Panama	<i>Pavona clavus</i>	November 1979
UVA 1	Gulf of Chiriqui	<i>Pavona clavus</i>	June 1983
SECAS 1	Gulf of Chiriqui	<i>Pavona clavus</i>	June 1983
UVA 56	Gulf of Chiriqui	<i>Pavona clavus</i>	November 1979
AZUERO	Gulf of Chiriqui	<i>Pavona gigantea</i>	June 1983

magnitude of observed seasonal variations in water temperatures. The skeletal $\delta^{18}\text{O}$ values of the Gulf of Panama coral samples have a range of 1.5 to 2.0‰ (Figures 8 through 10) which corresponds to a seasonal water temperature range (Figure 3) of 8-10°C. Coral skeletal $\delta^{18}\text{O}$, however, is influenced by both water temperature and salinity. Variations in skeletal $\delta^{18}\text{O}$ data for the URABA, SOUTH SHORE CONTADORA, and CONTADORA 9 sample over the upwelling to non-upwelling season of 1982 is approximately 1.5‰ (Figures 8 through 10). Water temperature variations for February through June 1982 are approximately 4°C (Figure 11), contributing 1‰ variation in skeletal $\delta^{18}\text{O}$, or about 70% of the total observed variation. The remaining 0.5 ‰, or about 30%, is attributed to the influence of salinity (Equation 2; Figure 12) (Dunbar and Wellington, 1981). The timing of seasonal variations in skeletal $\delta^{18}\text{O}$ and water temperature correspond closely. The CONTADORA 9 sample (Figure 10) was stained (by G. Wellington) with Alizarin red on May 24, 1979 and September 25, 1979. During May 1979, the skeletal $^{18}\text{O}/^{16}\text{O}$ ratios were decreasing as a result of increasing water temperatures (Figure 3). Likewise, in September, 1979 skeletal $^{18}\text{O}/^{16}\text{O}$ ratios are low due to elevated water temperatures (Figure 3).

The SOUTH SHORE CONTADORA and URABA data show increasing skeletal $^{18}\text{O}/^{16}\text{O}$ ratios at the top of the coral, implying low water temperature at the time they were collected. However, the SOUTH SHORE CONTADORA and URABA samples were collected in June, 1983, when water temperatures were high. Coral growth may have ceased at some time prior to sampling as a result of the 1982-1983 El Niño. Further evidence of the effects of thermal stressing on coral skeletal $^{18}\text{O}/^{16}\text{O}$ ratios is shown in Figure 8. Skeletal $^{18}\text{O}/^{16}\text{O}$ and $^{13}\text{C}/^{12}\text{C}$ ratios are highly variable in the region of the profiles corresponding to growth during 1972-1973. A strong El Niño occurred during

Figure 8:

Seasonal variations in coral relative skeletal density and stable isotopes. Shaded areas represent regions of high relative skeletal densities. The influence of light intensity, salinity, and water temperature on skeletal stable isotopes is indicated. Sample is Pavona gigantea, collected from Uraba Island, Gulf of Panama, June, 1983.

URABA

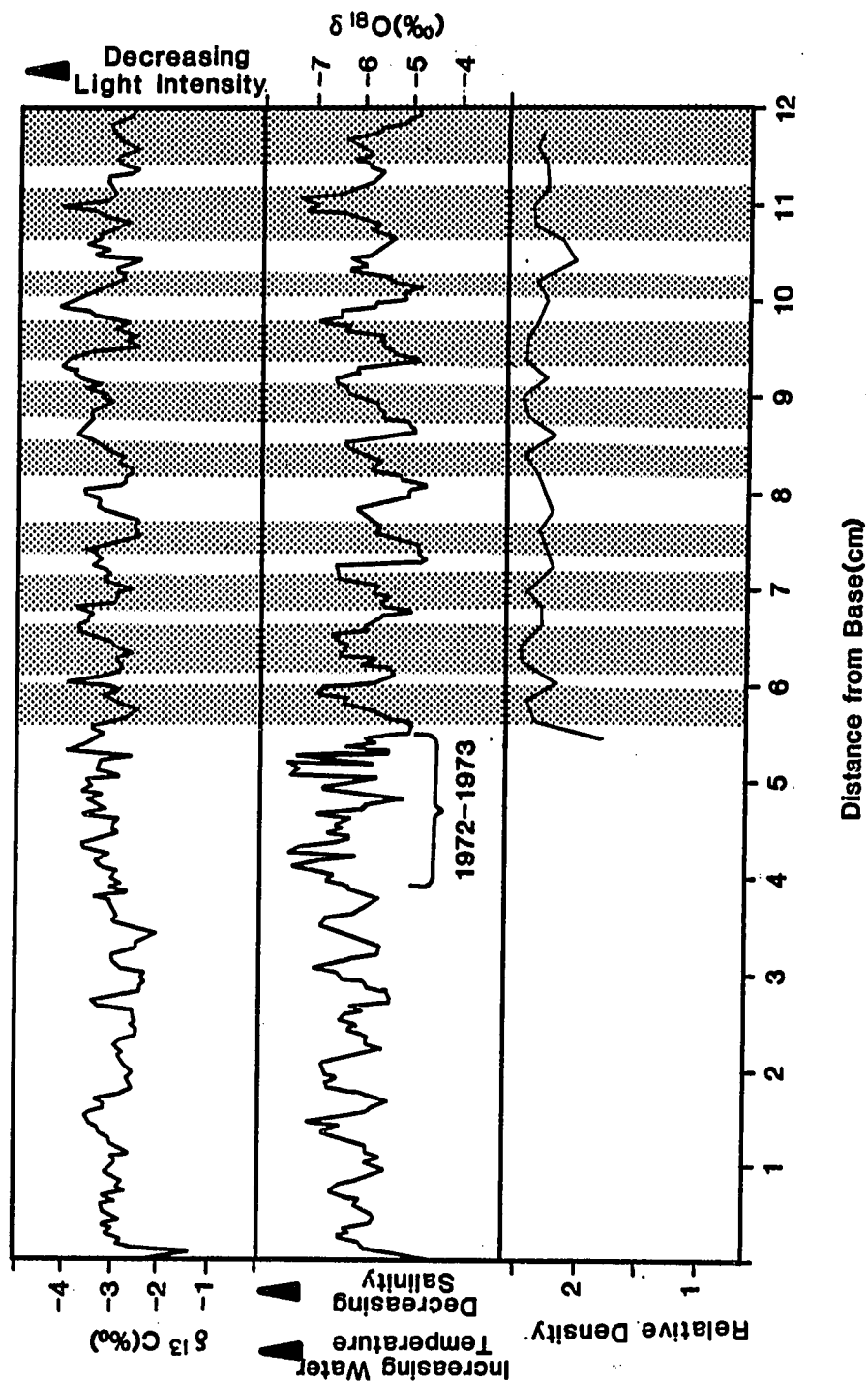


Figure 9:

Seasonal variation in coral relative skeletal density and stable isotope ratios. The shaded areas represent regions of high relative skeletal densities. The influence of water temperature, salinity, and light intensity on skeletal stable isotopes is indicated. The sample is Pavona gigantea, collected from the Gulf of Panama, Perlas Islands, June, 1983.

SOUTH SHORE CONTADORA

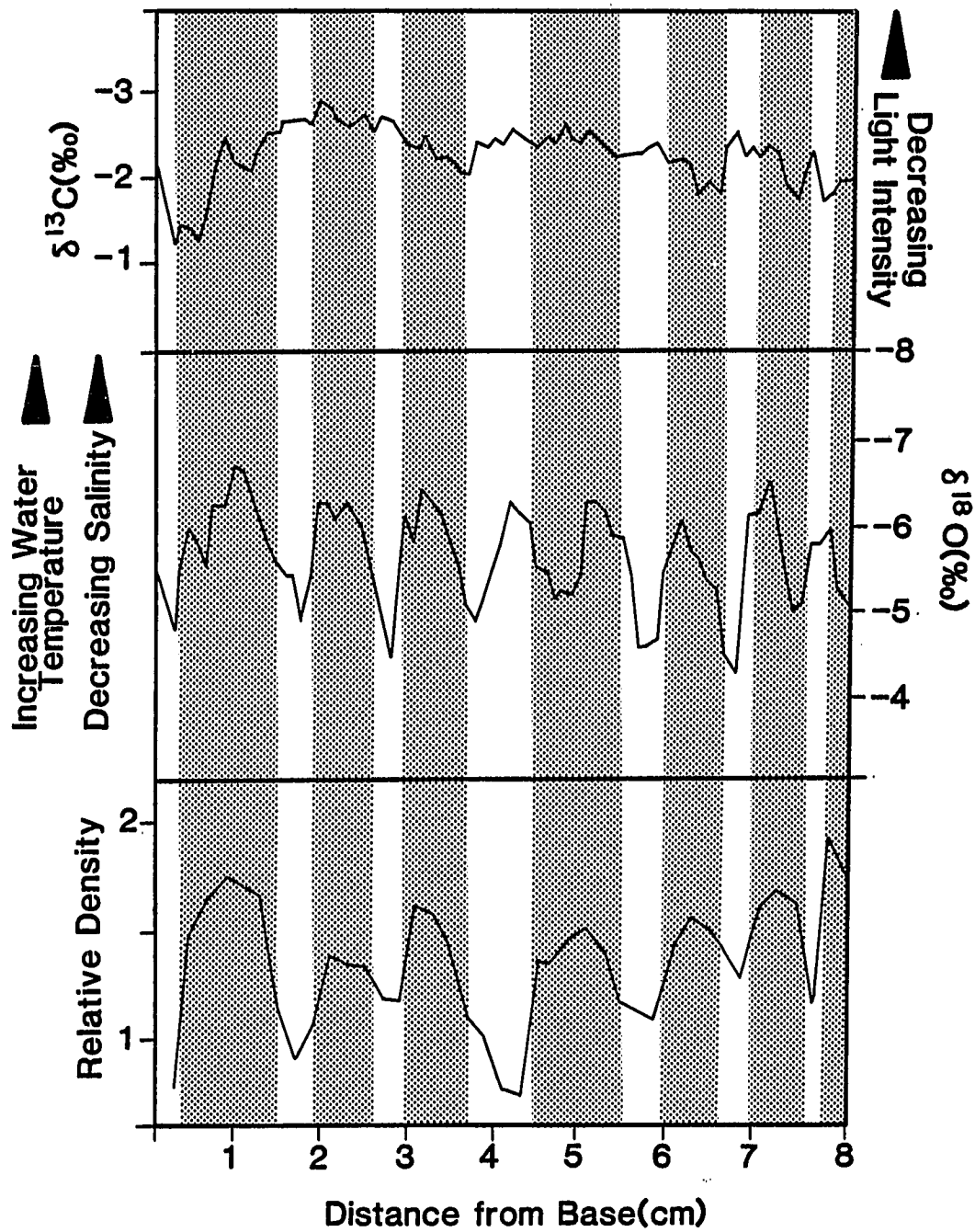


Figure 10:

Seasonal variations in coral relative skeletal density and stable isotope ratios. The shaded areas represent regions of high relative skeletal densities based on visual inspection of the coral X-radiograph. The vertical dashed lines indicate Alizarin Red staining episodes. The influence of water temperature, salinity, and light intensity on skeletal stable isotopes is indicated. The sample is Pavona clavus, collected by G. Wellington from the Perlas Islands, Gulf of Panama, November, 1979.

CONTADORA 9

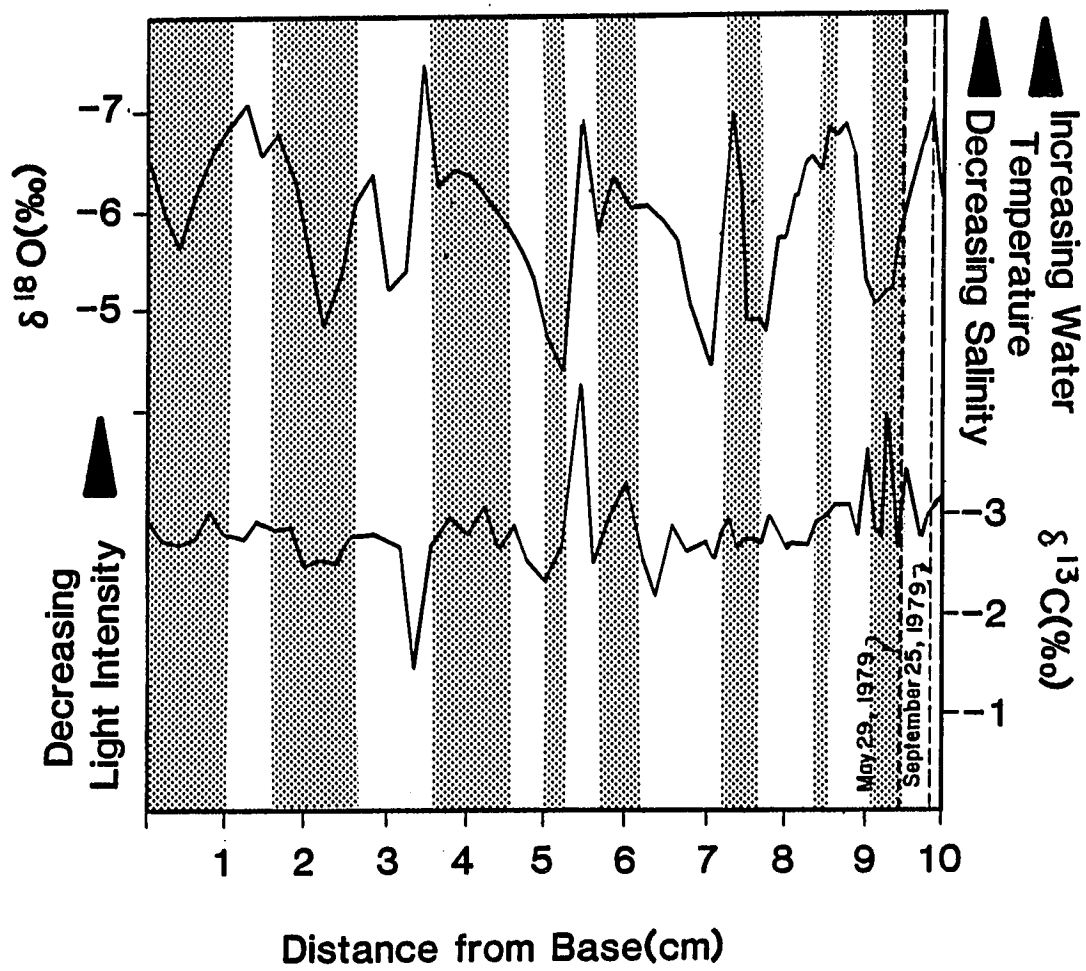


Figure 11:

Seasonal sea surface temperature variations ($^{\circ}\text{C}$) in the Gulf of Panama from January, 1982 through January, 1984 (from the Smithsonian Tropical Research Institute, Balboa, Panama; Dr. Jeremy Jackson, personal communication).

SEA SURFACE TEMPERATURE

Gulf of Panama

January 1982-January 1984

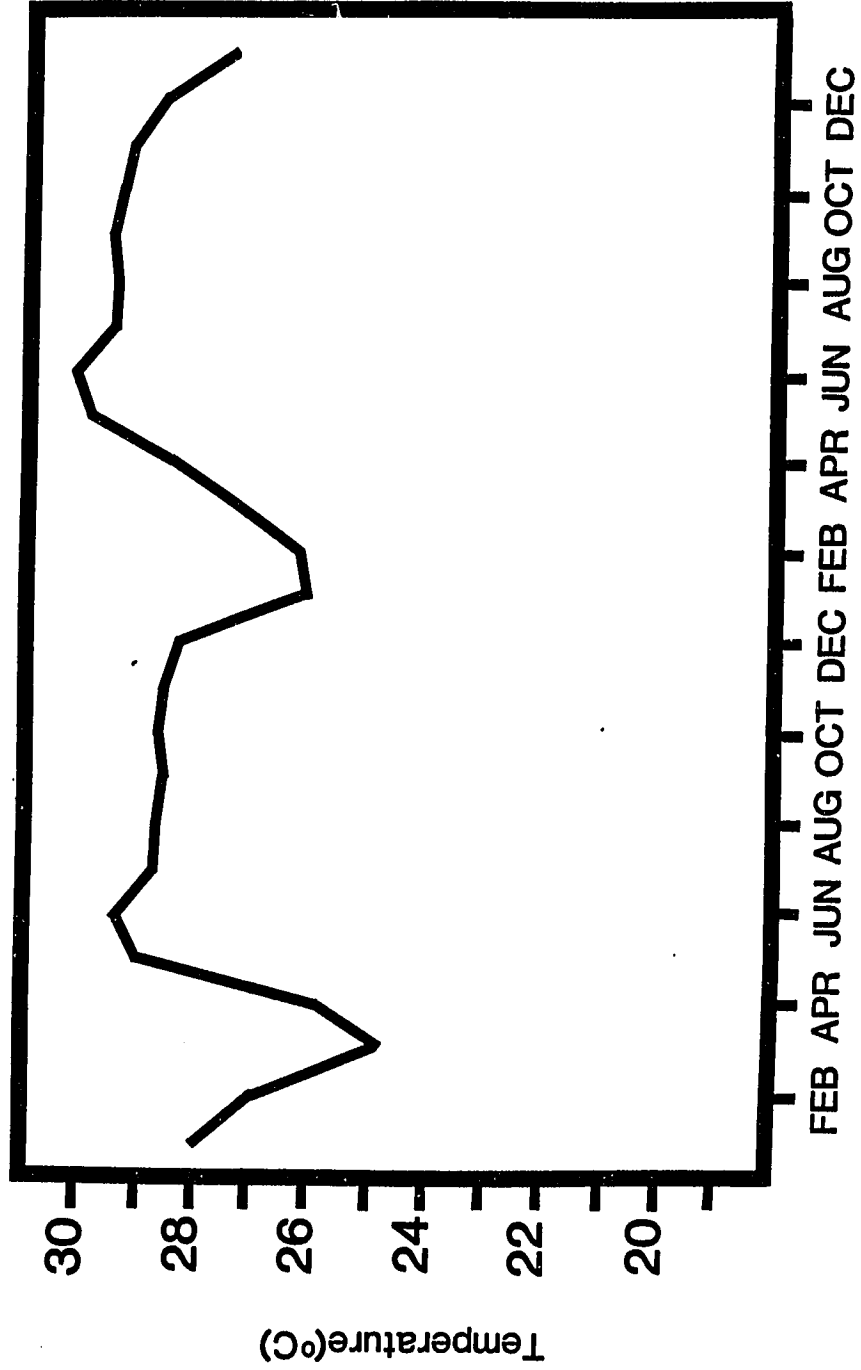


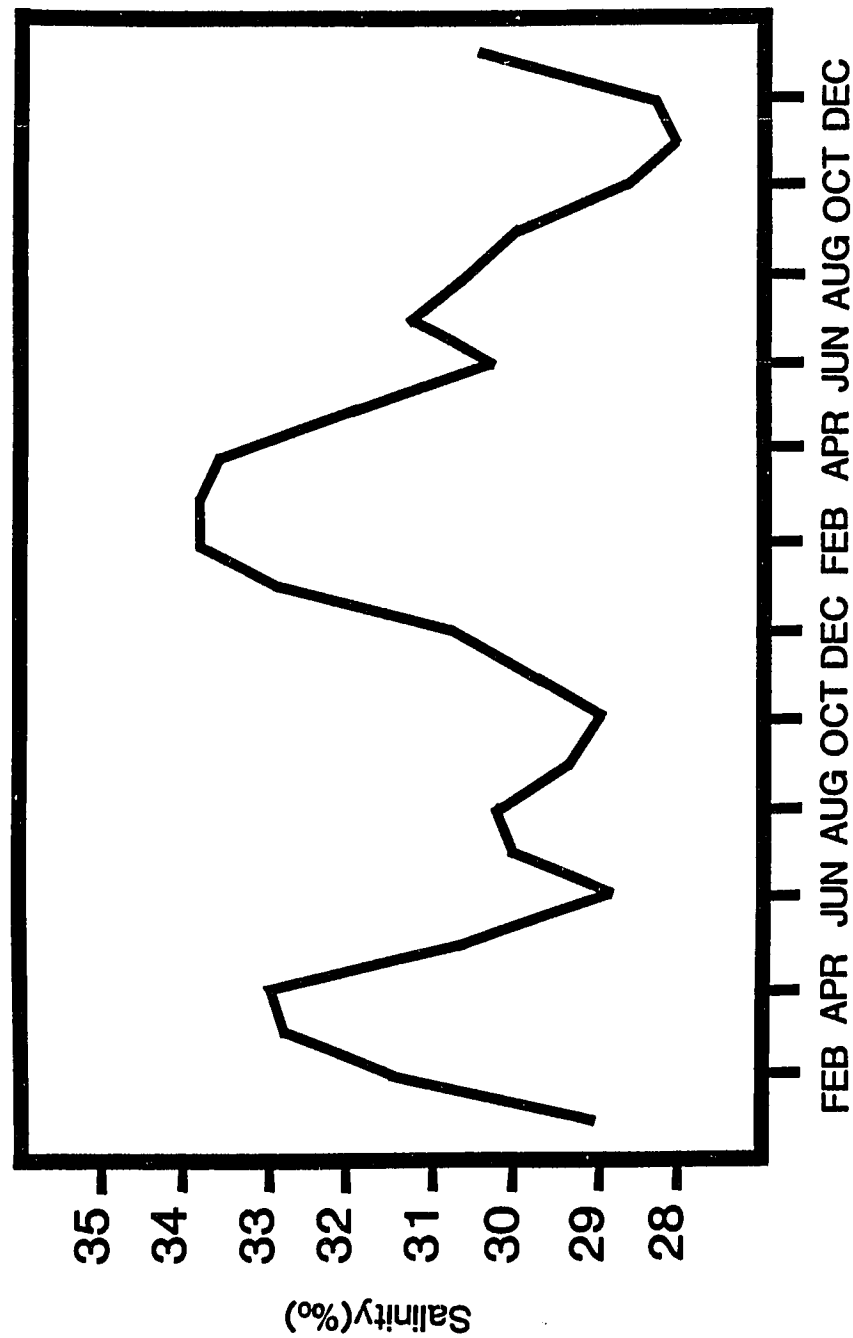
Figure 12:

Seasonal sea surface salinity variations (‰) in the Gulf of Panama from January, 1982 through January, 1984 (from the Smithsonian Tropical Institute, Balboa, Panama; Dr. Jeremy Jackson, personal communication).

SEA SURFACE SALINITY

Gulf of Panama

January 1982-January 1984



1972-1973 (Wooster and Guillen, 1974) at which time water temperatures exceeded 28°C in the eastern tropical Pacific (Firing *et al.*, 1983; Philander, 1983; Wooster and Guillen, 1974).

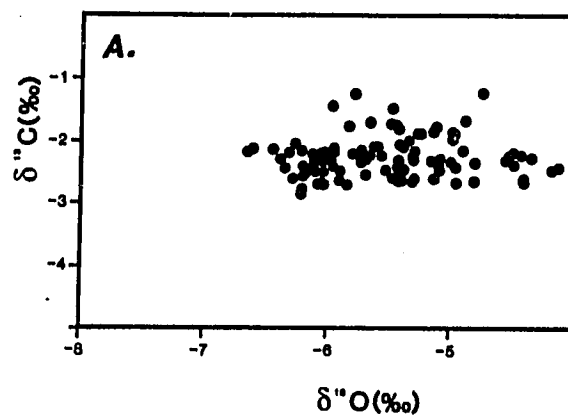
Interpretation of $\delta^{13}\text{C}$

Skeletal $\delta^{18}\text{O}$ and $\delta^{13}\text{C}$ data are compared to each other and certain environmental parameters to determine whether variations in these stable isotopes accurately monitor variations in water temperature, salinity, and light intensity. Quantitative comparison of variations in skeletal $\delta^{18}\text{O}$ and $\delta^{13}\text{C}$ in the SOUTH SHORE CONTADORA sample shows that no correlation exists between $\delta^{18}\text{O}$ and $\delta^{13}\text{C}$ ($r = 0.101$, $p = 0.37$) (Figure 13a). Large seasonal variations in $\delta^{13}\text{C}$ were not present in the SOUTH SHORE CONTADORA and CONTADORA 9 samples (Figures 9 and 10) possibly due to only minor seasonal variations in light intensity. Increased turbidity associated with upwelling in the dry season and increased cloud cover in the wet season reduce seasonal variations in light intensity on the reef. Variation in the URABA $\delta^{13}\text{C}$ data shows a more pronounced seasonality and lags behind seasonal variations in $\delta^{18}\text{O}$. Variations in skeletal $\delta^{18}\text{O}$ are plotted against variations in skeletal $\delta^{13}\text{C}$ (Figure 13b). The correlation is significant and positive ($r = 0.128$, $p = 0.05$). Eliminating the slight lag between $\delta^{18}\text{O}$ and $\delta^{13}\text{C}$ yields a better correlation ($r = 0.366$) (Figure 13c). The skeletal $\delta^{13}\text{C}$ data of this coral sample support the model proposed by Fairbanks and Dodge (1979) and Weber *et al.* (1975) using variations in light intensity to explain observed skeletal $\delta^{13}\text{C}$ variations, that is, lower skeletal $^{13}\text{C}/^{12}\text{C}$ ratios result from decreased light intensity. This implies that when water temperatures are high ($^{18}\text{O}/^{16}\text{O}$ ratios are low), cloud cover is high ($^{13}\text{C}/^{12}\text{C}$ ratios are low). Water temperature and cloud cover data support this observation (Figure 3).

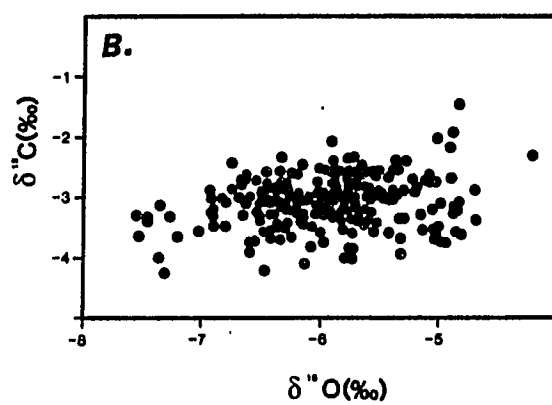
Figure 13:

(a) Relationship between skeletal $\delta^{18}\text{O}$ and $\delta^{13}\text{C}$ for the SOUTH SHORE CONTADORA sample data. Correlation coefficients and probabilities calculated using Pearson Product-Moment Correlation . $R = 0.101$; $N = 80$; $p = 0.37$; (b) relationship between skeletal $\delta^{18}\text{O}$ and $\delta^{13}\text{C}$ for URABA sample, $r = 0.128$, $N = 240$, $p = 0.05$; (c) same as (b) except that skeletal $\delta^{18}\text{O}$ values have been shifted 0.15 cm along the maximum vertical growth axis with respect to skeletal $\delta^{13}\text{C}$ values, $r = 0.366$, $N = 238$.

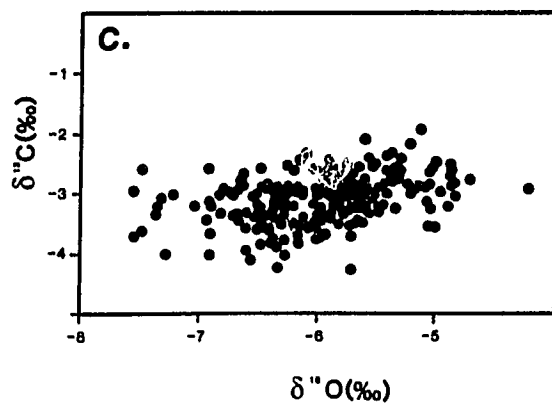
SOUTH SHORE CONTADORA



URABA



URABA



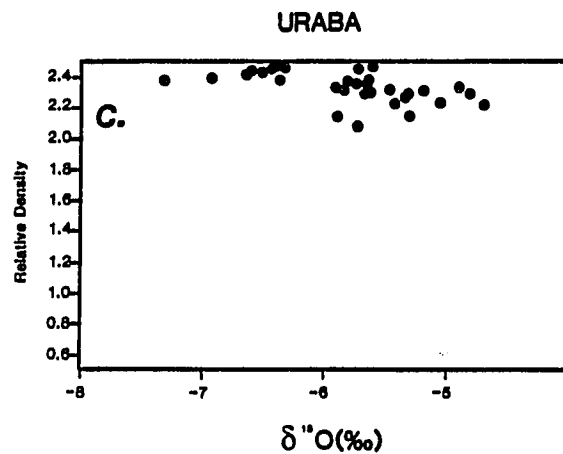
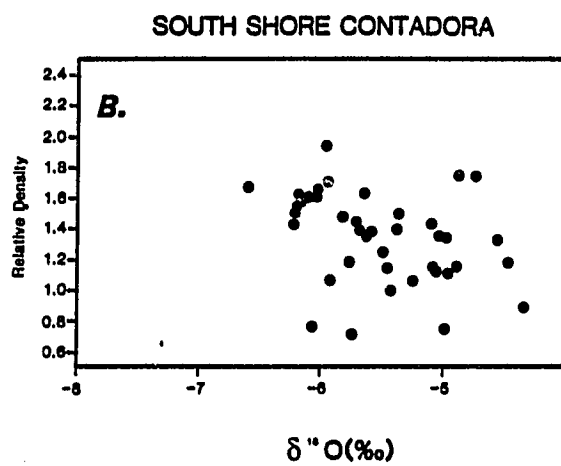
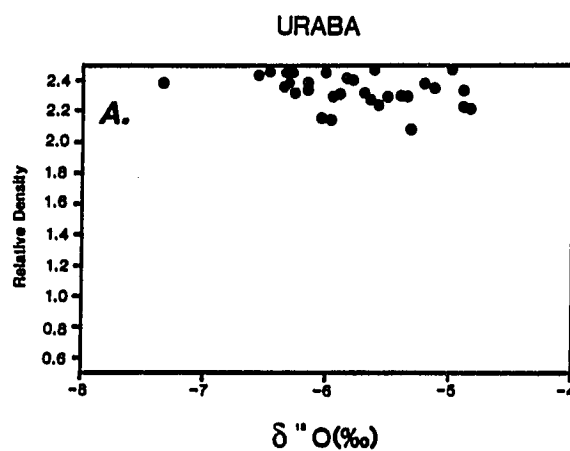
Comparison of coral stable isotopes with observed variations in water temperature, salinity, and cloud cover in the Gulf of Panama indicate that $\delta^{18}\text{O}$ and $\delta^{13}\text{C}$ accurately record seasonal changes in these environmental parameters. The timing and magnitude of variations in skeletal $\delta^{18}\text{O}$ correlate well with observed variations in water and salinity, while $\delta^{13}\text{C}$ may be a useful indicator of the degree to which light intensity varies seasonally on the reef.

Correlation of Stable Isotopes with Density Banding

Stable isotopes are correlated with density banding to test the model put forth by Wellington and Glynn (1983) for coral density band development. The shaded areas in Figures 8 through 10 represent regions of high relative skeletal density. Generally, high relative skeletal density correspond to low skeletal $^{18}\text{O}/^{16}\text{O}$ ratios in these samples. Quantitative correlation between relative skeletal density and $\delta^{18}\text{O}$ in the URABA and SOUTH SHORE CONTADORA samples are significant and negative ($r = -0.332$, $p = 0.05$ for URABA; $r = -0.512$, $p = 0.0019$ for SOUTH SHORE CONTADORA) (Figures 14a and 14b). However, the correlation was not perfect. The number of $\delta^{18}\text{O}$ "peaks" do not equal the number of high density bands in the CONTADORA 9 and SOUTH SHORE CONTADORA samples (Figures 9 and 10). The thickness of the CONTADORA 9 and SOUTH SHORE CONTADORA sample slabs were slightly greater than one polyp diameter (2-3 mm). Skeletal density variations, therefore, are on a smaller scale than the seasonal variations in the environmental parameters which influence skeletal $\delta^{18}\text{O}$ and $\delta^{13}\text{C}$, making a strict correlation difficult. The thickness of the URABA sample slab, however, was roughly twice the polyp diameter, yielding larger scale variations in skeletal density which is supported by the excellent correlation between the number of "high" density bands and $\delta^{18}\text{O}$ "peaks". However, many $\delta^{18}\text{O}$ "peaks" exhibit slight leads and lags with

Figure 14:

(a) Relationship between skeletal $\delta^{18}\text{O}$ and relative skeletal density for the URABA sample. Correlation coefficients and probabilities calculated using the Pearson Product-Moment Correlation, $R = -0.322$; $N = 32$; $p = 0.06$; (b) relationship between skeletal $\delta^{18}\text{O}$ and relative skeletal density for the SOUTH SHORE CONTADORA sample, $r = 0.512$, $N = 40$, $p = 0.0019$; (c) same as (a) except that skeletal $\delta^{18}\text{O}$ values have been shifted 0.10 cm along the maximum vertical growth axis with respect to relative skeletal density values, $r = -0.561$, $N = 32$, $p = 0.008$.



respect to the high density banding. In the URABA sample, a better correlation ($r = -0.561$, $p = 0.008$) was achieved when skeletal $\delta^{18}\text{O}$ values were shifted 0.15 cm along the maximum vertical growth axis with respect to relative skeletal density values, indicating a slight lag between skeletal density and $\delta^{18}\text{O}$ (Figure 14c). Quantitative correlation of skeletal $\delta^{13}\text{C}$ and relative skeletal density for the SOUTH SHORE CONTADORA sample (Figure 15a) shows a slight positive correlation ($r = 0.206$, $p = 0.241$). Correlation of skeletal $\delta^{13}\text{C}$ with relative skeletal density data of the URABA sample shows a negative relationship ($r = -0.349$, $p = 0.05$; Figure 15b). This implies that light levels are low (decreased $^{13}\text{C}/^{12}\text{C}$ ratios) during the formation of high density bands. During the formation of high density bands in the Gulf of Panama, light levels are, in fact, reduced due to increased cloud cover.

Comparison of skeletal $\delta^{18}\text{O}$ and $\delta^{13}\text{C}$ values with relative skeletal densities indicates that larger scale variations in skeletal density exhibited, for example, by the URABA sample, correlate well with variations in skeletal $\delta^{18}\text{O}$ and $\delta^{13}\text{C}$. However, statistical comparison of skeletal stable isotopes with relative skeletal density shows that a slightly better correlation exists between skeletal density and $\delta^{13}\text{C}$ than skeletal density and $\delta^{18}\text{O}$ in the URABA sample.

Gulf of Chiriqui

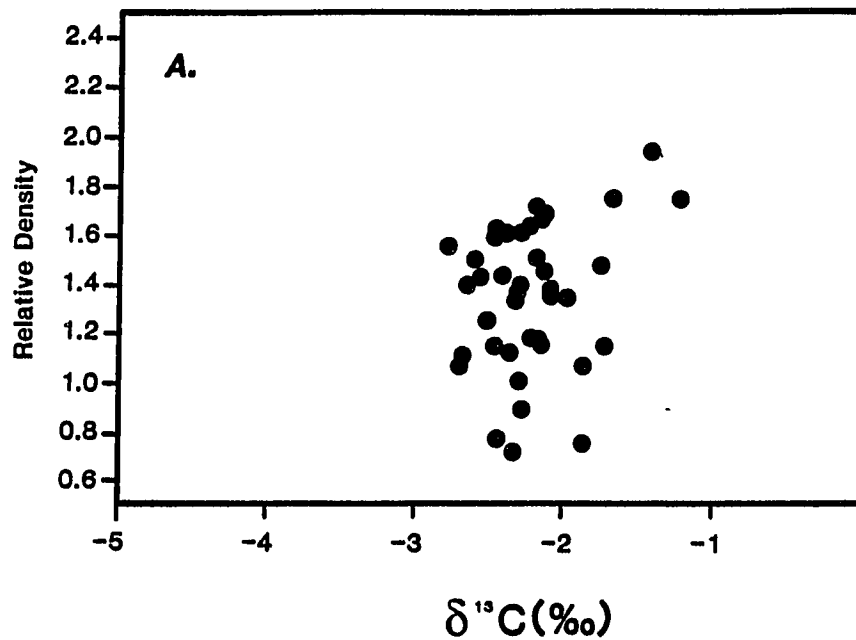
Interpretation of $\delta^{18}\text{O}$

Seasonal variations in skeletal $\delta^{18}\text{O}$ of the Gulf of Chiriqui samples are approximately 1‰ (Figures 16 through 18). Seasonal variations in water temperature are on the order of 4°C (Figure 3). The degree to which salinity affects skeletal $\delta^{18}\text{O}$ in the Gulf of Chiriqui has not been quantified, however, large salinity variations are not required to explain the observed isotope data.

Figure 15:

(a) Relationship between skeletal $\delta^{13}\text{C}$ and relative skeletal density for SOUTH SHORE CONTADORA sample. Correlation coefficients and probabilities calculated using the Pearson Product-Moment Correlation, $R = 0.206$; $N = 40$; $p = 0.241$; (b) relationship between skeletal $\delta^{13}\text{C}$ and relative skeletal density for the URABA sample, $r = -0.349$, $N = 32$, $p = 0.05$.

SOUTH SHORE CONTADORA



URABA

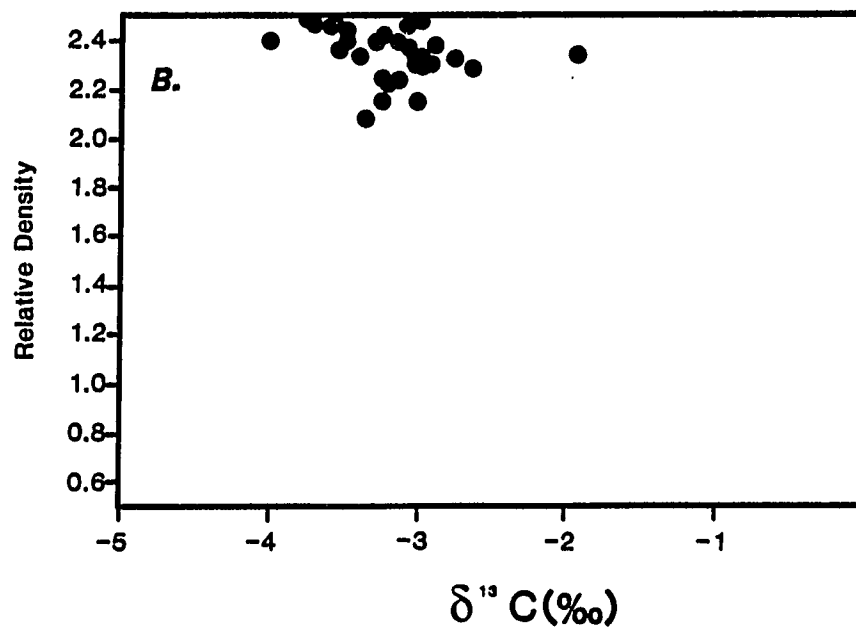


Figure 16:

Seasonal variations in coral relative skeletal density and stable isotope ratios. The shaded areas represent regions of high relative skeletal densities based on visual inspection of the coral X-radiograph. The influence of salinity, water temperature, and light intensity on skeletal stable isotopes is indicated. The sample is Pavona clavus, collected by G. Wellington from Uva Island, Gulf of Chiriqui, November, 1979.

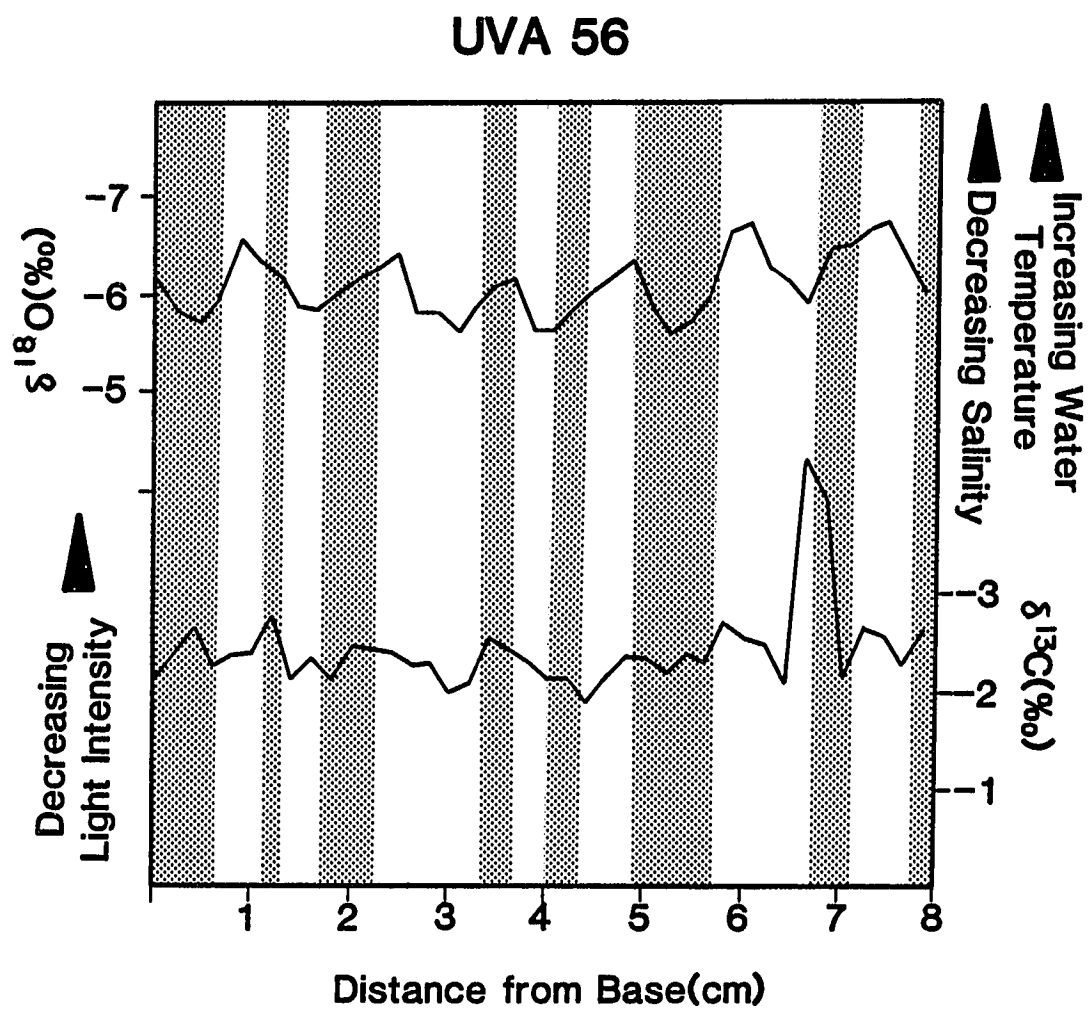


Figure 17:

Seasonal variations in coral relative skeletal density and stable isotope ratios. The shaded areas represent regions of high relative skeletal densities. The influence of water temperature, salinity, and light intensity on skeletal stable isotopes is indicated. The sample is Pavona clavus, collected from Uva Island, Gulf of Chiriqui, June, 1983.

UVA 1

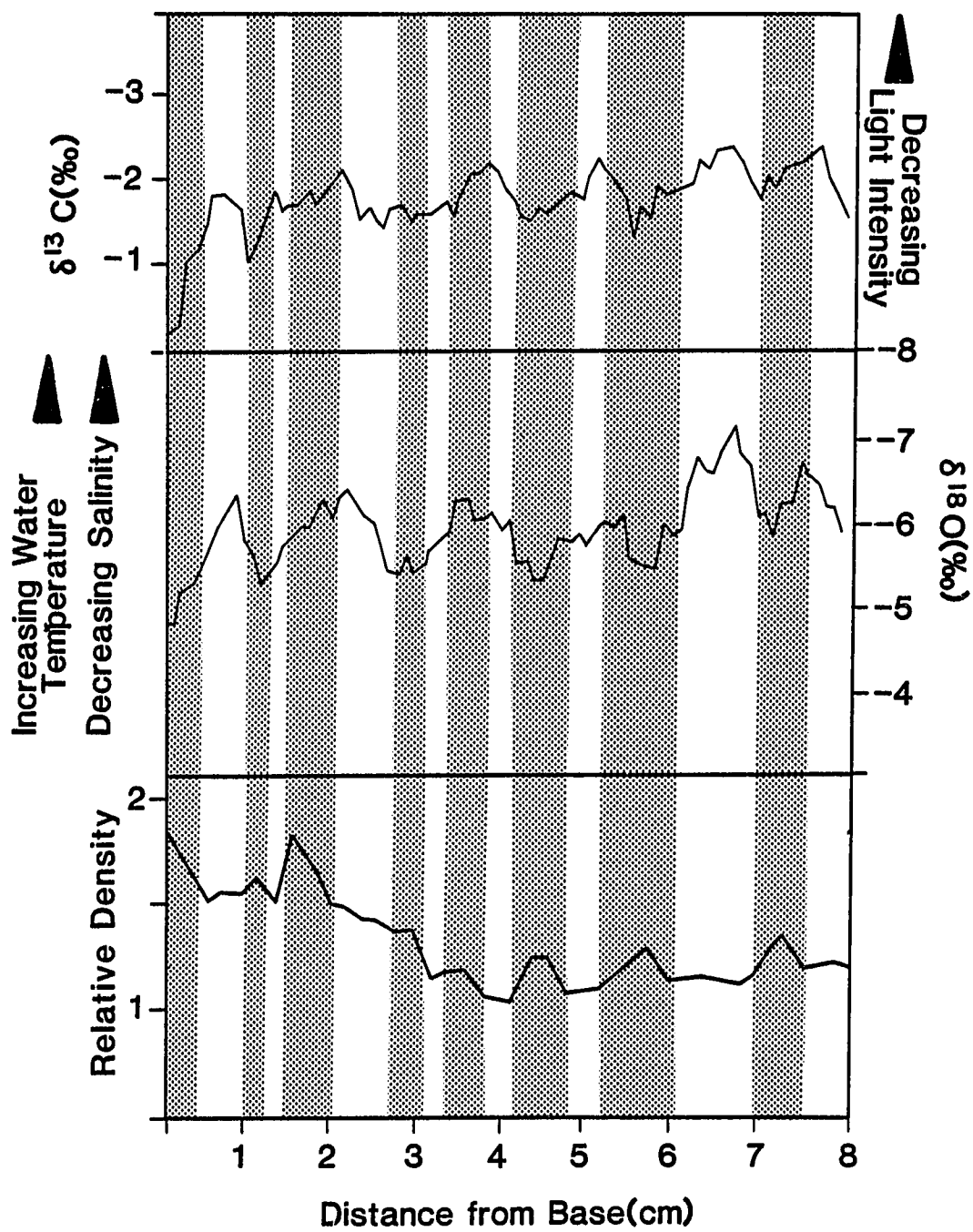
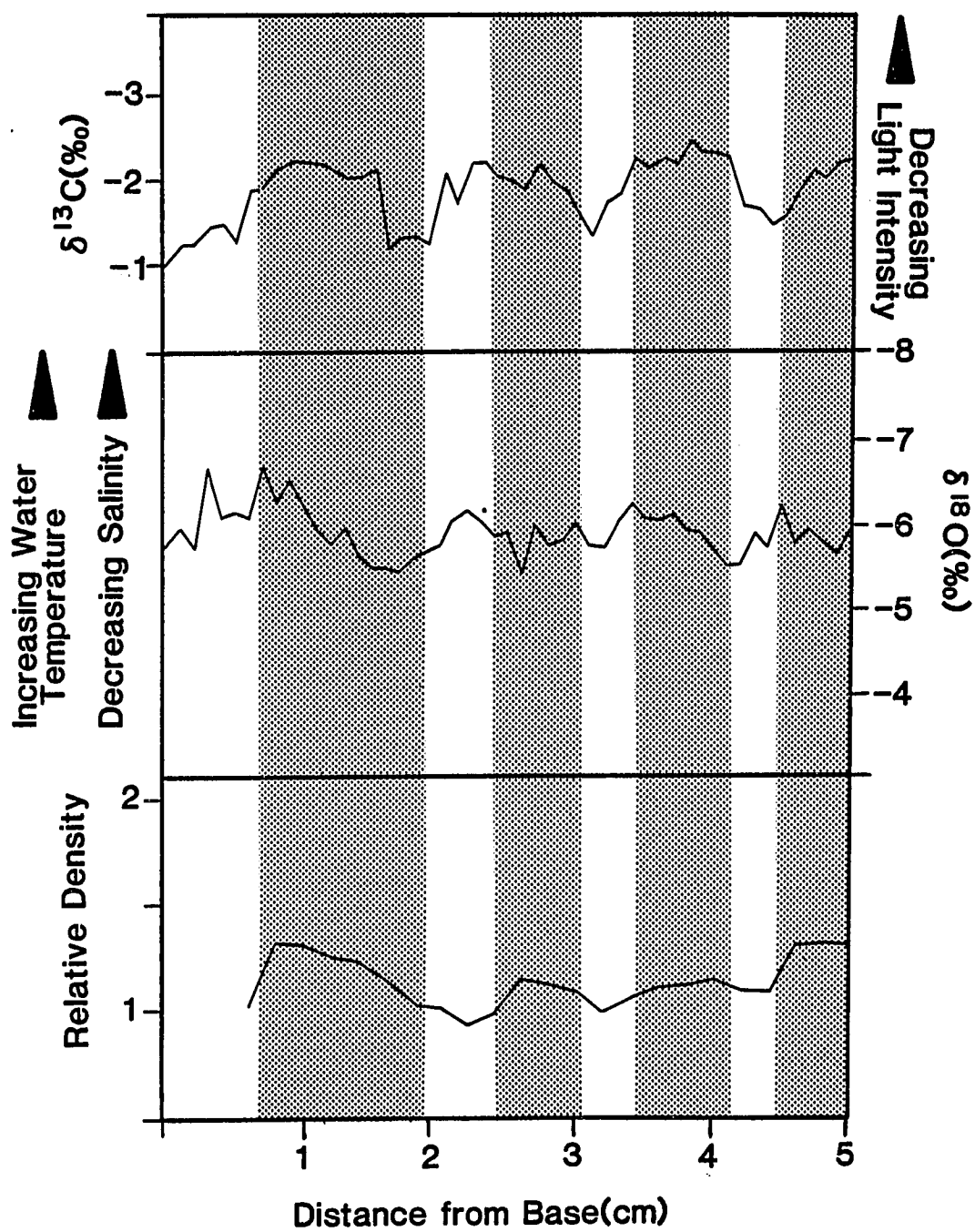


Figure 18:

Seasonal variations in coral relative skeletal density and stable isotope ratios. The shaded areas represent regions of high relative skeletal densities. The influence of water temperature, salinity, and light intensity on skeletal stable isotopes is indicated. The sample is Pavona clavus, collected from the Secas Islands, Gulf of Chiriqui, June, 1983.

SECAS 1



Seasonal variations in skeletal $\delta^{18}\text{O}$ are more pronounced in the UVA 1 and UVA 56 samples (Figures 16 and 17) than in the SECAS 1 sample (Figure 18). The reason for this is unknown. Skeletal $^{18}\text{O}/^{16}\text{O}$ ratios of the UVA 56 and UVA 1 samples (Figures 16 and 17) are relatively high at the time the samples were collected, implying that water temperatures were at a seasonal low. Water temperature data for the Gulf of Chiriqui (Figure 3) show that water temperatures are relatively low from June through November.

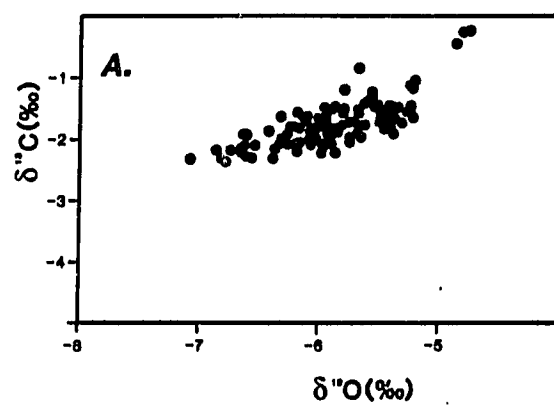
Interpretation of $\delta^{13}\text{C}$

Generally, seasonal variations in skeletal $\delta^{13}\text{C}$ values for the Gulf of Chiriqui corals are more pronounced than those for the Gulf of Panama samples presumably due to greater seasonal variation in light intensity in the Gulf of Chiriqui. Quantitative correlation of skeletal $\delta^{18}\text{O}$ and $\delta^{13}\text{C}$ data for UVA 1 show that there is a significant and positive correlation ($r = 0.76$, $p = 0.001$), implying that water temperatures are high during periods of low light intensity (Figure 19a). Water temperature and cloud cover data show that during periods of increased cloud cover (wet season), water temperatures are at a seasonal low (Figure 3), which would result in a negative correlation between $\delta^{13}\text{C}$ and $\delta^{18}\text{O}$. However, periods of increased and decreased salinity would account for the observed positive correlation. Previous studies (Glynn, 1977) have shown that seasonal salinity variations in the Gulf of Chiriqui are approximately 6‰, which are comparable to those in the Gulf of Panama. A 6‰ variation in salinity would correspond to a 0.75‰ variation in skeletal $\delta^{18}\text{O}$, following the relationship between salinity and $\delta^{18}\text{O}$ established by Dunbar and Wellington (1981). The observed variation in skeletal $\delta^{18}\text{O}$, however, is approximately 1‰. Water temperature and salinity variations act in opposition, that is, water temperatures are low when salinity values are low,

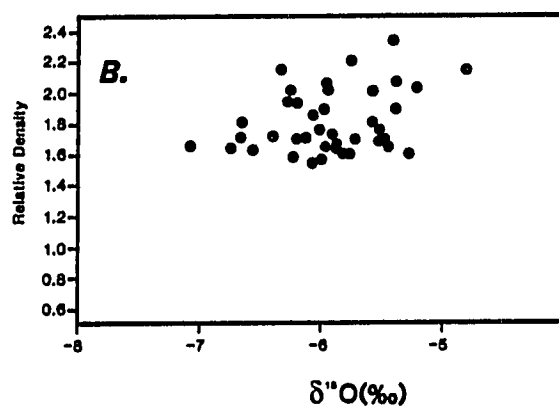
Figure 19:

(a) Relationship between skeletal $\delta^{18}\text{O}$ and $\delta^{13}\text{C}$ data from UVA 1 sample. Correlation coefficients and probabilities calculated using the Pearson Product-Moment Correlation. $R = 0.760$; $N = 80$; $p = 0.001$; (b) relationship between skeletal $\delta^{18}\text{O}$ and relative skeletal density for the UVA 1 sample, $r = 0.305$, $N = 40$, $p = 0.05$; (c) relationship between skeletal $\delta^{13}\text{C}$ and relative skeletal density for the UVA 1 sample, $r = 0.434$, $N = 40$, $p = 0.0005$.

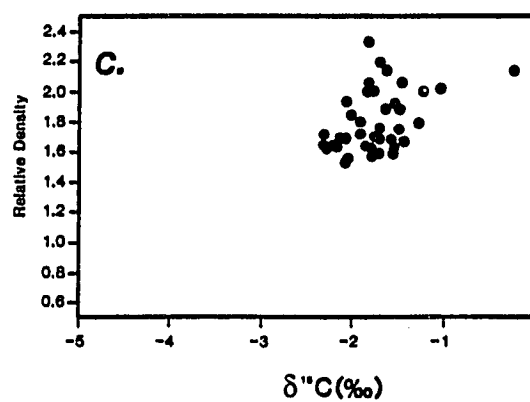
UVA 1



UVA 1



UVA 1



even further reducing the effect of salinity on skeletal $\delta^{18}\text{O}$. More detailed measurements of salinity, light intensity, and water temperature variations in the Gulf of Chiriqui are required before an empirical relationship between stable isotopes and these environmental parameters can be determined.

Correlation of Stable Isotopes with Density Banding

Shaded areas in Figures 16 through 18 represent regions of high relative skeletal density. Skeletal $^{18}\text{O}/^{16}\text{O}$ and $^{13}\text{C}/^{12}\text{C}$ ratios of the UVA 1 sample correlate positively ($r = 0.305$, $p = 0.05$ for ^{18}O ; $r = 0.433$, $p = 0.005$ for ^{13}C) with relative skeletal densities (Figures 19b and 19c), implying that high density bands form during periods of increased light intensity and either increased salinity or decreased water temperature. High density bands form during the wet season in the Gulf of Chiriqui when salinity, light levels, and water temperatures are seasonally low. However, at the time the UVA 1 sample was collected (June, 1983), skeletal densities should have been increasing. Relative skeletal density appears to be relatively low at the top of the coral, however. A possible explanation may be that coral growth ceased at some time prior to sampling as a result of the El Niño which affected this region in early 1983. The poor correlation between the number of "high" density bands and $\delta^{18}\text{O}$ "peaks" is the result of comparison of small scale skeletal density variations and larger scale variations in skeletal stable isotopes and the environmental parameters they monitor.

Azuero Peninsula

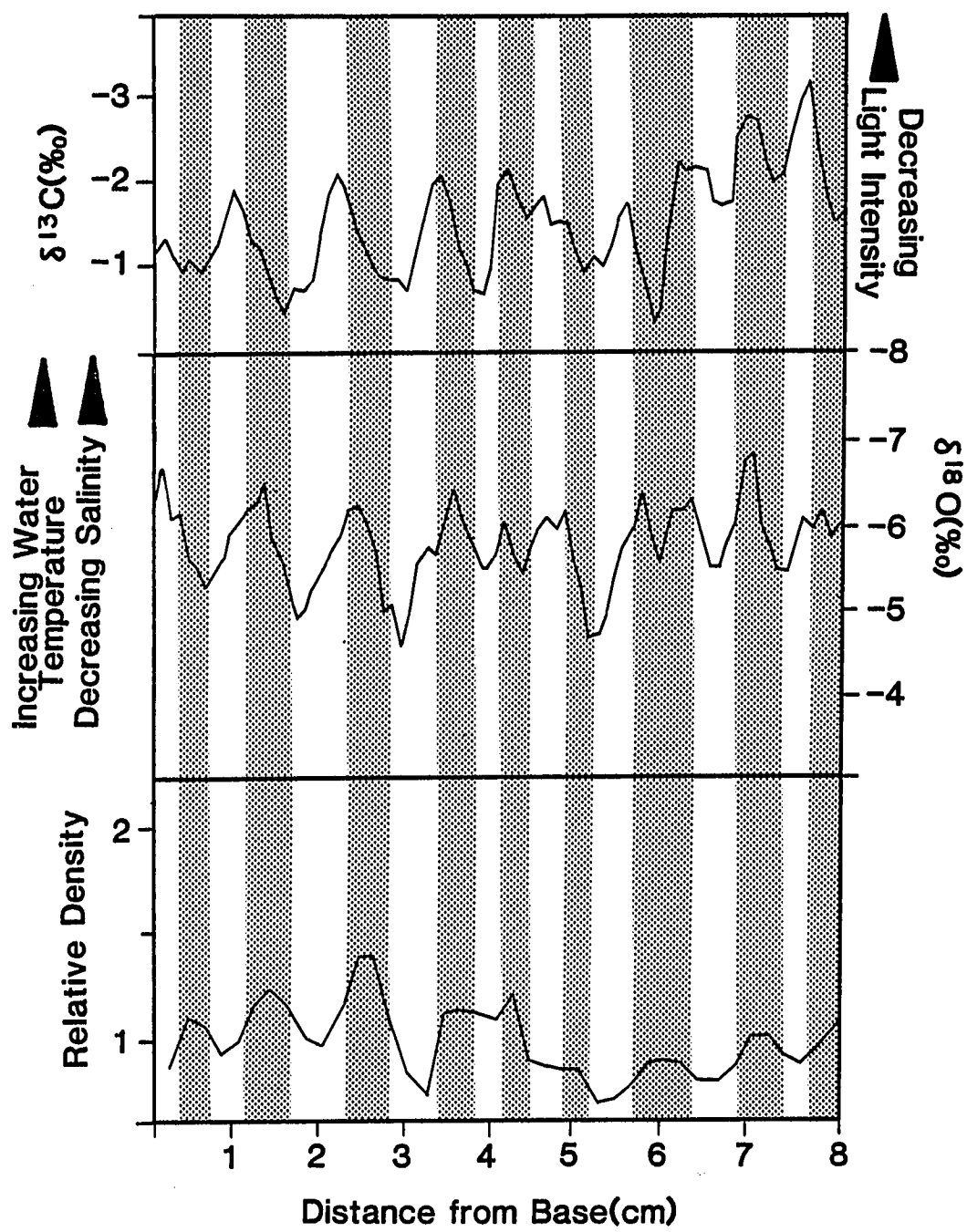
Interpretation of $\delta^{18}\text{O}$

The AZUERO sample (Figure 20) was collected from within the thermal boundary zone off the Azuero Peninsula (Figure 2). The thermal boundary zone

Figure 20:

Seasonal variations in coral relative skeletal density and stable isotope ratios. The shaded areas represent regions of high relative skeletal densities. The influence of water temperature, salinity, and light intensity on skeletal stable isotopes is indicated. The sample is Pavona gigantea, collected from the Thermal Boundary Zone, Azuero Peninsula, June, 1983.

AZUERO



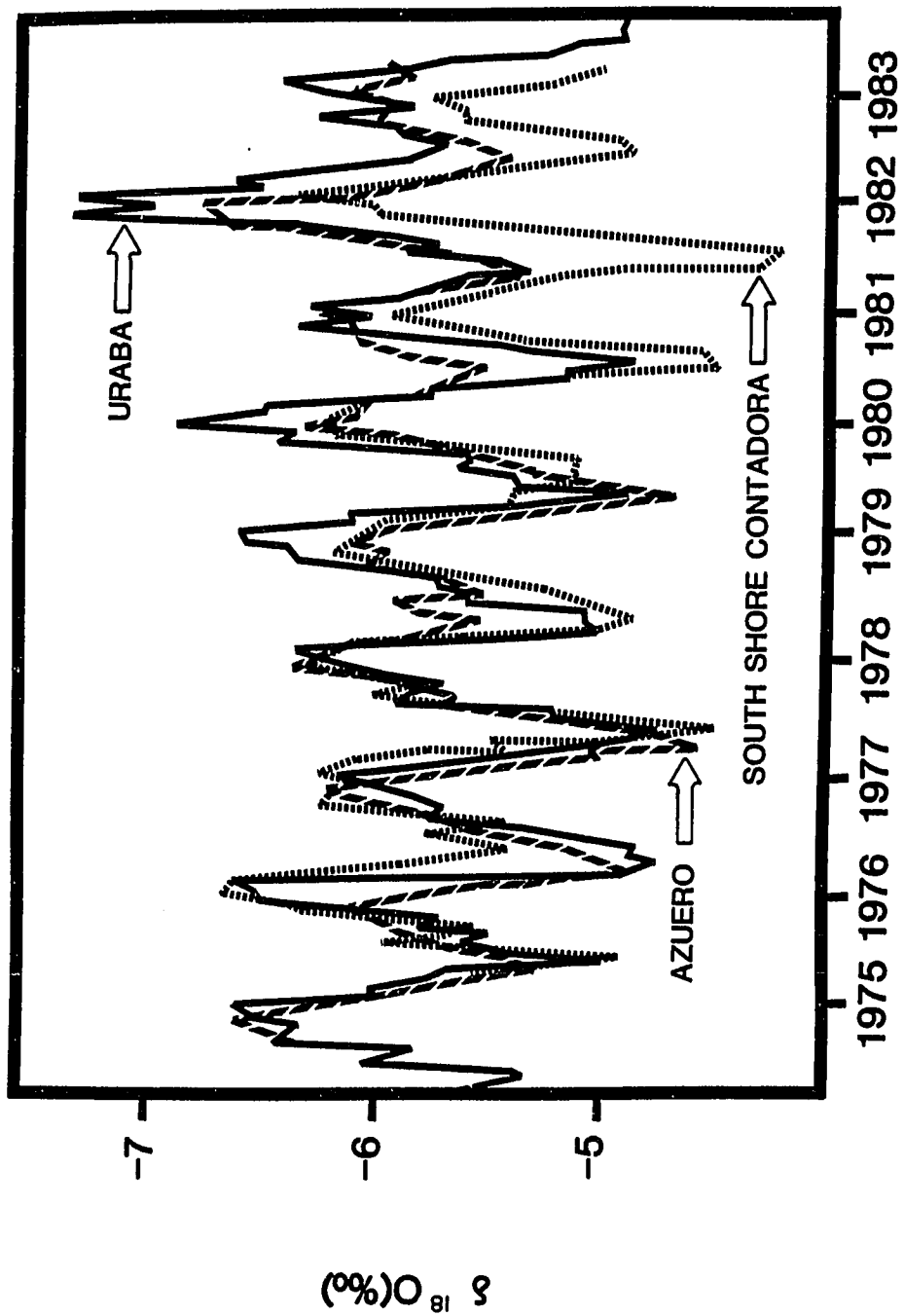
represents the transition between upwelling and non-upwelling conditions. The magnitude of seasonal $\delta^{18}\text{O}$ variations is approximately 1.5‰, roughly comparable to those of the Gulf of Panama data. Water temperature and salinity data are not currently available for this region. The degree to which salinity and water temperature influence skeletal $\delta^{18}\text{O}$ have, therefore, not been quantified. Skeletal $^{18}\text{O}/^{16}\text{O}$ ratios are relatively low at the top of the coral implying that water temperatures were high at the time the sample was collected. The AZUERO sample was collected in June, 1983, at which time upwelling had ceased and the thermal gradient which characterizes this region had disappeared.

Interpretation of $\delta^{13}\text{C}$

Skeletal $\delta^{13}\text{C}$ variations are more pronounced than in either the Gulf of Panama or Gulf of Chiriqui data implying an even greater seasonal variation in light intensity. Cloud cover data is not currently available for this region, however. Generally, skeletal $\delta^{13}\text{C}$ variations are in phase with skeletal $\delta^{18}\text{O}$, implying that periods of decreased light intensity correspond to periods of increased water temperatures and/or decreased salinity. Environmental conditions in the thermal boundary zone, therefore, appear to be similar to those found in the Gulf of Panama. This is supported by evidence presented in Figure 21, where the $\delta^{18}\text{O}$ profile of the AZUERO coral has been superimposed on specimens of Pavona gigantea from the Gulf of Panama. The stable isotope profiles of these three corals show the same relative changes in the magnitude of the $\delta^{18}\text{O}$ signals. Offsets in the $\delta^{18}\text{O}$ data result from varying degrees of influence of water temperature (upwelling) and salinity (freshwater input). The URABA sample was collected from Uraba Island, located at the Pacific entrance to the freshwater Panama Canal (Figure 2). The lower overall skeletal

Figure 21:

Superimposed stable oxygen isotope profiles of three Gulf of Panama corals (Pavona gigantea), adjusted for differences in growth rates. Note the similarity in magnitude of the $\delta^{18}\text{O}$ profile variations, particularly during 1982-1983.



Tropical Wet Seasons

$^{18}\text{O}/^{16}\text{O}$ ratios of this sample reflect the influence of sea surface salinity variations, which are probably greater than those at locations further offshore. The SOUTH SHORE CONTADORA sample was collected from the Perlas Islands, located 18 km from the Panamanian coast. Decreased water temperatures associated with seasonal upwelling in the Gulf of Panama result in the higher skeletal $^{18}\text{O}/^{16}\text{O}$ ratios of the SOUTH SHORE CONTADORA sample. Although salinity variations occur as well, they represent approximately 30% of the observed variation in skeletal $\delta^{18}\text{O}$ in the Gulf of Panama (Dunbar and Wellington, 1981).

Correlation of Stable Isotopes with Density Banding

The shaded areas in Figure 20 represent regions of high relative skeletal density. Generally, high skeletal $^{18}\text{O}/^{16}\text{O}$ and $^{13}\text{C}/^{12}\text{C}$ ratios correspond to high relative skeletal densities, implying that high density bands form during the wet season when water temperature and cloud cover are high and salinity is low. Discrepancies in the correlation between skeletal stable isotopes and density band patterns is attributed to differences in the scales of the stable isotope and skeletal density variations.

CONCLUSIONS

Seasonal variations in skeletal density, $\delta^{18}\text{O}_{\text{PDB}}$, and $\delta^{13}\text{C}_{\text{PDB}}$ of Pavona clavus and P. gigantea, collected from the Gulf of Panama and the Gulf of Chiriqui, correlate well with observed seasonal climatic variations. Comparison of coral relative skeletal densities, $^{18}\text{O}/^{16}\text{O}$ ratios, and $^{13}\text{C}/^{12}\text{C}$ ratios for the Gulf of Panama and Gulf of Chiriqui samples, implies that a close correlation exists between density "banding" and stable isotope variations but that

subannual banding is often present. However, discrepancies in the correlation of stable isotopes with density band patterns is probably the result of differences in the magnitude of the scales of stable isotopes and skeletal density variations. Reproductive status may be an alternative factor influencing density band patterns. Reproduction in pavonid corals occurs during the formation of high density bands when energy normally used for tissue growth and linear extension may be reallocated to reproduction (Wellington and Glynn, 1983).

Anomalous conditions associated with El Niño have been documented in the Galapagos Islands, Ecuador and off the coast of Peru. Although the Gulf of Panama salinity and tidal data appeared normal during the 1982-1983 El Niño, high water temperatures were recorded (Figure 11). However, the manifestation of the 1982-1983 El Niño, and other El Niños, is not obvious in the coral stable isotope records. Interpretation of the coral stable isotopes, therefore, is more complex than originally thought. Coral metabolism may slow down during El Niño events to the point where CaCO_3 accretion ceases. In this event, there would be a hiatus in both the $\delta^{18}\text{O}$ and skeletal density band records.

Paleoclimatological studies using variations in coral stable isotope ratios combined with sclerochronology could yield valuable information regarding changing circulation in the eastern tropical Pacific through time. Coral cores are available from these regions dating back approximately 250 years, providing paleoclimatological data as far back as the Little Ice Age (150-400 years B.P.) and the onset of upwelling in the Gulf of Panama.

REFERENCES

- Baker, P.A. and Weber J.N.(1975) Coral growth rate: variation with depth, *Earth Plan. Sci. Lett.*, v. 27, 57-61.
- Buddemeier, R.W. (1974) Environmental controls over annual and lunar monthly cycles in hermatypic coral calcification, *Proc. 2nd Int. Symp. Coral Reefs, Australia*, v. 2, 259-267.
- Buddemeier, R.W. and Kinzie R.A. (1974) The chronometric reliability of contemporary corals. Paper presented at Interdisc. Winter Conference on Biological Clocks and changes in earth's rotation. Newcastle upon Tyne, Jan 8-10.
- Buddemeier, R.W., Maragos J.E., and Knutson D.K.(1974) Radiographic studies of reef coral exoskeleton: rates and patterns of growth, *J. Exp. Marine Biol. Ecol.*, v. 14, 197-200.
- Craig, H. and Gordon L. (1965) Deuterium and $\delta^{18}\text{O}$ variations in the ocean and marine atmosphere. In: *Symposium on marine geochemistry: Graduate of School of Oceanogr., University of Rhode Island, Occ. Publ.*, v. 3, 277-374.
- Dodge, R.E., Aller R.C., and Thompson J.(1974) Coral growth related to resuspension of bottom sediments, *Nature*, v. 247, 574-577.
- Dunbar, R.B. (1981) Sedimentation and the history of upwelling and climate in high fertility areas of the northeast Pacific Ocean, PhD dissertation, University of Southern California, San Diego, CA.
- Dunbar, R.B. and Wellington G.M. (1981) Stable isotopes in a branching coral monitor seasonal temperature variation , *Nature*, v. 293, no. 5832, 453-455.
- Emiliani,C. (1966) Paleotemperature analysis of Caribbean cores P6304-9 and a generalized temperature curve for the past 450,000 years, *J. Geol.*, v. 74, 109-126.
- Emiliani, C., Hudson J.H., Shinn E.A., and George R.Y. (1978) Oxygen and carbon isotopic growth record in a reef coral from the Florida Keys and a deep-sea coral from Blake Plateau, *Science*, v. 202, 627-629.
- Emrich, K., Enhalt D.H., and Vogel J.C.(1970) Carbon isotope fractionation during the precipitation of CaCO_3 , *Earth Plan, Sci. Lett.*, v. 8, 363-371.
- Epstein, S., Buchsbaum R., Lowenstam H., and Urey H.C. (1953) Revised carbonate-water isotopic temperature scale, *Bull. Geol. Soc. Am.*, v. 64, 1315-1326.
- Epstein, S. and Mayeda T.K. (1953) Variations of the $^{18}\text{O}/^{16}\text{O}$ ratio in natural waters, *Geochim. Cosmochim. Acta*, v. 4, 213-224.
- Erez, J. (1978) Vital effect on stable-isotope composition seen in foraminifera and coral skeletons, *Nature*, v. 273, 199-202.

- Fairbanks, R.G. and Dodge R.E. (1979) Annual periodicity of the $^{18}\text{O}/^{16}\text{O}$ and $^{13}\text{C}/^{12}\text{C}$ ratios in the coral Montastrea annularis, *Geochim. Cosmochim. Acta*, v. 43, 1009-1020.
- Firing E., Lukas R., Sadler J., and Wyrtki K. (1983) Equatorial Undercurrent disappears during 1982-1983 El Niño, *Science*, v. 222, 1121-1123.
- Glynn, P.W. (1983) Extensive 'bleaching' and death of reef corals on the Pacific coast of Panama, *Env. Cons.*, v. 10(2), 149-154.
- Glynn, P.W. (1977) Coral growth in upwelling and non-upwelling areas off the Pacific coast of Panama, *J.M.R.*, v. 35(3), 567-585.
- Glynn, P.W. (1974) The importance of Acanthaster on corals and coral reefs in the eastern tropical Pacific, *Env. Cons.*, v. 1(4), 295-303.
- Glynn, P.W., Druffel E., and Dunbar R.B. (1983) A dead Central American coral reef tract: Possible link with the Little Ice Age, *J. Mar. Res.*, v. 41, 605-637.
- Glynn, P.W. and Macintyre I. (1977) Growth rate and age of coral reefs on the Pacific coast of Panama, *Proc. 3rd Int. Coral Reef Sympos. 2*, RSMAS, Miami, U.S.A., 251-260.
- Glynn, P.W., and Stewart (1973) Distribution of coral reefs in the Pearl Islands (Gulf of Panama) in relation to thermal conditions, *Limnol. Oc.*, v. 18(3), 367-379.
- Goreau, T.J. (1977) Coral skeletal chemistry: physiological and environmental regulation of stable isotopes and trace metals in Montastrea annularis, *Proc. R. Soc. Lond. B*, v. 196, 291-315.
- Goreau, T.F. (1961) Problems of growth and calcium deposition in reef corals, *Endeavour*, v. 20, 32-39.
- Goreau, T.F. (1959) The ecology of Jamaican coral reefs, species composition and zonation, *Ecology*, v. 10, 67-90.
- Halpern, D., Hayes S.P., Leetmaa A., Hansen D.V., Philander S.G.H. (1983) Oceanographic observations of the 1982 warming of the tropical eastern Pacific, *Science*, v. 221, 1173-1175.
- Highsmith, R.C. (1979) Coral growth rates and environmental control of density banding, *J. Exp. Mar. Biol. Ecol.*, v. 37, 105-125.
- Houck, J.E. (1978) The potential utilization of scleractinian corals in the study of the marine environment, PhD dissertation, Oceanogr. University of Hawaii, Honolulu.
- Killingly, J.S. and Berger W.H. (1979) Stable isotopes in a mollusk shell: detection of upwelling events, *Science*, v. 205, 186-188.
- Knutson, D.W., Buddemeier R.W., and Smith S.V. (1972) Coral chronometers: seasonal growth bands in reef coral, *Science*, v. 177, 270-272.

- Land, L.S., Lang, J.C., and Smith S.V. (1975) Preliminary observation on the C isotopic composition of some reef corals and symbiotic zooxanthellae, *Limnol. Oc.*, v. 20, 283-287.
- Lasker, H.R., Peters E.C., Coffroth M.A. (1984) Bleaching of reef coelenterates in the San Blas Islands, Panama, *Coral Reefs*, v. 3, 183-190.
- Macintyre, I.G. and Smith S.V. (1974) X-radiographic studies of skeletal development in coral colonies, *Proc. 2nd Int. Coral Reef Symp.*, v. 2, 277-287.
- Malmgren, B.A. and Kennett J.P. (1978) Late Quaternary Paleoclimatic application of mean size variation in Globergerina bulloides (D'Orbigny) in the S. Indian Ocean, *J. Paleont.*, v. 52(6), 1195-1207.
- Moore, W.S. and Krishnaswami S. (1974) Correlation of X-radiography revealed banding in corals with radiometric growth rates, *Procs. 2nd Int. Symp. Coral Reefs*, Australia, v. 2, 267-276.
- Philander, S.G.H. (1983) El Niño-Southern Oscillation Phenomena, *Nature*, v. 302, 295-301.
- Rasmusson, E.M. and Carpenter T.H. (1982) Variations in tropical sea surface temperature and surface wind fields associated with Southern Oscillation/El Niño, *Monthly Weather Review*, v. 110(1), 354-384.
- Sokal, R.R. and Rohlf F.J. (1969) Biometry, W.H. Freeman and Company, San Francisco, California.
- Swart, P.K. and Coleman M.L. (1980) Isotopic data for scleractinian corals explain their paleotemperature uncertainties, *Nature*, v. 283, 557-559.
- Weber, J.N., Deines D., Weber P.H., and Baker P.A. (1976) Depth related changes in the $^{13}\text{C}/^{12}\text{C}$ ratio of skeletal carbonate deposited by the Caribbean reef-frame building coral M. annularis: further implications of a model for stable isotopic fractionation by scleractinian corals, *Geochim. Cosmochim. Acta*, v. 40, 31-39.
- Weber, J.N., White E.W., and Weber P.H. (1975) Correlation of density banding in reef coral skeletons with environmental parameters: the basis for interpretation of chronology records preserved in the coralla of corals, *Paleobiol.*, v. 1, 137-149.
- Weber, J.N. and Woodhead P.M.J. (1972) Temperature dependence of oxygen-18 concentration in reef coral carbonates, *J. of Geophys. Res.*, v. 77(3), 463-473.
- Weber, J.N. and Woodhead P.M.J. (1971) Diurnal variations in the isotopic composition of dissolved inorganic carbon in seawater from coral reef environments, *Geochim. Cosmochim. Acta*, v. 35, 891-902.
- Wefer, G. and Berger W.H. (1980) Stable isotope composition of benthic calcareous algae from Bermuda, *J. of Sed. Petrol.*, v. 51(2), 459-465.

- Weil, S.M., Buddemeier R.W., Smith S.V., and Kroopnick P.M. (1981) The stable isotopic composition of coral skeletons: control by environmental variables, *Geochim. Cosmochim. Acta*, v. 45, 1147-1153.
- Wellington, G.M. and Glynn P.W. (1983) Environmental influences on skeletal banding in eastern Pacific (Panama) corals, *Coral Reefs*, v. 1, 215-222.
- Wellington, G.M. (1982) An experimental analysis of the effects of light and zooplankton on coral zonation, *Oecologia*, v. 52, 311-320.
- Williams, D.F. (1976) Late Quaternary fluctuations of the polar front and subtropical convergence in the SE Indian Ocean, *Mar. Microp.*, v. 1, 363-375.
- Wooster, W.S. and Guillen O. (1974) Characteristics of El Niño in 1972, *J. Mar. Res.*, v. 32, 387-403.

APPENDIX A

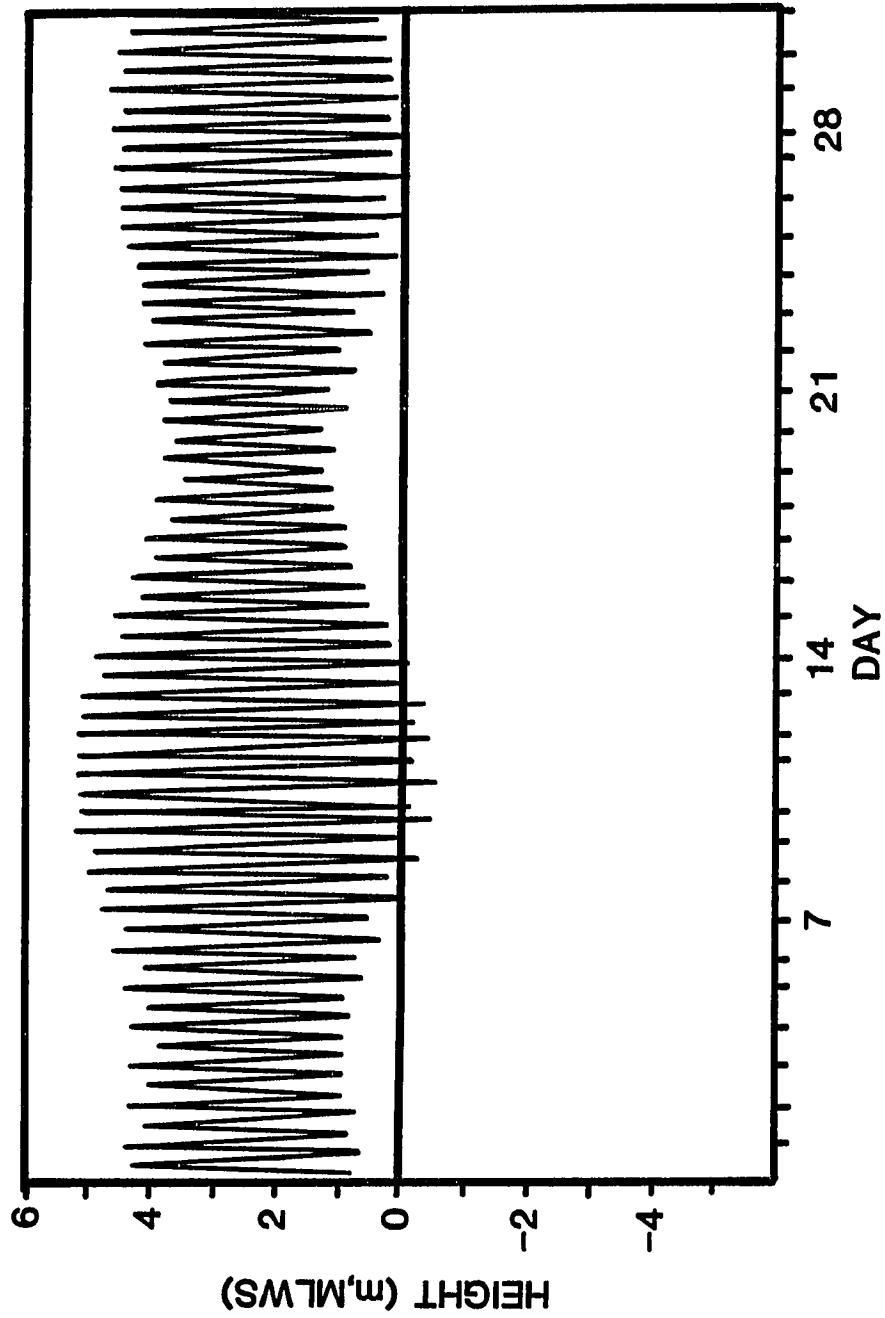
APPENDIX A

High and low tide heights for January-June, 1982 and January-December, 1983 were measured at Balboa, Panama (Pacific) relative to Mean Low Water Springs (MLWS) datum which is approximately 8.4 ft. (2.56 m) below mean sea level at Balboa (U.S. Coast and Geodetic Survey). The first six plots are daily measurements; the last three plots are weekly averages. Tide data is taken from the Tide Tables published by the U. S. Department of Commerce (1982-1983).

HIGH AND LOW TIDE HEIGHTS

JANUARY 1982

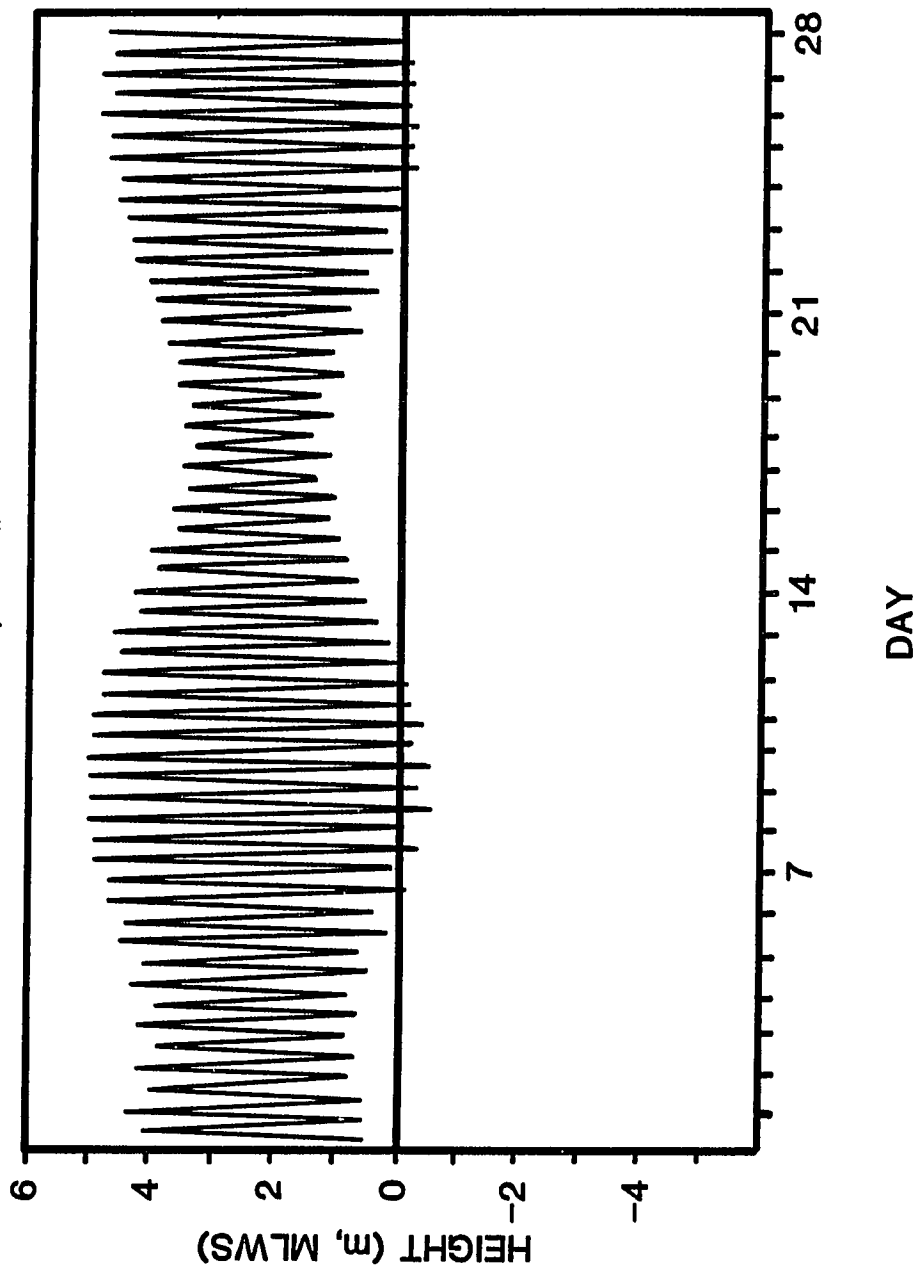
Balboa, Panama



HIGH AND LOW TIDE HEIGHTS

FEBRUARY 1982

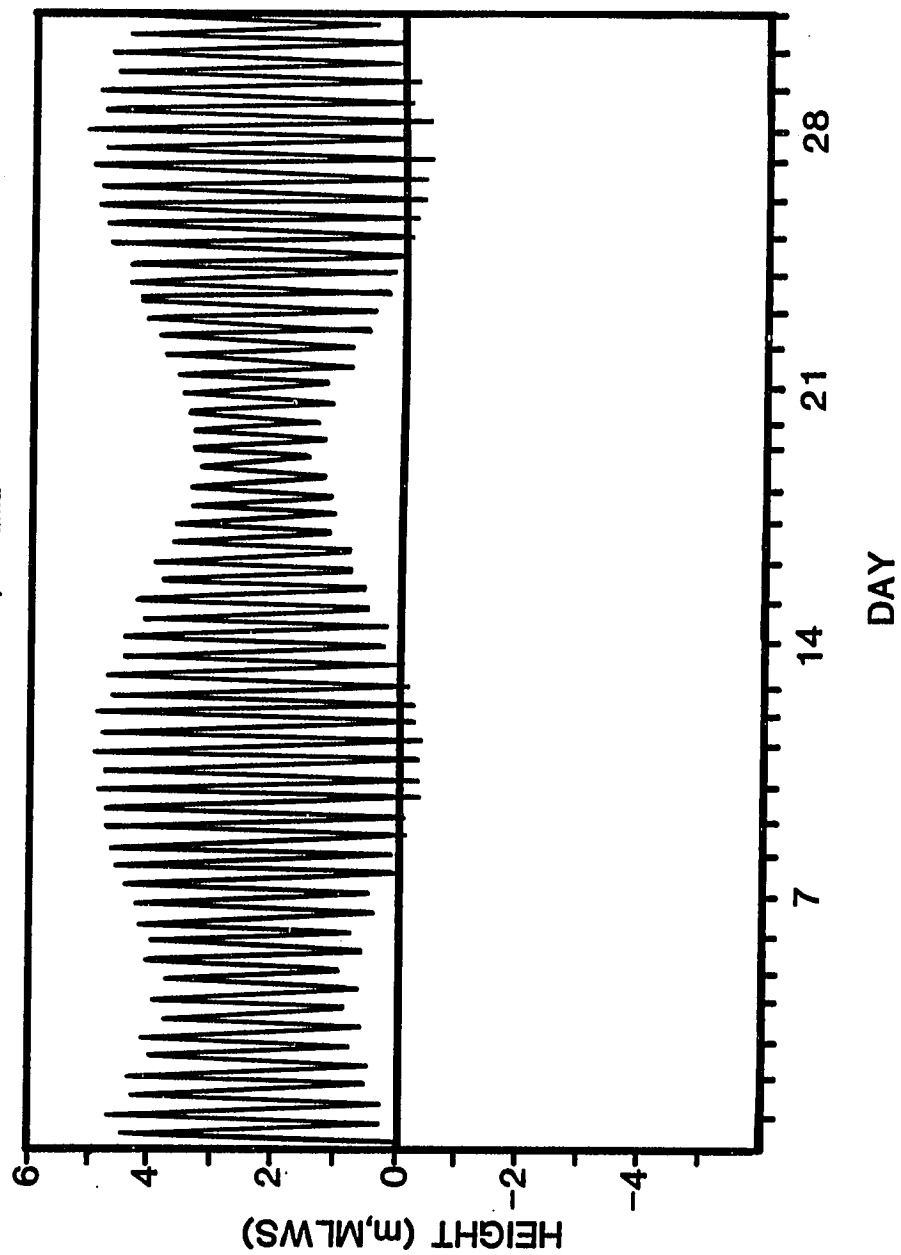
Balboa, Panama



HIGH AND LOW TIDE HEIGHTS

MARCH 1982

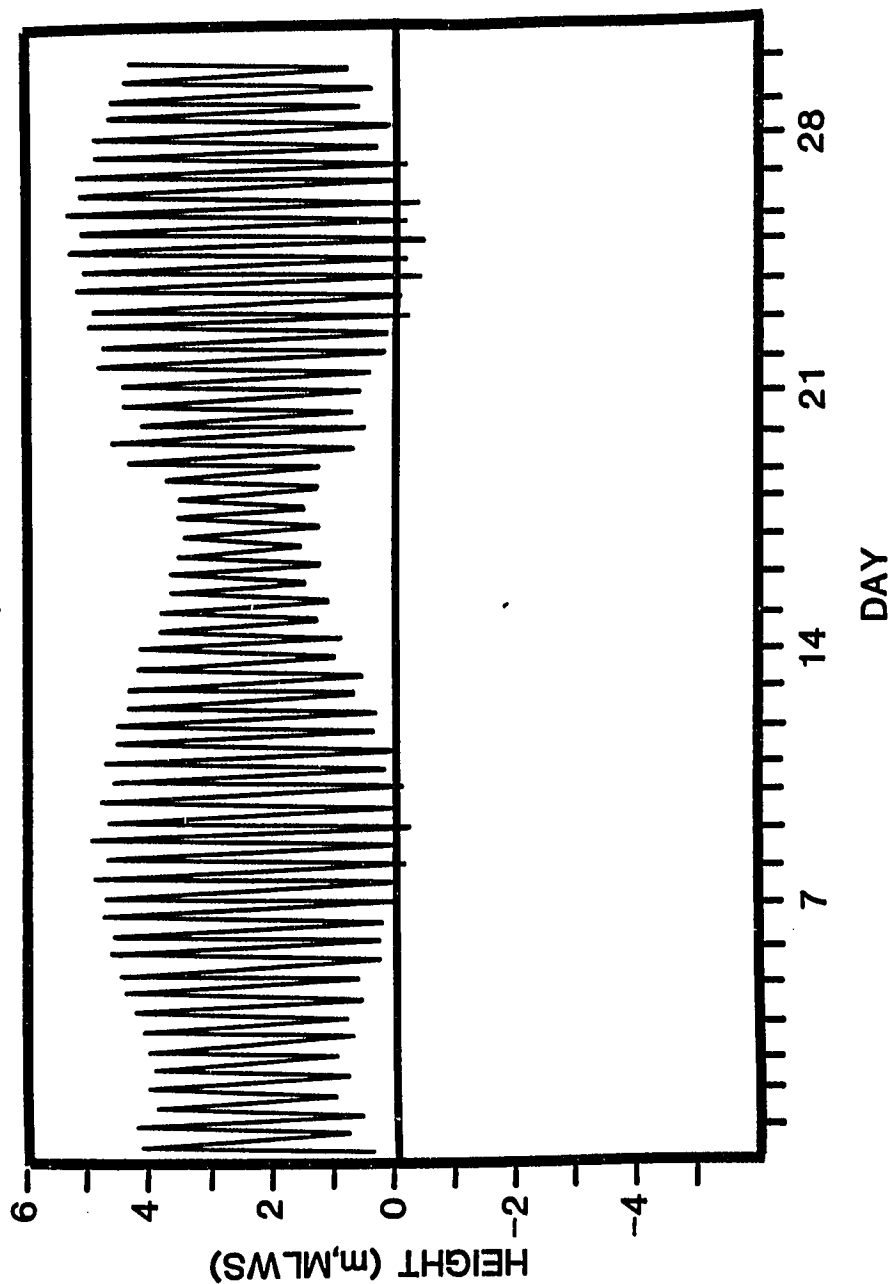
Balboa, Panama



HIGH AND LOW TIDE HEIGHTS

APRIL 1982

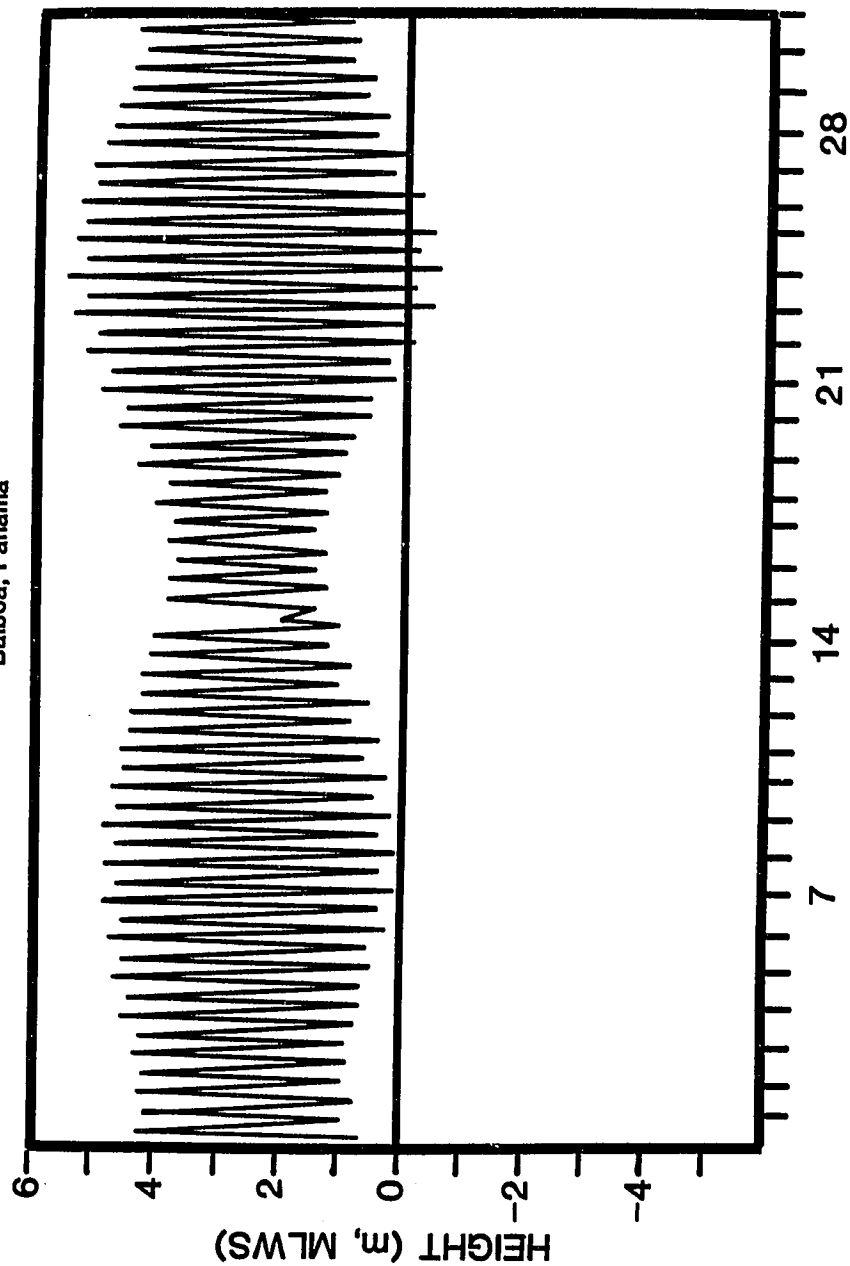
Balboa, Panama



HIGH AND LOW TIDE HEIGHTS

MAY 1982

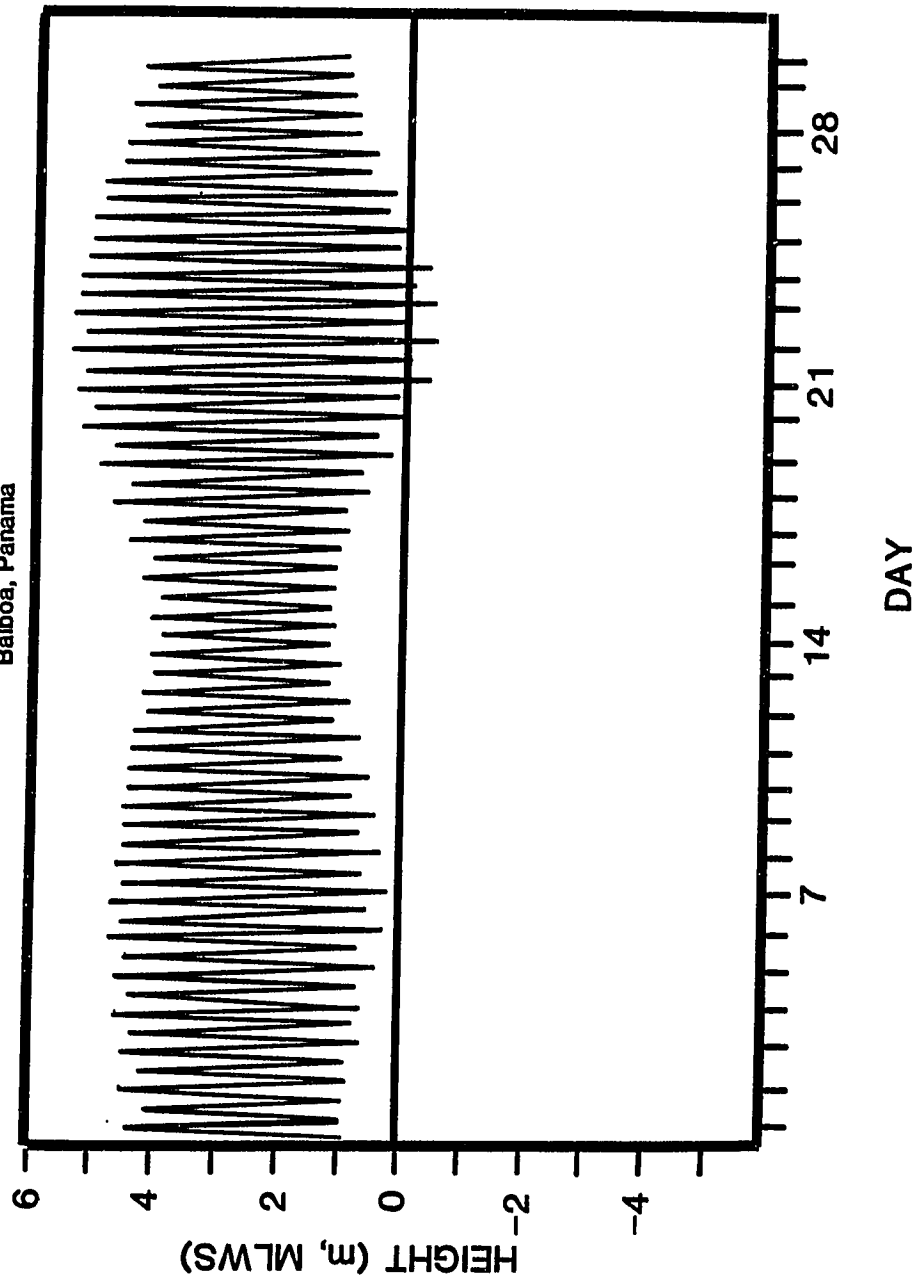
Balboa, Panama



HIGH AND LOW TIDE HEIGHTS

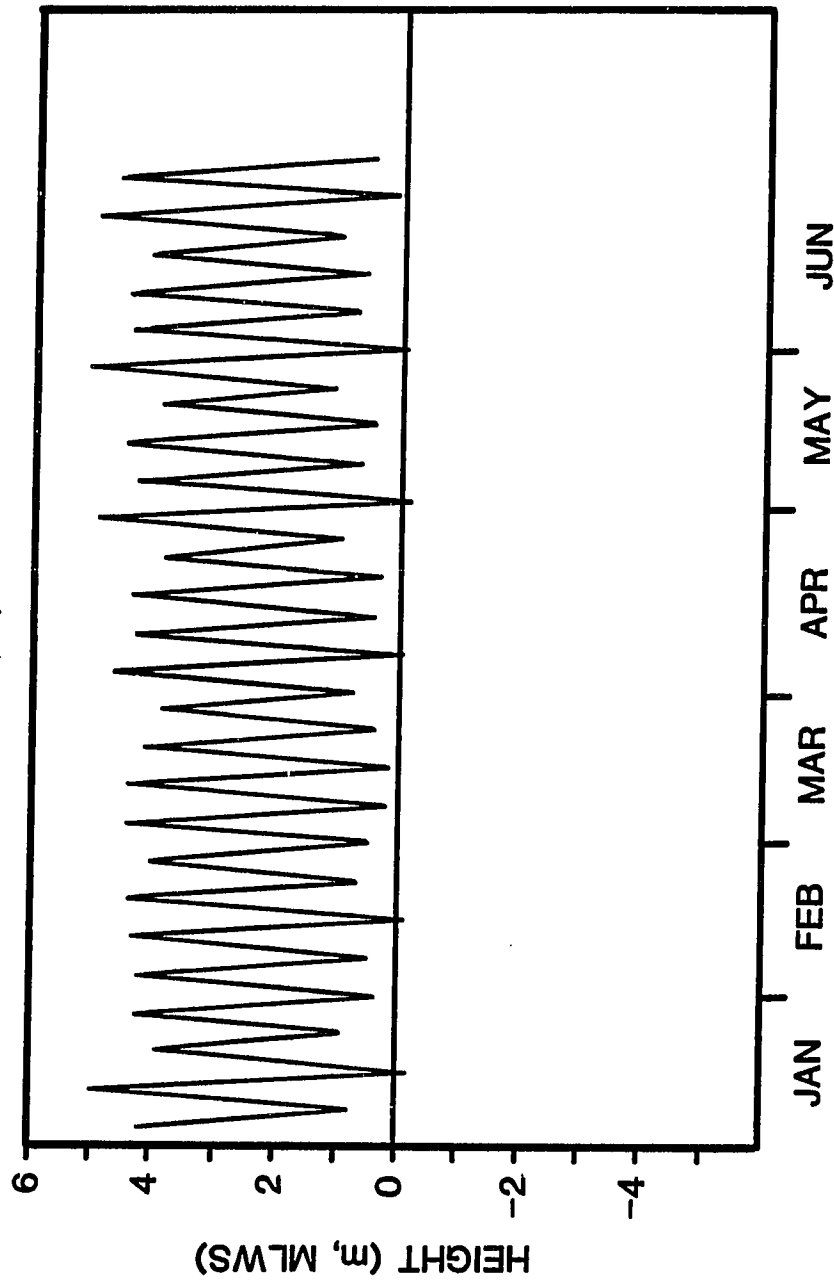
JUNE 1982

Balboa, Panama



WEEKLY AVERAGE TIDE HEIGHTS

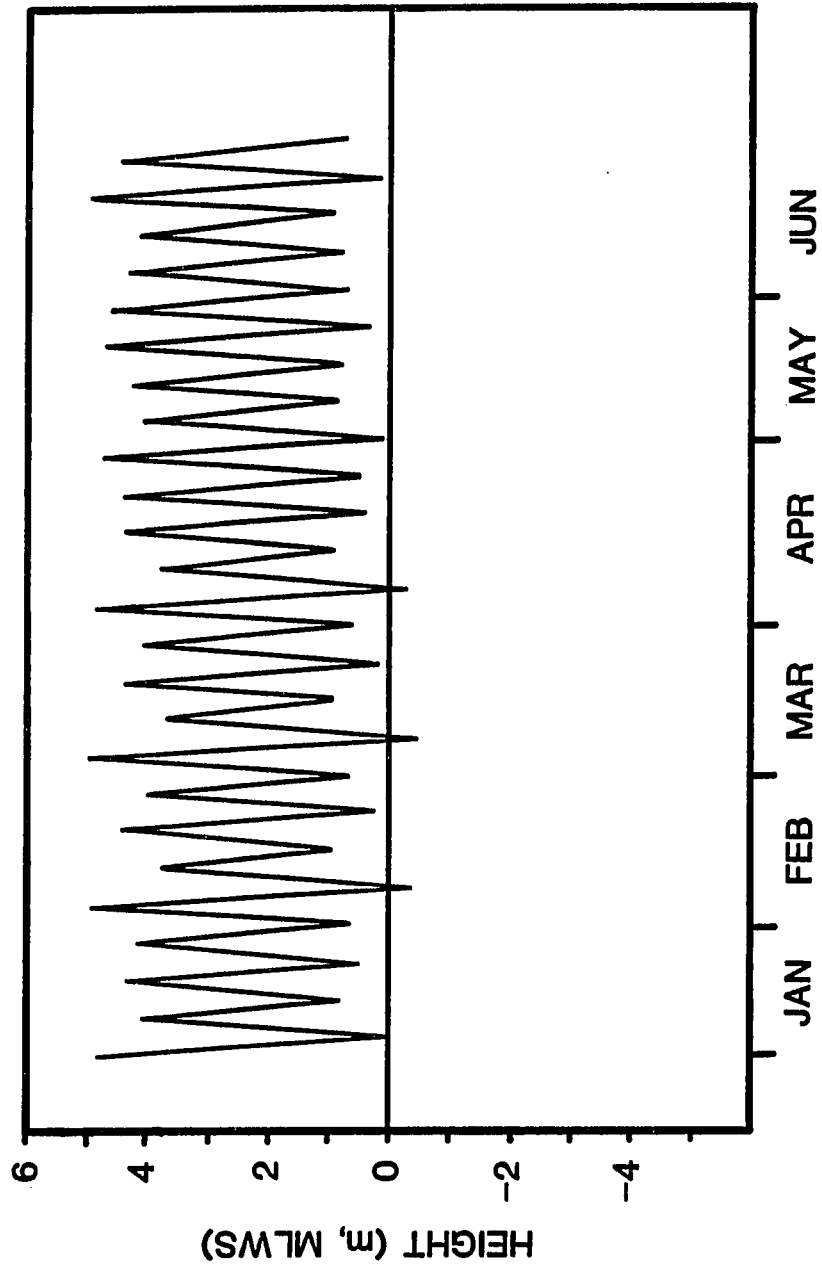
BALBOA, PANAMA



1982

WEEKLY AVERAGE TIDE HEIGHTS

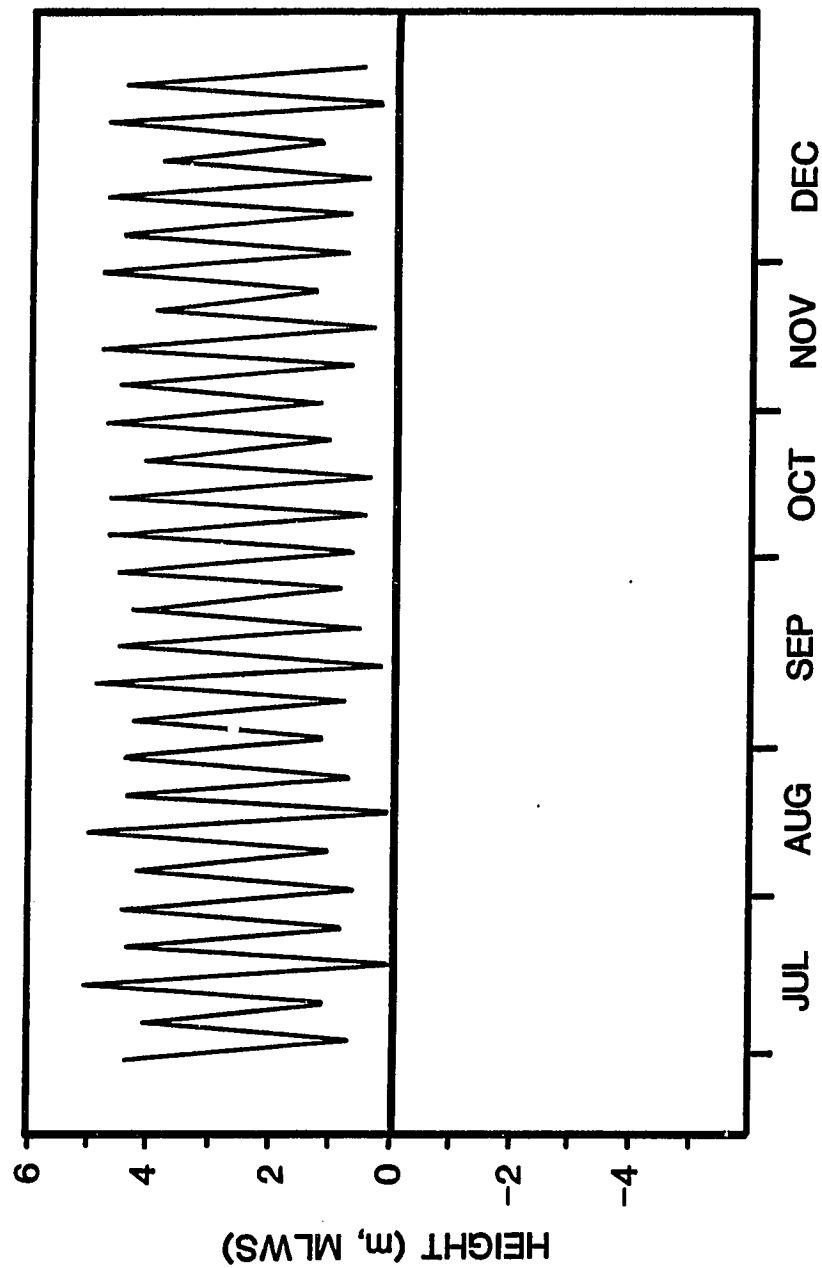
BALBOA, PANAMA



1983

WEEKLY AVERAGE TIDE HEIGHTS

BALBOA, PANAMA



1983

APPENDIX B

APPENDIX B

Included here are tables of the mean standard deviations of the stable isotope replicates for each coral head. Also included is the standard deviation of the stable isotope values of an internal lab isotope standard, RICE-1, relative to PDB.

Coral stable isotope data are listed versus distance along the maximum vertical growth axis of the coral for each coral head. Isotope values for samples and the standard are reported in standard delta notation relative to PDB as discussed in the text.

Rice University
Intralaboratory Isotope Standard
RICE-1

85

PARAMETER	REPORTED VALUE(%)	STD DEV	SUGGESTED VALUE(%)*
$\delta^{18}\text{O}$	-1.06	0.15	-0.99
$\delta^{13}\text{C}$	-0.78	0.11	-0.81

*Based on 25 replicate analyses of RICE-1 analyzed in
conjunction with the known isotope standard, NBS-20.

Delta O-18(‰)

Delta C-13(‰)

1.12	0.86
1.20	0.83
1.17	0.88
0.90	0.84
1.06	0.86
0.80	0.78
1.20	0.84
0.83	0.78
1.06	0.82
1.28	0.80
1.12	0.80
1.11	0.78
1.15	0.80
0.97	0.84
1.15	0.80
0.88	0.89
0.83	0.82
1.19	0.90
1.17	0.85
1.09	0.84
0.97	0.86
1.10	0.94
1.13	0.99
1.11	0.87
1.29	0.86
1.21	0.85
1.28	0.67
1.26	0.77
1.04	0.79
0.91	0.53
1.24	0.65
0.95	0.42
0.84	0.74
0.96	0.72
1.16	0.81
1.13	0.89
0.98	0.85
0.97	0.83
0.97	0.79
1.16	0.86
0.94	0.85
1.15	0.27
1.16	0.65
1.11	0.69
0.95	0.83
1.08	0.61

0.91	0.69
1.06	0.70
1.07	0.78
0.82	0.65
0.97	0.60
1.15	0.79
0.82	0.54
1.23	0.67
1.33	0.89
1.08	0.78
0.96	0.77
0.94	0.96
0.97	0.86
1.02	0.71
0.80	0.81
0.81	0.78
0.95	0.73
1.13	0.67
0.87	0.74
1.13	0.78
0.95	0.43
1.24	0.84
1.24	0.75
0.98	0.70
1.18	0.73
0.70	0.66
1.07	0.68
0.96	0.73
1.09	0.71
1.09	0.83
0.97	0.87
1.08	0.77
1.09	0.74
0.94	0.85
1.17	0.82
1.02	0.90
1.12	0.86
1.10	0.85
1.10	0.88
1.22	0.64
1.39	0.80
1.05	0.85
1.28	0.84
1.33	0.82
1.12	0.88
1.39	0.91
0.74	0.84
0.99	0.86
0.59	0.84
0.76	0.88

1.18	0.79
1.03	0.77
1.15	0.69
0.85	0.77
0.90	0.91
0.89	0.84
1.04	0.78
1.17	0.81
0.97	0.84
1.25	0.89
1.14	0.73
1.32	0.84
1.10	0.89
1.26	0.85
1.06	0.83
1.02	0.78
1.12	0.82
0.90	0.77
1.07	0.74
1.03	0.87
0.80	0.60
0.99	0.81
1.26	0.86
1.16	0.77
1.08	0.73
1.19	0.80
1.05	0.81
0.94	0.46
1.34	0.80
0.90	0.66
1.16	0.79
1.19	0.69
1.20	0.74
1.16	0.74

STANDARD DEVIATIONS

89

<u>IDENTIFICATION</u>	<u>§180</u>	<u>§130</u>
SOUTH SHORE CONTADORA	0.12	0.07
CONTADORA 9	ND	ND
URABA	0.24	0.21
UVA 56	ND	ND
UVA 1	0.12	0.14
SECAS 1	0.15	0.13
AZUERO	0.04	0.08

Distance from top (cm)	Delta O-18(‰)	Delta C-13(‰)
0.00	-5.87	-2.24
0.10	-5.60	-2.20
0.20	-5.90	-2.05
0.20	-5.66	-2.00
0.30	-5.89	-2.09
0.40	-5.91	-2.01
0.40	-5.57	-1.78
0.50	-6.21	-1.56
0.60	-5.74	-1.67
0.60	-5.62	-1.30
0.70	-5.85	-1.68
0.80	-5.41	-1.70
0.80	-5.56	-1.73
0.90	-5.49	-2.27
1.00	-5.76	-2.29
1.00	-5.61	-2.42
1.10	-5.88	-2.33
1.20	-5.91	-2.38
1.20	-5.89	-2.54
1.30	-6.08	-2.17
1.40	-6.00	-2.25
1.40	-6.06	-2.23
1.50	-6.04	-2.14
1.60	-6.20	-2.24
1.60	-6.22	-2.29
1.70	-5.98	-1.86
1.80	-5.71	-1.77
1.90	-5.73	-1.36
2.00	-5.94	-1.39
2.00	-6.04	-1.75
2.10	-5.80	-1.88
2.20	-5.74	-1.95
2.30	-5.97	-2.17
2.40	-5.33	-1.96
2.40	-5.39	-1.81
2.50	-5.86	-2.02
2.60	-5.95	-2.03
2.60	-5.70	-2.03
2.70	-6.01	-2.22
2.80	-6.02	-2.15
2.80	-6.23	-2.25
2.90	-6.04	-1.72
3.00	-5.74	-2.10
3.10	-5.68	-1.30
3.20	-5.59	-1.31

3.20	-5.55	-1.38
3.30	-5.41	-1.34
3.40	-5.46	-1.19
3.50	-5.48	-2.11
3.60	-5.67	-2.12
3.60	-5.51	-2.00
3.70	-5.94	-2.04
3.80	-5.67	-2.10
3.80	-5.83	-2.12
3.90	-5.91	-2.17
4.00	-6.21	-2.23
4.00	-6.16	-2.18
4.10	-6.50	-2.22
4.20	-6.35	-2.24
4.20	-6.16	-2.05
4.30	-6.66	-1.92
4.40	-5.92	-1.79
4.40	-6.18	-1.96
4.50	-6.12	-1.27
4.60	-5.97	-1.44
4.60	-6.16	-1.53
4.70	-6.65	-1.45
4.80	-5.73	-1.26
4.90	-6.08	-1.35
4.90	-5.84	-1.14
5.00	-5.76	-1.07

URABA

Distance from top (cm)	Delta O-18 (‰)	Delta C-13 (‰)
0.00	-4.76	-1.84
0.00	-5.03	-2.03
0.05	-4.92	-2.18
0.10	-4.91	-2.67
0.15	-5.13	-2.72
0.20	-5.18	-2.74
0.20	-5.26	-3.04
0.25	-5.70	-3.20
0.30	-5.82	-3.17
0.35	-6.44	-3.06
0.40	-6.40	-2.94
0.40	-6.15	-2.98
0.45	-6.03	-2.75
0.50	-5.85	-2.57
0.55	-6.31	-2.87
0.60	-6.06	-2.98
0.60	-5.84	-3.09
0.65	-5.88	-2.96
0.70	-5.68	-2.53
0.75	-5.75	-2.74
0.80	-5.90	-3.34
0.80	-5.80	-3.13
0.85	-6.26	-3.21
0.90	-6.65	-3.12
0.95	-6.49	-3.07
1.00	-7.41	-3.15
1.00	-7.29	-3.12
1.05	-6.92	-3.23
1.10	-7.32	-4.25
1.15	-6.37	-3.44
1.20	-6.03	-3.47
1.20	-5.93	-3.02
1.25	-5.71	-2.76
1.30	-5.90	-2.95
1.35	-5.48	-3.04
1.40	-5.45	-3.36
1.40	-5.22	-3.35
1.45	-5.60	-3.40
1.50	-5.74	-3.57
1.55	-5.89	-3.28
1.60	-6.40	-3.27
1.60	-6.25	-3.69
1.65	-6.01	-2.52
1.70	-6.38	-2.81
1.75	-5.99	-3.03

1.80	-5.39	-2.93
1.80	-5.65	-2.90
1.85	-5.39	-2.87
1.90	-4.83	-3.09
1.95	-5.17	-3.29
2.00	-5.14	-3.60
2.00	-5.15	-3.46
2.05	-5.75	-3.84
2.10	-5.75	-4.01
2.15	-6.47	-4.22
2.20	-6.56	-3.47
2.20	-6.41	-3.65
2.25	-6.91	-3.47
2.30	-6.33	-2.75
2.35	-6.44	-3.08
2.40	-5.45	-2.84
2.40	-5.80	-3.13
2.45	-5.60	-2.57
2.50	-5.62	-2.81
2.55	-5.40	-2.54
2.60	-5.28	-3.07
2.60	-5.45	-2.87
2.65	-4.84	-3.60
2.70	-5.33	-3.94
2.75	-6.14	-4.10
2.80	-5.96	-3.74
2.80	-6.20	-3.88
2.85	-6.60	-3.89
2.90	-6.56	-3.73
2.95	-6.40	-3.27
3.00	-6.41	-3.93
3.00	-6.27	-3.47
3.05	-5.97	-3.23
3.10	-5.74	-3.36
3.15	-5.71	-3.11
3.20	-5.56	-3.23
3.20	-5.63	-3.26
3.25	-5.56	-3.55
3.30	-5.07	-3.53
3.35	-5.05	-3.60
3.40	-5.00	-3.74
3.45	-5.72	-3.82
3.50	-6.41	-3.68
3.55	-6.37	-3.44
3.60	-6.32	-3.36
3.60	-6.01	-3.21
3.65	-5.94	-3.06
3.70	-5.66	-2.83
3.75	-5.81	-2.97
3.80	-5.85	-2.79

3.80	-5.96	-2.72
3.85	-5.23	-2.69
3.90	-5.20	-2.84
3.95	-4.71	-2.86
4.00	-4.74	-3.27
4.00	-5.06	-2.99
4.05	-5.05	-3.68
4.10	-5.44	-3.58
4.15	-5.82	-3.39
4.20	-6.26	-3.45
4.20	-6.07	-3.34
4.25	-6.05	-3.26
4.30	-5.92	-2.78
4.35	-5.79	-2.60
4.40	-5.78	-2.61
4.40	-5.56	-2.65
4.45	-5.74	-2.59
4.50	-5.35	-2.51
4.55	-5.05	-2.75
4.60	-4.87	-3.32
4.60	-4.85	-3.08
4.65	-4.87	-3.57
4.70	-4.71	-3.37
4.75	-4.89	-3.28
4.80	-6.73	-3.45
4.80	-6.43	-3.52
4.85	-6.54	-3.24
4.90	-6.52	-3.09
4.95	-6.11	-3.32
4.95	-6.29	-3.21
5.00	-5.71	-2.99
5.05	-5.79	-2.64
5.10	-5.48	-2.95
5.15	-5.62	-2.97
5.20	-5.24	-3.03
5.20	-5.58	-3.03
5.25	-4.96	-3.76
5.30	-5.64	-3.45
5.35	-5.75	-3.56
5.40	-6.08	-3.69
5.40	-5.95	-3.48
5.45	-5.97	-3.76
5.50	-6.61	-3.75
5.55	-6.52	-3.36
5.60	-6.19	-2.88
5.60	-6.39	-3.29
5.65	-6.38	-3.04
5.70	-6.45	-2.78
5.75	-5.79	-2.72
5.80	-6.13	-3.09

5.80	-5.97	-2.94
5.85	-5.39	-2.89
5.90	-5.32	-2.89
5.95	-5.54	-3.42
6.00	-5.78	-3.65
6.00	-5.83	-4.36
6.05	-6.80	-3.09
6.10	-6.94	-2.90
6.15	-6.28	-3.22
6.20	-6.18	-2.93
6.20	-6.54	-3.20
6.25	-6.02	-2.88
6.30	-5.66	-2.47
6.35	-5.52	-2.56
6.40	-5.09	-2.73
6.40	-5.09	-2.62
6.45	-5.00	-3.08
6.50	-5.02	-3.50
6.55	-5.97	-3.23
6.60	-5.83	-3.37
6.60	-5.55	-3.31
6.65	-6.31	-3.51
6.70	-5.34	-3.69
6.75	-7.37	-4.00
6.80	-5.69	-2.59
6.85	-7.55	-3.30
6.90	-7.28	-3.33
6.95	-7.48	-3.33
7.00	-5.40	-2.97
7.00	-5.80	-2.73
7.05	-6.42	-3.53
7.10	-6.82	-3.48
7.15	-6.25	-3.66
7.20	-5.02	-3.19
7.20	-5.11	-3.20
7.25	-5.82	-3.53
7.30	-5.98	-3.29
7.35	-6.90	-3.18
7.40	-6.40	-3.96
7.40	-5.91	-3.29
7.45	-6.50	-2.89
7.50	-6.26	-2.99
7.55	-6.69	-3.00
7.60	-5.92	-2.78
7.60	-6.46	-3.13
7.65	-6.52	-3.32
7.70	-7.22	-3.65
7.75	-7.55	-3.61
7.80	-5.83	-2.97
7.80	-6.22	-3.24

7.85	-6.91	-3.30
7.90	-7.48	-3.37
7.95	-6.92	-3.23
8.00	-6.45	-3.02
8.00	-6.74	-2.94
8.05	-6.71	-2.99
8.10	-6.28	-2.88
8.15	-6.20	-3.07
8.20	-5.90	-2.78
8.20	-5.87	-2.51
8.25	-5.70	-3.38
8.30	-5.82	-3.02
8.35	-5.94	-3.01
8.40	-6.40	-3.10
8.40	-5.84	-2.96
8.45	-6.72	-2.98
8.50	-6.83	-3.02
8.55	-6.55	-2.72
8.60	-6.30	-2.36
8.60	-6.00	-2.48
8.65	-5.93	-2.07
8.70	-5.73	-2.34
8.75	-5.57	-2.58
8.80	-5.75	-2.73
8.80	-5.45	-2.42
8.85	-6.10	-2.99
8.90	-6.49	-3.01
8.95	-6.92	-2.99
9.00	-6.54	-2.65
9.00	-6.23	-3.17
9.05	-6.33	-2.33
9.10	-5.90	-2.40
9.15	-5.78	-2.36
9.20	-5.33	-2.49
9.20	-5.42	-2.36
9.25	-5.29	-2.42
9.30	-5.42	-3.01
9.35	-6.15	-3.44
9.40	-5.93	-3.30
9.40	-5.89	-3.34
9.45	-6.27	-2.61
9.50	-6.36	-2.57
9.55	-5.96	-2.54
9.60	-6.17	-2.46
9.60	-6.23	-2.78
9.65	-5.88	-2.54
9.70	-5.77	-2.58
9.75	-5.77	-2.83
9.80	-5.29	-3.14
9.80	-5.78	-2.79

9.85	-6.03	-2.93
9.90	-6.43	-2.86
9.95	-6.75	-2.86
10.00	-6.68	-2.79
10.05	-6.64	-2.67
10.10	-6.47	-2.59
10.15	-6.66	-2.69
10.20	-6.49	-2.83
10.20	-6.76	-2.42
10.25	-5.92	-2.58
10.30	-5.71	-2.84
10.35	-5.31	-3.34
10.40	-5.84	-3.08
10.40	-5.46	-3.30
10.45	-5.83	-3.21
10.50	-6.29	-3.44
10.55	-7.04	-3.56
10.60	-6.19	-3.58
10.60	-6.53	-3.42
10.65	-6.67	-3.31
10.70	-6.42	-3.28
10.75	-6.04	-3.11
10.80	-5.65	-3.07
10.80	-5.94	-3.07
10.85	-5.76	-2.91
10.90	-5.54	-2.63
10.95	-5.73	-3.00
11.00	-5.55	-2.94
11.00	-5.44	-2.95
11.05	-5.42	-3.06
11.10	-5.65	-3.17
11.15	-5.91	-3.06
11.20	-6.03	-2.55
11.20	-6.55	-3.11
11.25	-6.51	-2.93
11.30	-6.29	-2.78
11.35	-5.93	-3.19
11.40	-6.10	-3.04
11.40	-5.85	-2.83
11.45	-5.78	-3.22
11.50	-5.64	-3.19
11.55	-5.59	-3.03
11.60	-5.86	-2.73
11.60	-5.34	-3.03
11.65	-6.21	-3.19
11.70	-6.15	-3.05
11.75	-6.34	-3.17
11.80	-6.12	-2.97
11.80	-5.63	-2.73
11.85	-5.78	-2.91

11.90	-5.44	-2.68
11.95	-4.85	-1.44
12.00	-4.22	-2.31

UVA 56

Distance from top (cm)	Delta O-18 (‰)	Delta C-13 (‰)
0.20	-6.04	-2.60
0.40	-6.38	-2.28
0.60	-6.77	-2.55
0.80	-6.69	-2.64
1.00	-6.54	-2.14
1.20	-6.49	-3.97
1.40	-5.94	-4.32
1.60	-6.15	-2.08
1.80	-6.28	-2.47
2.00	-6.75	-2.52
2.20	-6.66	-2.69
2.40	-6.01	-2.27
2.60	-5.76	-2.36
2.80	-5.65	-2.18
3.00	-5.93	-2.32
3.20	-6.38	-2.35
3.40	-6.21	-2.15
3.60	-6.06	-1.87
3.80	-5.88	-2.11
4.00	-5.68	-2.10
4.20	-5.67	-2.28
4.40	-6.21	-2.39
4.60	-6.13	-2.50
4.80	-5.96	-2.06
5.00	-5.67	-1.96
5.20	-5.86	-2.27
5.40	-5.86	-2.23
5.60	-6.42	-2.35
5.80	-6.27	-2.39
6.00	-6.19	-2.42
6.20	-6.06	-2.08
6.40	-5.90	-2.29
6.60	-5.92	-2.08
6.80	-6.26	-2.70
7.00	-6.38	-2.35
7.20	-6.63	-2.32
7.40	-5.98	-2.20
7.60	-5.78	-2.59
7.80	-5.89	-2.33
8.00	-6.12	-2.10

Distance from top (cm)	Delta O-18(‰)	Delta C-13(‰)
0.10	-6.02	-3.24
0.20	-7.01	-2.95
0.30	-6.81	-2.79
0.40	-6.44	-2.99
0.50	-6.11	-3.43
0.60	-5.76	-2.66
0.70	-5.23	-4.01
0.80	-5.19	-2.73
0.90	-5.07	-2.81
1.00	-5.25	-3.64
1.10	-5.76	-2.70
1.20	-6.54	-3.05
1.30	-6.89	-3.06
1.40	-6.77	-3.04
1.50	-6.83	-2.95
1.60	-6.40	-2.91
1.70	-6.54	-2.64
1.80	-6.45	-2.65
1.90	-6.15	-2.67
2.00	-5.75	-2.61
2.10	-5.76	-2.79
2.20	-5.39	-2.95
2.30	-4.80	-2.68
2.40	-4.89	-2.71
2.50	-4.87	-2.69
2.60	-6.25	-2.61
2.70	-7.03	-2.88
2.80	-6.12	-2.72
2.90	-4.81	-2.50
3.00	-4.50	-2.68
3.20	-5.01	-2.56
3.40	-5.71	-2.86
3.60	-5.93	-2.08
3.80	-6.05	-2.47
4.00	-6.02	-3.24
4.20	-6.35	-2.95
4.40	-5.77	-2.42
4.60	-6.86	-4.30
4.80	-4.38	-2.61
5.00	-4.71	-2.26
5.20	-5.40	-2.45
5.40	-5.71	-2.83
5.60	-5.96	-2.61
5.80	-6.17	-2.99
6.00	-6.36	-2.75

6.20	-6.41	-2.90
6.40	-6.25	-2.66
6.60	-7.45	-1.35
6.80	-5.39	-2.60
7.00	-5.21	-2.66
7.20	-6.35	-2.74
7.40	-6.11	-2.72
7.60	-5.35	-2.44
7.80	-4.89	-2.49
8.00	-5.71	-2.41
8.20	-6.37	-2.80
8.40	-6.78	-2.80
8.60	-6.55	-2.88
8.80	-7.08	-2.66
9.00	-6.86	-2.71
9.20	-6.58	-2.93
9.40	-6.20	-2.64
9.60	-5.60	-2.60
9.80	-5.98	-2.65
10.00	-6.54	-2.81

UVA 1

Distance from top (cm)	Delta O-18(‰)	Delta C-13(‰)
0.10	-5.80	-1.51
0.10	-5.90	-1.51
0.20	-6.12	-1.77
0.30	-6.09	-2.00
0.30	-6.17	-1.82
0.40	-6.39	-2.32
0.50	-6.61	-2.28
0.50	-6.38	-2.17
0.60	-6.66	-2.15
0.70	-6.20	-2.21
0.70	-6.18	-2.06
0.80	-6.19	-2.10
0.90	-5.73	-1.95
0.90	-5.85	-1.83
1.00	-6.06	-2.02
1.10	-6.06	-1.83
1.10	-5.95	-1.69
1.20	-6.65	-1.93
1.30	-6.86	-2.18
1.30	-6.66	-2.20
1.40	-7.08	-2.33
1.50	-6.82	-2.32
1.50	-6.79	-2.37
1.60	-6.56	-2.30
1.70	-6.54	-2.10
1.70	-6.63	-2.11
1.80	-6.74	-2.18
1.90	-6.62	-1.92
1.90	-6.27	-1.90
2.00	-5.87	-1.87
2.10	-5.91	-1.82
2.10	-5.69	-1.82
2.20	-5.96	-1.82
2.30	-5.47	-1.84
2.30	-5.39	-1.93
2.40	-5.45	-1.56
2.50	-5.50	-1.61
2.50	-5.47	-1.66
2.60	-5.57	-1.29
2.70	-6.01	-1.80
2.70	-6.11	-1.63
2.80	-5.90	-1.93
2.90	-6.03	-2.02
2.90	-5.90	-2.08
3.00	-5.87	-2.22

3.10	-5.66	-1.98
3.10	-5.75	-2.06
3.20	-5.82	-1.78
3.30	-5.77	-1.76
3.30	-5.69	-1.91
3.40	-5.77	-1.72
3.50	-5.43	-1.56
3.50	-5.41	-1.78
3.60	-5.28	-1.57
3.70	-5.31	-1.73
3.70	-5.28	-1.57
3.80	-5.52	-1.51
3.90	-5.44	-1.59
3.90	-5.54	-1.47
4.00	-6.01	-1.71
4.10	-6.05	-1.91
4.10	-5.67	-1.78
4.20	-6.07	-2.08
4.30	-5.99	-2.22
4.30	-5.98	-2.09
4.40	-5.99	-2.06
4.50	-6.17	-2.08
4.50	-6.34	-2.07
4.60	-6.23	-1.80
4.70	-6.02	-1.66
4.70	-5.63	-1.41
4.80	-5.72	-1.72
4.90	-5.63	-1.78
4.90	-5.68	-1.52
5.00	-5.48	-1.58
5.10	-5.41	-1.66
5.10	-5.35	-1.48
5.20	-5.52	-1.46
5.30	-5.43	-1.72
5.30	-5.23	-1.65
5.40	-5.39	-1.65
5.50	-5.61	-1.39
5.50	-5.42	-1.45
5.60	-5.97	-1.50
5.70	-6.12	-1.71
5.70	-5.96	-1.63
5.80	-6.19	-1.56
5.90	-6.33	-2.00
5.90	-6.42	-1.87
6.00	-6.27	-2.08
6.10	-5.95	-2.07
6.10	-6.09	-1.89
6.20	-6.25	-1.79
6.30	-5.94	-1.91
6.30	-5.88	-1.48

6.40	-5.94	-1.86
6.50	-5.85	-1.88
6.50	-5.81	-1.56
6.60	-5.75	-1.71
6.70	-5.42	-1.67
6.70	-5.68	-1.58
6.80	-5.41	-1.84
6.90	-5.24	-1.61
6.90	-5.25	-1.46
7.00	-5.57	-1.24
7.10	-5.80	-1.19
7.10	-5.68	-0.85
7.20	-6.33	-1.64
7.30	-6.07	-1.90
7.30	-6.15	-1.63
7.40	-5.95	-1.83
7.50	-5.74	-2.00
7.50	-5.51	-1.71
7.60	-5.38	-1.47
7.70	-5.25	-1.14
7.70	-5.22	-1.18
7.80	-5.21	-1.05
7.90	-4.87	-0.45
7.90	-4.76	-0.23
8.00	-4.90	-0.25

SOUTH SHORE CONTADORA

Distance from top (cm)	Delta Q-18(%)	Delta C-13(%)
0.00	-4.99	-1.87
0.10	-5.14	-1.86
0.20	-5.83	-1.75
0.30	-5.65	-1.69
0.40	-5.66	-2.23
0.50	-4.98	-1.89
0.60	-4.88	-1.68
0.70	-5.27	-1.88
0.70	-5.42	-1.80
0.80	-5.95	-2.19
0.90	-6.38	-2.28
1.00	-6.03	-2.16
1.10	-6.01	-2.27
1.20	-4.90	-2.16
1.30	-4.18	-2.50
1.30	-4.12	-2.44
1.40	-4.34	-2.28
1.50	-5.12	-1.77
1.60	-5.25	-1.88
1.70	-5.49	-1.73
1.80	-5.60	-2.09
1.90	-5.95	-2.12
2.00	-5.64	-2.10
2.10	-5.30	-2.14
2.10	-5.39	-2.10
2.20	-4.56	-2.33
2.30	-4.50	-2.21
2.30	-4.48	-2.39
2.40	-4.43	-2.23
2.40	-4.51	-2.23
2.50	-5.32	-2.22
2.60	-5.77	-2.21
2.70	-5.80	-2.20
2.80	-6.11	-2.30
2.90	-6.19	-2.42
3.00	-6.17	-2.48
3.10	-5.39	-2.48
3.10	-5.30	-2.30
3.20	-5.10	-2.42
3.30	-5.14	-2.60
3.40	-5.16	-2.32
3.40	-4.96	-2.42
3.50	-5.38	-2.44
3.60	-5.43	-2.30
3.70	-5.96	-2.39

3.80	-6.03	-2.50
3.80	-6.12	-2.40
3.90	-6.20	-2.51
4.00	-5.75	-2.34
4.10	-5.44	-2.41
4.20	-5.08	-2.30
4.20	-5.00	-2.34
4.30	-4.80	-2.36
4.40	-4.99	-1.98
4.50	-5.42	-2.03
4.50	-5.34	-1.99
4.60	-5.72	-2.14
4.70	-6.06	-2.19
4.80	-6.31	-2.17
4.80	-6.13	-2.19
4.90	-6.34	-2.43
5.00	-5.69	-2.30
5.10	-6.03	-2.35
5.20	-5.09	-2.47
5.30	-4.40	-2.67
5.30	-4.41	-2.63
5.40	-4.96	-2.68
5.50	-5.41	-2.49
5.60	-5.84	-2.70
5.60	-6.03	-2.70
5.70	-6.21	-2.58
5.70	-6.05	-2.66
5.80	-6.28	-2.61
5.80	-6.18	-2.54
5.90	-5.91	-2.62
5.90	-6.09	-2.69
6.00	-6.20	-2.79
6.10	-6.21	-2.86
6.20	-5.45	-2.60
6.20	-5.29	-2.61
6.30	-4.81	-2.66
6.40	-5.39	-2.65
6.50	-5.43	-2.65
6.50	-5.31	-2.65
6.60	-5.48	-2.58
6.60	-5.53	-2.47
6.70	-5.90	-2.48
6.70	-5.69	-2.55
6.80	-6.10	-2.49
6.80	-5.98	-2.31
6.90	-6.44	-2.13
6.90	-6.26	-2.03
7.00	-6.60	-2.13
7.10	-6.65	-2.18
7.20	-6.18	-2.46

7.30	-6.21	-2.15
7.40	-5.46	-1.73
7.50	-5.79	-1.24
7.60	-5.96	-1.43
7.70	-5.47	-1.48
7.80	-4.74	-1.24
8.00	-5.56	-2.23

AZUERO

Distance from top (cm)	Delta O-18 (‰)	Delta C-13 (‰)
0.00	-6.06	-1.49
0.00	-5.80	-1.60
0.10	-5.80	-1.45
0.20	-6.11	-1.83
0.30	-5.91	-2.44
0.40	-6.02	-3.17
0.50	-5.71	-2.88
0.60	-5.43	-2.43
0.70	-5.45	-1.99
0.80	-5.72	-1.91
0.90	-6.03	-2.24
0.90	-5.96	-2.16
1.00	-6.80	-2.64
1.10	-6.68	-2.79
1.10	-6.65	-2.60
1.20	-6.03	-2.45
1.30	-5.76	-1.69
1.40	-5.46	-1.67
1.50	-5.47	-1.72
1.60	-5.90	-2.06
1.60	-5.75	-2.10
1.70	-6.25	-2.09
1.80	-6.12	-2.10
1.90	-6.26	-2.24
1.90	-6.01	-2.12
2.00	-5.85	-1.48
2.10	-5.50	-0.46
2.20	-5.80	-0.30
2.30	-6.35	-0.71
2.40	-5.93	-1.19
2.50	-5.72	-1.70
2.60	-5.43	-1.52
2.70	-4.97	-1.17
2.80	-4.70	-0.96
2.90	-4.64	-1.03
3.00	-5.25	-0.93
3.10	-5.44	-1.06
3.10	-5.56	-1.15
3.20	-5.96	-1.48
3.20	-6.26	-1.42
3.30	-5.98	-1.48
3.30	-5.85	-1.45
3.40	-5.99	-1.42
3.40	-6.12	-1.48
3.50	-5.93	-1.78

3.60	-5.71	-1.62
3.70	-5.38	-1.53
3.80	-5.61	-1.75
3.90	-5.99	-2.17
4.00	-5.61	-1.96
4.10	-5.51	-0.97
4.20	-5.51	-0.66
4.30	-5.79	-0.71
4.40	-5.96	-1.02
4.40	-6.08	-0.98
4.50	-6.37	-1.18
4.60	-5.98	-1.70
4.70	-5.62	-2.02
4.80	-5.70	-1.96
4.90	-5.51	-1.41
5.00	-5.10	-1.08
5.00	-4.80	-0.97
5.10	-4.59	-0.71
5.10	-4.49	-0.72
5.20	-5.04	-0.81
5.30	-4.94	-0.82
5.40	-5.65	-0.86
5.50	-5.98	-0.99
5.60	-6.21	-1.33
5.60	-6.18	-1.14
5.70	-6.19	-1.43
5.70	-6.09	-1.50
5.80	-5.87	-1.89
5.90	-5.67	-2.08
6.00	-5.43	-1.87
6.10	-5.25	-1.34
6.20	-4.98	-0.82
6.30	-4.90	-0.69
6.40	-5.11	-0.72
6.40	-4.96	-0.70
6.50	-5.51	-0.44
6.60	-5.75	-0.63
6.60	-5.80	-0.56
6.70	-6.45	-0.90
6.80	-6.20	-1.23
6.80	-6.20	-1.18
6.90	-6.15	-1.26
7.00	-6.01	-1.63
7.10	-5.90	-1.85
7.20	-5.57	-1.54
7.30	-5.35	-1.20
7.30	-5.43	-1.23
7.40	-5.27	-1.03
7.40	-5.27	-1.15
7.50	-5.46	-0.95

7.60	-5.59	-1.07
7.70	-6.10	-0.95
7.80	-6.06	-1.12
7.90	-6.69	-1.33
8.00	-6.20	-1.19

APPENDIX C

APPENDIX C

Based on a method developed by Buddemeier (1974), Houck (1978) derived a computer algorithm for calculating actual coral skeletal density using the relationship between the densitometer response to the film emulsion of the coral slab and the Al stepwedge from the same emulsion. Houck's (1978) algorithm was rewritten into a Fortran disk program for use on an IBM-PC and is included here with coral skeletal density data.

The first step in the algorithm involves the calculation of the linear absorption coefficient for Al:

$$(a) \ln(R_{Al}) = (\mu_{Al})(X_{Al}) + C$$

and, likewise, for coral:

$$(b) \ln(R_{CrI}) = (\mu_{CrI})(X_{CrI}) + C$$

where R_{Al} and R_{CrI} are the densitometer responses to the film emulsion exposed by X-rays passing through the Al stepwedge and coral, respectively; X_{Al} and X_{CrI} are the respective thicknesses of the Al stepwedge and coral slab; C is a constant dependent on film properties, exposure time, X-ray output and densitometer sensitivity; and μ_{Al} and μ_{CrI} are the linear absorption coefficients for Al and coral, respectively.

The next step involves calculation of the mass absorption coefficient for Al, which is simply the linear absorption coefficient divided by the density of the material. The mass absorption coefficient of coral is linearly related to the

mass absorption coefficient of Al over a wide range of X-ray energies, so that calculating the weight fraction of each of the coral aragonite elemental components was not necessary.

Formulas (a) and (b) can be equated by considering the thickness of Al needed to produce the same densitometer response as the coral slab:

$$(c) R_{Al} = R_{CrI}$$

or

$$(d) e^{(\mu_{Al})(X_{Al})} = e^{(\mu_{CrI})(X_{CrI})}$$

By taking the natural logarithm of both sides of equation (d), the equation for the coral density can then be derived:

$$(e) \rho_{CrI} = (\ln(R_{CrI}) - C) / (\mu / \rho_{CrI})(X_{CrI})$$

where R_{CrI} , X_{CrI} , and C are the same as in equation (b); and μ / ρ_{CrI} is the mass absorption coefficient of the coral.

Although Houck's (1978) algorithm generates values which represent actual skeletal densities (g/cc), relative skeletal densities are reported in this study due to insufficient thickness of the coral slabs. Coral slabs should be cut 2 to 3 times the diameter of a single coral polyp to avoid detection of variations in densities of skeletal elements of a single polyp rather than overall skeletal density variations. The X-ray emulsion densities of the CONTADORA 9 and UVA 56 coral samples were outside the range of the X-ray emulsion densities of

the Al stepwedge, precluding calculation of relative skeletal densities for those samples .


```

        DIMENSION RA(25), TA(25),RCRL(25), TCRL(25), BRA(25),
        1,BTA(25), BRC(25), BTRC(25), ALBRA(25),VAL(24),
        1,WL(24), UC(24), ALBRC(25)
C      RA(I) is densitometer response to aluminum thickness
        TA(I).
C      RCRL(I) is densitometer response to coral thickness
        TCRL(I).
C      TA(I) and TCRL(I) in centimeters.
C      NUM is X-Ray film number, each card must be numbered.
C      Any number of aluminum step wedge values and any
C      number of coral measurements can be made per X-Ray
C      film number(25 max).
C      NUM is also used as sentinel, 0 after each X-Ray set,
C      -1 at end of data.
C      Data output for coral samples in same order as input.
C      Coral density out put is grams per cc.
C      X-Ray number, RA(I), TA(I), RCRL(I), and TCRL(I) data
C      are listed for each X-Ray film before calculated
        values.
        CHARACTER*6 FNAME
        OPEN(4,FILE='OUT.PUT', STATUS='NEW')
        WRITE(*,1)
1      FORMAT(' INPUT FILE NAME')
2      READ(*,3)FNAME
3      FORMAT(A)
        OPEN(5,FILE=FNAME)
4      WRITE(*,99)
99     FORMAT(1X,'NUM',3X,'RA(I)',3X,'TA(I)',1X,'RCRL(I)'
1,1X,'TCRL(I))
5      I=1
        J=0
        Z=0.0
        L=0
        STA=0.0
        SQSTA=0.0
        SLBRA=0.0
        SQBRA=0.0
        SPROD=0.0
C
10     READ(5,100) NUM, RA(I), TA(I), RCRL(I), TCRL(I)
100    FORMAT(I3,4F8.3)
        WRITE(*,100) NUM, RA(I), TA(I), RCRL(I), TCRL(I)
105    WRITE(4,151) NUM, RA(I), TA(I), RCRL(I), TCRL(I)
151    FORMAT(1X,I3,4F8.3)
C
110    IF(NUM) 860,300,120
120    KNUM=NUM
130    IF(RA(I).EQ.0) GO TO 160
        BRA(I)=RA(I)
        BTA(I)=TA(I)
        Z=Z+1.0
        L=L+1

```

```

C
160 IF(RCRL(I).NE.0) GO TO 170
    GO TO 200
170 J=J+1
    BRC(J)=RCRL(I)
    BTCR(J)=TCRL(I)
    IF(RA(I).EQ.0) GO TO 10
C
200 STA=STA+BTA(I)
    SQSTA=SQSTA+BTA(I)**2
    ALBRA(I)=ALOG(BRA(I))
    SLBRA=SLBRA+ALBRA(I)
    SQBRA=SQBRA+ALBRA(I)**2
    SPROD=SPROD+(BTA(I)*ALBRA(I))
    I=I+1
    GO TO 10
C
300 SLOPE=(SPROD-((STA*SLBRA)/Z))/(SQSTA-((STA**2)/Z))
    RSQ=((SPROD-((STA*SLBRA)/Z))**2)/((SQSTA-((STA**2)/Z)
1 )*(SQBRA-((SLBRA**2)/Z)))
    ALNA=(SLBRA/Z)-((SLOPE*STA)/Z)
    UPAL=SLOPE/2.702
C
    IF(UPAL.LT..16.OR.UPAL.GE.25.30) GO TO 840
C
    VAL(1)=.16
    VAL(2)=.18
    VAL(3)=.25
    VAL(4)=.36
    VAL(5)=.54
    VAL(6)=.72
    VAL(7)=1.04
    VAL(8)=1.43
    VAL(9)=1.92
    VAL(10)=2.51
    VAL(11)=3.21
    VAL(12)=4.00
    VAL(13)=5.05
    VAL(14)=6.10
    VAL(15)=7.30
    VAL(16)=8.60
    VAL(17)=10.05
    VAL(18)=11.75
    VAL(19)=13.50
    VAL(20)=15.45
    VAL(21)=17.50
    VAL(22)=19.85
    VAL(23)=22.45
    VAL(24)=25.30
C
    M=0
    DO 400 M=1,24
    BZ=M

```

WL(M)=.05+(BZ*.05)
400 CONTINUE

C

UC(1)=.18
UC(2)=.20
UC(3)=.32
UC(4)=.52
UC(5)=.79
UC(6)=1.17
UC(7)=1.68
UC(8)=2.31
UC(9)=3.09
UC(10)=4.00
UC(11)=5.06
UC(12)=6.30
UC(13)=7.85
UC(14)=9.50

C

Sr K EDGE AT .75 ANGSTROMS
IF(UPAL.GE.6.13.AND.UPAL.LT.7.30) UC(14)=8.75
UC(15)=10.45
UC(16)=12.35
UC(17)=14.50
UC(18)=16.80
UC(19)=19.45
UC(20)=22.15
UC(21)=25.25
UC(22)=28.55
UC(23)=32.25
UC(24)=36.20

C

MA=0
DO 500 MA=1,23
MB=MA+1
IF(UPAL.GE.VAL(MA).AND.UPAL.LT.VAL(MB)) GO TO 450
GO TO 500
450 FRAC=(UPAL-VAL(MA))/(VAL(MB)-VAL(MA))
WAF=FRAC*.05
WAV=WAF+WL(MA)
UCRL=(FRAC*(UC(MB)-UC(MA)))+UC(MA)
E=12.4/WAV
500 CONTINUE

C

WRITE(*,550) KNUM, L, RSQ, UPAL, UCRL, WAV, E
550 FORMAT(1X,'X-RAY FILM NUMBER',I4/1X,
1 'NUMBER OF STEP WEDGE VALUES',I4/1X,
2 'COEFF. OF DETERM.(R SQUARED)=',F6.3/1X,
3 'MASS ABSORPTION COEF. AL=',F8.3/1X,
4 'MASS ABSORPTION COEF. CORAL=',F8.3/1X,
5 'EFFECTIVE X-RAY WAVELENGTH IN ANGSTROMS=',F8.3/1X,
6 'EFFECTIVE X-RAY ENERGY IN KeV.',F8.3)

C

MC=0

```
DO 800 MC=1,J  
  ALBRC(MC)=ALOG(BRC(MC))  
  ETAL=(ALBRC(MC)-ALNA)/SLOPE  
  D=(SLOPE*ETAL)/(UCRL*BTCR(MC))
```

C

```
  WRITE(*,600) KNUM, MC, D  
600  FORMAT(1X,'X-RAY FILM NUMBER',I4/1X,  
  1 'CORAL SAMPLE',I4/1X,  
  2 'CORAL DENSITY=',F8.3)  
800  CONTINUE  
      CLOSE(5,STATUS='KEEP')  
820  WRITE(*,830)  
830  FORMAT(' INPUT ANOTHER FILE NAME')  
      GO TO 2
```

C

```
840  WRITE(*,850) KNUM  
850  FORMAT(1X,'ENERGY OUTSIDE LIMITS FOR X-RAY FILM',I4)  
      GO TO 820  
860  STOP  
      END
```

INPUT FILE NAME

AZUERO

NUM	RA(I)	TA(I)	RCRL(I)	TCRL(I)
3	5.560	.120	6.300	.430
3	6.640	.240	6.820	.450
3	8.170	.360	6.700	.440
3	9.060	.480	6.470	.450
3	9.670	.600	6.700	.475
3	.000	.000	7.050	.470
3	.000	.000	7.200	.470
3	.000	.000	7.100	.490
3	.000	.000	6.800	.490
3	.000	.000	6.800	.510
3	.000	.000	7.200	.500
3	.000	.000	7.700	.495
3	.000	.000	7.750	.500
3	.000	.000	6.950	.500
3	.000	.000	6.500	.500
3	.000	.000	6.280	.505
3	.000	.000	7.120	.510
3	.000	.000	7.190	.515
3	.000	.000	7.200	.520
3	.000	.000	7.180	.530
3	.000	.000	7.450	.525
3	.000	.000	6.720	.530
3	.000	.000	6.650	.530
3	.000	.000	6.650	.535
3	.000	.000	6.830	.560
3	.000	.000	6.800	.560
3	.000	.000	6.600	.560
3	.000	.000	6.620	.570
3	.000	.000	6.800	.570
3	.000	.000	7.130	.570
3	.000	.000	7.150	.570
3	.000	.000	6.900	.575
3	.000	.000	6.830	.575
3	.000	.000	7.000	.570
3	.000	.000	7.300	.575
0	.000	.000	.000	.000

X-RAY FILM NUMBER 3

NUMBER OF STEP WEDGE VALUES 5

COEFF. OF DETERM. (R SQUARED)= .958

MASS ABSORPTION COEF. AL= .437

MASS ABSORPTION COEF. CORAL= .636

EFFECTIVE X-RAY WAVELENGTH IN ANGSTROMS= .271

EFFECTIVE X-RAY ENERGY IN KeV.= 45.681

X-RAY FILM NUMBER 3

CORAL SAMPLE 1

CORAL DENSITY= .839

X-RAY FILM NUMBER 3

CORAL SAMPLE 2

CORAL DENSITY= 1.079
X-RAY FILM NUMBER 3
CORAL SAMPLE 3
CORAL DENSITY= 1.040
X-RAY FILM NUMBER 3
CORAL SAMPLE 4
CORAL DENSITY= .895
X-RAY FILM NUMBER 3
CORAL SAMPLE 5
CORAL DENSITY= .963
X-RAY FILM NUMBER 3
CORAL SAMPLE 6
CORAL DENSITY= 1.144
X-RAY FILM NUMBER 3
CORAL SAMPLE 7
CORAL DENSITY= 1.215
X-RAY FILM NUMBER 3
CORAL SAMPLE 8
CORAL DENSITY= 1.120
X-RAY FILM NUMBER 3
CORAL SAMPLE 9
CORAL DENSITY= .982
X-RAY FILM NUMBER 3
CORAL SAMPLE 10
CORAL DENSITY= .943
X-RAY FILM NUMBER 3
CORAL SAMPLE 11
CORAL DENSITY= 1.142
X-RAY FILM NUMBER 3
CORAL SAMPLE 12
CORAL DENSITY= 1.367
X-RAY FILM NUMBER 3
CORAL SAMPLE 13
CORAL DENSITY= 1.373
X-RAY FILM NUMBER 3
CORAL SAMPLE 14
CORAL DENSITY= 1.031
X-RAY FILM NUMBER 3
CORAL SAMPLE 15
CORAL DENSITY= .820
X-RAY FILM NUMBER 3
CORAL SAMPLE 16
CORAL DENSITY= .705
X-RAY FILM NUMBER 3
CORAL SAMPLE 17
CORAL DENSITY= 1.085
X-RAY FILM NUMBER 3
CORAL SAMPLE 18
CORAL DENSITY= 1.104
X-RAY FILM NUMBER 3
CORAL SAMPLE 19
CORAL DENSITY= 1.098
X-RAY FILM NUMBER 3

CORAL SAMPLE 20
CORAL DENSITY= 1.069
X-RAY FILM NUMBER 3
CORAL SAMPLE 21
CORAL DENSITY= 1.190
X-RAY FILM NUMBER 3
CORAL SAMPLE 22
CORAL DENSITY= .872
X-RAY FILM NUMBER 3
CORAL SAMPLE 23
CORAL DENSITY= .841
X-RAY FILM NUMBER 3
CORAL SAMPLE 24
CORAL DENSITY= .833

X-RAY FILM NUMBER 3
CORAL SAMPLE 1
CORAL DENSITY= .832
X-RAY FILM NUMBER 3
CORAL SAMPLE 2
CORAL DENSITY= .679
X-RAY FILM NUMBER 3
CORAL SAMPLE 3
CORAL DENSITY= .688
X-RAY FILM NUMBER 3
CORAL SAMPLE 4
CORAL DENSITY= .754
X-RAY FILM NUMBER 3
CORAL SAMPLE 5
CORAL DENSITY .853
X-RAY FILM NUMBER 3
CORAL SAMPLE 6
CORAL DENSITY= .871
X-RAY FILM NUMBER 3
CORAL SAMPLE 7
CORAL DENSITY= .859
X-RAY FILM NUMBER 3
CORAL SAMPLE 8
CORAL DENSITY= .775
X-RAY FILM NUMBER 3
CORAL SAMPLE 9
CORAL DENSITY= .770
X-RAY FILM NUMBER 3
CORAL SAMPLE 10
CORAL DENSITY= .844
X-RAY FILM NUMBER 3
CORAL SAMPLE 11
CORAL DENSITY= .975
X-RAY FILM NUMBER 3
CORAL SAMPLE 12
CORAL DENSITY= .982
X-RAY FILM NUMBER 3
CORAL SAMPLE 13

CORAL DENSITY= .876
X-RAY FILM NUMBER 3
CORAL SAMPLE 14
CORAL DENSITY= .848
X-RAY FILM NUMBER 3
CORAL SAMPLE 15
CORAL DENSITY= .924
X-RAY FILM NUMBER 3
CORAL SAMPLE 16
CORAL DENSITY= 1.030